Otto Dodz SA21

NASA-CR-192414

Rockwell International

Rocketdyne Division
6633 Canoga Avenue
Canoga Park, California 91304

489092
84p.

RSS-8826-28

TECHNOLOGY TEST BED ENGINE

REAL-TIME FAILURE CONTROL

FINAL REPORT

P/E OCTOBER 1992

21 OCTOBER 1992

Contract NAS8-40000

Task 21

PREPARED BY

Hagop V. Panossian, Ph.D.
Principal Investigator
Principal Engineer
Control/Structure
System Dynamics

Victoria R. Kemp
Member of Technical Staff
System Dynamics

APPROVED BY

J. M. Hamilton for

Mike H. Taniguchi
Manager
System Dynamics

for

Sally Stohler
Manager
SSME Technology
Support Team

1. TABLE OF CONTENTS

Page

2. LIST OF FIGURES

2. LIST OF FIGURES (continued)

3. LIST OF TABLES

4. SUMMARY

The Real-Time Failure Control (RTFC) program involves development of a failure detection algorithm, for the Space Shuttle Main Engine (SSME). This failure detection approach is signal-based and entails monitoring SSME measurement signals based on predetermined as well as on-line computed mean and standard deviation values. Twenty-four engine measurements are monitored in the algorithm and provisions are made to add more parameters if needed. Each of the first values of every measurement signal at the algorithm start is checked against safety limits placed around a pre-computed engine-to-engine mean value (MV) with a bandwidth equal to a given multiple of the pre-computed standard deviation (SD). If several parameters are out of the bounds of these limits a failure is signaled. During the first two seconds (after algorithm start) a moving average (MA) and a SD is computed on-line in real-time. The moving average of each parameter is computed by averaging the incoming signal measurement with the four most recent previous signal measurements. The moving average is updated at every sampling interval (40 msec) and is checked against a similar safety band around the initial signal value for each parameter. If several anomalies are registered, a failure is signalled by the algorithm. At the end of the two-second interval the MA is fixed as the mean value for the rest of the algorithm operation and a safety band is placed above and below this value equal to a multiple of the computed SD. However, the safety band is adjusted by adjusting the mean value when propellant tank repressurization and venting take place. "Influence Coefficients" are used to make the necessary adjustments to the safety limits of those parameters that are affected by repressurization and venting or valve closure and opening. The MA is, in both cases, continuously updated and checked against the safety band. Once more, if several parameters exceed the limits a failure is signalled. At the start of every scheduled power transient the algorithm is stopped. It is re-initiated after two seconds from the termination of the power transient and the process is repeated.

This final report is divided into four major sections. The most encompassing of all is the discussion section that has sub-sections on: 1) RTFC algorithm development, 2) RTFC simulations, 3) RTFC current limitations, and 4) enhancements planned for. The report will cover background information, new developments, and future plans for the algorithm implementation and enhancements.

5. INTRODUCTION

Anomalous behavior during Space Shuttle Main Engine (SSME) hot-fire testing is presently detected via measurement redlines that monitor key measured parameters. In order to avoid the cost incurred and the impact on the SSME flight schedule due to failures, it is desirable to have an advanced failure detection system that detects anomalies early enough to minimize damage and that can identify as many failures as possible, quickly and efficiently, prior to catastrophes. The safe operation of any complex system, such as the SSME, rests on the reliability of the control and fault detection systems and the speed of detection and identification of component, sensor, or actuator failures. In the recent past, fault detection and isolation has raised the interest of many researchers [1-7]. Most major techniques to failure detection can be categorized as either model-based or signal-based approaches.

Model-based techniques rely on analytical redundancy [4-8]. Analytically generated "measurement" outputs are compared with hardware measurements by using present and/or previous values of some variables in conjunction with their mathematical relationships. The fault detection process herein encompasses three major tasks: 1) residual generation that entails taking the difference between the analytical and measured values, 2) statistical testing and signature generation, and 3) diagnostics and decision making.

On the other hand, signal-based techniques are hardware intensive and sensor/actuator driven. In this approach, the major undertakings include: 1) limit/trend checking by comparison of plant outputs with normal operational limits, 2) sensor/actuator/component redundancy, whereby a single value from measurements of several identical sensors is used according to some decision mechanism, 3) frequency spectrum analyses by using plant measurements, wherein frequency spectrums are compared with normal spectrums [9-12].

An algorithm is hereby developed, referred to as Real-Time Failure Control Algorithm (RTFCA) that permits fault detection during SSME hot-fire testing by a simple signal-based approach.

The method entails monitoring the signal averages for twenty-four engine parameters and comparing the signal averages to upper and lower signal safety limits. The

reason for monitoring the averages of signals, rather than their actual values, is to smooth or filter out most of the undesirable effects of sensor noise. Moreover, the safety limits are placed above and below the fixed average value for each parameter with a bandwidth of n*SD, where n is a pre-determined constant that is large enough to avoid false alarms and small enough to make the algorithm sensitive to actual failures.

The RTFC algorithm, as it is currently configured, works during SSME steady-state operation, starting at five seconds following engine start or two seconds following initiation of a new power transient. Moreover, an added safety feature is included that checks the value of each parameter at the first incoming measurement against upper and lower bounds around a predicted mean value. In case several parameters exceed or are below their expected limits then a failure is signalled. This feature will ensure the normal engine operation by identifying any failure that could have happened during start/power transients. Also, if any sensor indicates a negative output, it is automatically disqualified and eliminated from the algorithm. However, there is no means of overall sensor failure detection in the present set-up.

Twelve simulations on actual data from SSME incident tests were carried out during the current phase of the RTFC contract. Over forty incident tests were carefully studied for useful information. Currently, the RTFCA can handle only steady-state operating conditions. However, the start anomaly check is really a post transient failure detection approach that will detect any anomalous developments that happen during start or power transients. Moreover, there are nonlinear effects that appear in the behavior of some parameters. For example, the HPOT pump discharge temperature takes over 60 seconds to reach steady state and has an excursion of over 50°R. Special provisions are needed for such parameters to avoid false alarms. In addition, the RTFCA performance is a function of the multiplying factor n, as well as of the number of parameters required to show anomalous behavior for an engine shutdown decision.

Nevertheless, the RTFCA as it is presently configured, is very effective (much better than redlines) in detecting slow developing failures and it is slightly better than the redlines in fast failures, such as structural ruptures. Several of the RTFCA advantages include: 1) the requirement of multiple parameter anomalies for a failure decision (this avoids false alarms), 2) the option of choosing a different bandwidth for different

parameters and even for different intervals, 3) the use of a moving average, that removes noise effects and is sufficiently short-term to enhance its sensitivity, 4) the use of SD values, computed on-line, that are characteristic of current signal behavior, 5) the capability to account for those parameter excursions that are due to repressurization or venting and valve closure or opening effects, and 6) the flexibility of the algorithm for further expansions and enhancements, among others.

There are means of modifying the algorithm that will make it more encompassing and that will be discussed in what follows. An automated selection of the optimal safety bandwidth, the best influence coefficients or gains for repressurization/venting and valve closure/ open effects, and the number of anomalous parameters required for a sure failure needs to be developed. Most of the shortcomings of the RTFCA can thus be eliminated and plans for accomplishing this will be discussed later.

This report covers: 1) background information on past SSME failures and problems involving their detection, 2) detailed descriptions and simulation plots of the RTFCA, 3) the accommodation of repressurization/venting effects as well as repressurization valve closure and opening effects, 4) limitations and advantages of the algorithm, and 5) plans for future work for the enhancement of the RTFCA.

The objective of the present contract is to further enhance the RTFCA for the SSME by the accommodation of and compensation for propellant tank repressurization/venting as well as valve/closure and opening effects, and to demonstrate the operability of the algorithm via engine simulations. It will be shown that the RTFCA is capable of detecting performance degradation and anomalous behavior of the SSME earlier and faster than the existing redline system.

6. DISCUSSION

Fault detection system design involves several complex issues, such as quick response prior to significant performance degradation or damage as well as consideration of system redundancy. Advanced fault detection algorithms, based on careful consideration of system dynamic characteristics, can often lead to significant reduction of hardware redundancy. There are three main concerns in any fault detection and identification process. The primary objective invariably is to establish that a failure has occurred with a high degree of certainty. The type and location of failure as well as the extent of degradation are two of the remaining concerns that should be addressed appropriately. The principal thrust of the present algorithm involves the fault detection problem.

6.1 BACKGROUND

There were four major tasks identified in the statement of work of the present contract. These included 1) analyses of existing SSME test data to study the characteristic behavior due to LOX and fuel tank venting and repressurization, as well as repressurization valve opening/closure transient effects, 2) development of an analytical repressurization to account for the above mentioned venting/repressurization and repressurization valve opening/closing effects, 3) performing computer simulations to evaluate the analytical approach, and 4) preparation of agreed-upon documentation. These tasks also involved identifying the availability of sensors required to meet the enhanced algorithm. In addition, other areas of algorithm refinement were identified.

Thus, repressurization and venting, as well as valve closure and opening effects on SSME parameters were identified and quantified. An analytical approach to account for these effects was incorporated in the RTFCA. In this approach, the signal limits are modified at each time step in an effort to track the transient behavior induced in the signals as a result of the above mentioned effects. The modifications are based on the expected parameter change per unit LOX and fuel engine inlet pressure change.

6.1.1 INCIDENTS

The occurrence of an anomaly or a failure is classified as a "major" or a "minor" incident based on: a) the extent of damage, b) pressure, temperature, speed and vibration levels in excess of normal end item operating levels, and c) internal and/or external fires or explosions [13].

RTFC Parameter Selection Criteria [14]:

A total of 40 tests were used to select the 24 parameters for the RTFC algorithm. Those measurement parameters chosen represent "key" aspects of SSME operation. Fifty-seven (57) measurements were examined for: a) anomaly induced percentage change from steady-state operation, b) rate of percentage change, c) interim from first indications of an anomaly to cut off. Each of the above factors were weighed and accordingly, the most appropriate parameters were selected for use in the algorithm.

A database was developed whereby all the generic and specific characteristics of various incident tests were listed. This data was used to evaluate the significant parameters for failure detection use (See Ref. 15).

Also included in the evaluations were failure mode qualitative characteristics where generic descriptions of the incident type and a sample of indicative parameters were studied. Moreover, 1) sensor measurement standard deviations, 2) test-to-test envelope database definition, 3) data for time-sliced value deviations from the average steady-state sensor measurements, and 4) 31 database inputs for each test were also studied.

Generated was information on engine parameters, mean values and standard deviations from actual and simulated data. For instance, for the high pressure oxygen turbopump (HPOT) discharge temperature channel B values, the engine-to-engine standard deviation for the predicted value at the 109% power level is 61.07373 while the actual value is 118.6592 (almost double). Differences of the above mentioned nature raise the concern of using pre-computed means and standard deviations. This fact is the fundamental reason for choosing the first incoming value of each parameter measurement as the basis for determining the actual mean value to be used by the

algorithm during its first two-second operation rather than using a pre-computed value.

6.1.1.1 SAMPLE INCIDENT DESCRIPTIONS

There are two major types of incidents: 1. Fast occurring structural failures, and 2. Slow occurring anomalies that build up over a longer duration. To provide a taste of such anomalies, a sample incident is described below.

1. Test No. 902-428
   Scheduled Duration (SDUR) = 700 seconds
   Achieved Duration (ADUR)= 204.12 seconds
   Engine NO. 2106
   Date: July 1, 1987

   Engine performance was nominal until engine start plus 163 seconds. At 163 seconds, HPOT discharge temp in Channel A (CHA) began to rise indicating the presence of a hot streak in the OPB injector, HPOT discharge temp in Channel B (CHB) did not respond. The hot streak was localized and due to the rotating effect of the turbine, only a Channel A sensor responded.

   Post test examination revealed erosion of the oxidizer preburner injector face and localized burn-through of the HPOTP turbine sheet metal adjacent to the injector erosion area. There was no external engine damage and heating was isolated to the areas noted above.

   REDLINE PARAMETER - HPFT discharge temp sensors (231,232) dropped below their lower limit. Pneumatic shutdown was initiated because a hydraulic lockup was in effect (part of the test plan).

6.1.1.2 SELECTION OF TESTS FOR RTFC SIMULATIONS

From past test histories, a selection of incident tests was derived for the purpose of simulations with the RTFC algorithm using real-test data. The selection was based on the need to cover a wide range of failure types. Thus, failures that have been simulated on the RTFC algorithm previously, failures that were representative of the most critical and most recurrent anomalies, as well as those that represented fast or slow occurring failures, both with and without repressurization/venting, were selected. Moreover, tests that were nominal and had repressurization and venting as well as valve closure/opening were also simulated. The selected list of incidents is presented in Table 6.1.

6.1.2 PARAMETER IDENTIFICATION (PID) NUMBER ASSOCIATION WITH TESTS

Every individual measurement parameter is associated with a PID number for each specific engine test. These PID numbers often change from test to test and from engine to engine, since in some cases, new sensors are added and in others, existing ones are removed. Thus, the redistribution of the measurement sensors create the need to identify the PID numbers for each test.

Processing test data of the SSME includes storage of measurement values in computer files that only accommodate 9 PIDs per file (meaning 9 measurements). This is apparently necessary for the failure mode effects analysis (FMEA) that is carried out after every failure occurrence.

6.1.3 CHARACTERISTIC EFFECTS OF REPRESSURIZATION AND VENTING ON RTFC PARAMETERS

During SSME testing, the LOX tank or the fuel tank, or both are either pressurized or vented several times during the course of a test in virtually every test. These repressurization/venting processes effect some of the parameter values over and above the power level variation effects. Eleven of the twenty-four monitored parameters are significantly affected by venting/pressurization of the oxygen tank. On the other hand, venting/repressurization of the fuel tank significantly affects only one parameter, the LPFTP speed. Additionally, closing of the fuel and GOX

repressurization valves results in rapid changes, essentially step function responses, in some parameters. Two parameters, the PBP discharge pressure and the LPFTP speed, are affected upon closing the fuel repressurization valve. One parameter, the HEX venturi delta-pressure, is affected upon closing the GOX repressurization valve.

Analyses on various engine data with and without LOX venting was carried out. Clearly, almost all parameters are affected, but only about half are significantly affected as to necessitate accommodation of the effects in the algorithm. Well-defined procedures are utilized to incorporate the effects of tank venting and pressurization as well as of repressurization valve closures on the RTFC parameters using existing SSME "influence coefficients."

6.2 RTFCA OBJECTIVE AND SCOPE

The main objective of the Real-Time Failure Control contract is to develop a real-time failure detection algorithm that is signal-based and that detects anomalous behavior of the SSME earlier than the existing redline system.

The RTFCA works, as it currently stands, only during SSME steady-state and repressurization and venting transient test conditions. It utilizes both low and high frequency measurement signals from twenty-four key parameters that are currently monitored. However, the option of expanding the monitored parameter list would not require extensive effort. Eight of these parameters are facility and sixteen are CADS. All major redline parameters are included, based on the fact that all these are key to safe engine operation.

6.2.1 THE CURRENT RTFC ALGORITHM

The RTFC algorithm in its present configuration starts at five seconds following engine start or two seconds following initiation of a new power transient. As a safety feature, the first measurement values (after algorithm start) of all the twenty-four monitored parameters are checked against safety limits formed by placing a safety band of N^*SD_p, where N is a predetermined multiplying factor (normally 4) and SD_p is the pre-computed SD. If several parameters (the number of which should be decided prior to a test, usually between 3 and 6) violate these limits then an engine shutdown is signalled. This check will detect any anomalous behavior that could have developed during start or a power transient. If no failures are detected at the first instant then the first measurement values of the twenty-four parameters are chosen as the mean values for the first two-second interval of the algorithm operation (i.e. first two-second failure detection). During this time an on-line real-time SD_p and a moving average (MA) are calculated. The latter is the average of 200 milliseconds worth of data for each parameter. This MA is updated at every sampling interval (40 milliseconds) by dropping the last value of the measurements and picking up and adding on the most recent one. This MA is checked against a safety band formed by placing safety limits around the above mentioned fixed average (the first incoming measurement value) of N_1^* SD_p bandwidth (where N_1 is a predetermined weighting factor). If several parameters simultaneously indicate anomalous behavior, an engine shutdown is signaled. Figures 1 and 2 show schematics of the RTFC algorithm's software structures and the operational features.

If no anomalies are detected during this two-second interval, and no repressurization or venting occurs, then the last computed MA is fixed as the mean value (MV) for each particular parameter for the rest of that power level (i.e. steady-state interval failure detection). A safety band is formed around this fixed MV by placing limits (above and below it) of N_2^* SD_c (where N_2 is a weighting factor and SD_c is the calculated SD). Then the on-line MA, that is continuously being updated, is checked against these safety limits at every sampling interval until the start of a scheduled power transient. If several parameters indicate violation of the safety limits, an engine shutdown is signalled.

In case of repressurization and venting, the MV of each parameter is adjusted, based on power levels and gain values derived from "influence coefficient" data. Moreover, the limits are also adjusted accordingly.

This process is stopped at the initiation of every scheduled power transient and is re-started two seconds thereafter, allowing time for the transient effects to settle out. For a visual picture of the algorithm operation see the schematic in Figure 2.

6.2.2 REPRESSURIZATION/VENTING AND VALVE CLOSURE/OPENING EFFECTS

Test Analyses:

Several tests, that were performed on test stands A1, A2 and A3 as well as tests from the technology Test Bed (TTB) engines, were analyzed and the effects of repressurization and venting (of LOX and fuel) were evaluated for various engine parameters. Tests 750-285, 801-008, 801-009, 801-011, 901-173, 901-340, 901-364, 901-498, 901-511, 901-550, 901-551, 902-398, 902-415, and 902-428 were examined for OPOV and FPOV actuator position as well as LPFP speed and HPFP discharge pres-sure changes due to repressurization and venting effects (as shown in Figures 3-7). Moreover, nine such tests were analyzed for the HPOT Discharge Temperature and HPFT Discharge Temperature. The tests studied included all of the above tests except 750-285, 901-173, 901-340, 901-364 and 801-008. Both Channel A and Channel B data were analyzed (see Figures 8 and 9). The test profile plots for some of the above mentioned tests were not available. However, test profiles for 750-285, 801-008, 801-009, 801-011, 901-173, 901-340, 901-364, 901-498, 901-511, 901-550, 901-551, 902-398, 902-415, 902-428, and 901-364 are shown in Figure 10.

Indications are that all of the above mentioned parameters are significantly effected by LOX repressurization and the effect of LOX venting is smaller but still measurable.

LOX repressurization decreases the OPOV opening by about 2.5% for 165 OPI (Oxidizer Pressure at Inlet). While only 1.5% reduction of the valve opening is registered for -80 NPSP venting at 107% RPL (see Figures 3). The effect of LOX venting and repressurization on the HPOT and HPFT Discharge Temperatures is similar.

Thus, LOX venting down to -20 NPSP increases the HPOT Discharge Temperature from 1290° to 1345° while repressurization up to 165 OPI (Oxidizer Pressure Inlet) reduces it from 1345° F to 1245° F at 104% RPL. These effects are even stronger at 109% RPL (which are currently being looked at (see Figures 8)). The thrust profiles of some of the above mentioned tests that were studied provide the venting/repressurization profiles as well as the power levels at various time slices (See Figure 10).

LOX repressurization decreases the LPFP speed by about 0.75 rpm/sec. for 47 NPSP. While only a minor change (.15 rpm/sec.) of the speed is registered for an equal degree of venting at 90% RPL (see Figure 5). The effect of LOX venting and repressurization on the HPFT Discharge Pressure is similar (Figure 6). Thus, LOX venting down from 220 psia to 135 psia increases the HPFT Discharge Pressure from 6728 psia to 6758 psia while repressurization from 90 psia to 220 psia reduces it from 6750 psia to 6720 psiaat 109% RPL. One of the tests, 902-398 indicates nonlinear behavior of the HPFP Discharge Pressure (see Figure 7). This is not seen in any other tests. Hence, it could have been a sensor problem.

It was found that fuel venting affected the Low Pressure Fuel Turbopump, (LPFTP) speed. A decrease of about 0.85 RPM/psi for fuel repressurization. Although it was noticed that very seldom fuel repressurization is performed (tests normally include only fuel venting). In addition, the High Pressure Fuel Pump (HPFP) radial accelerometers are also slightly affected by fuel repressurization amplitude by an increase of about 0.06g, and venting reduces it by about the same amount.

Out of the 24 RTFC monitored parameters, only 3 seem to be affected by opening/closing the fuel and GOX repressurization valves. The HPOTP Boost Pump (or, as it is more often called, the Preburner Boost Pump (PBP)) discharge pressure rises by 20 psi when the fuel repressurization valve is opened and drops by 20 psi when it is closed. The Low Pressure Fuel Pump (LPFP) speed, on the other hand increases by about 90 RPM when the fuel repressurization valve opens and decreases by about the same amount when it is closed.

The Heat Exchanger (HEX) Venturi delta pressure drops down by about 68 psi when the Gaseous Oxidizer (GOX) valve closes. Table 2 summarizes the effects of fuel/LOX venting/repressurization and repressurization valve opening/closure as a result of examination of actual test data

Analytical Approach:

An analytical approach to account for the effects of propellant tank venting and repressurization has been incorporated into the RTFC algorithm. The signal limits are modified at each time step in an effort to track the transient behavior induced in the signals as a result of tank venting and repressurization. The signal limits are computed by the standard methods used for steady-state behavior at algorithm start and again at two seconds following algorithm start, respectively. These signal limits are then modified at each time step according to any change in fuel and LOX inlet pressures and the corresponding "Influence Coefficient " (IC) values.

These IC, or gain, values represent the expected parameter change per unit fuel or LOX engine inlet pressure change. Thus, the computational expressions for the signal limits consist of three components which represent signal behavior due to: 1) steady state behavior, 2) LOX venting and repressurization effects, and 3) fuel venting and repressurization effects.

The ICs were derived by both SSME Power Balance model (PBM) and SSME Digital Transient model (DTM) calculations as well as from the data analyses of actual tests discussed previously. The first approach encompasses generating perturbations in the PBM by changing a given independent engine parameter by a certain amount at each specified power level, ranging from 65% to Rated Power Level (RPL) to 109% RPL, to compute the effects on all the dependent parameters at each of these power levels. Generally no assumption of cavitation of the High-Pressure Oxidizer Pump (HPOP) or even the High-Pressure Fuel Pump (HPFP) was made. There are independent parameters to simulate various degrees of HPOP and HPFP cavitation, that can occur at minimum LOX inlet and fuel inlet pressures or under poor hardware conditions.

The IC generation includes the comparison of each perturbed value of a parameter to a nominal value at each power level and the creation of a least-squares curve fit of up to order three, which approximates the percent change in each dependent variable at a given power level for a known dependent parameter perturbation. The coefficients of these equations, that result from the curve fits are the ICs. These can be represented as a matrix of independent and dependent parameters of engine operating conditions. Only those parameters that had larger than 2% change in their percent variation were evaluated. Table 3 summarizes the effects of LOX tank venting/repressurization based on PBM calculations.

For a given power level the IC of a certain parameter can be found from the following equation:

$$IC = A_0 + A_1 * PL + A_2 * PL + A_3 * PL$$

Where A_0, A_1, A_2, A_3 are the coefficients of the curve-fit and PL is the ratio of actual power level to the RPL. This number is the percent change in the dependent parameter for a 1% change in the independent parameter. Thus,

$$IC = \frac{dD}{D} * \frac{dI}{I}$$

Where d (.) is the perturbation of the dependent or independent variables. The total gain will then be the IC multiplied by the actual value of the parameter measurement signal.

An analytical approach to account for the effects of opening and closing the fuel and GOX repressurization valves has also been formulated and incorporated into the algorithm. Only three of the twenty-four parameters are significantly affected, and show either a step increase or decrease at the time of valve opening or closing. The amounts by which these parameters change are indicated in Table 6.2.2.1.

TABLE 6.2.2.1

ID	Parameter	Fuel Valve Open	Fuel Valve Close	GOX Valve Close
6	HPOTP Boost Pump Dis Pres	+20 psi	-20 psi	N/E
16	LPFTP Speed	+90 rpm	-90 rpm	N/E
21	HEX Venturi Delta-Pres	N/E	N/E	-68 psi

Extensive SSME hot-fire test data has been analyzed and actual variations of dependent parameter values have been evaluated based on known variations of independent parameters. Thus, at various power levels, known variations in tank pressures (independent variables) were studied against the effects on all twenty-four engine parameters (dependent variables) that are currently monitored. Then, the gains were derived based on actual calculations of the percent change of each dependent variable at a given power level for a known independent variable excursion.

6.2.3 COMPUTER SIMULATIONS

In this task, SSME hot-fire test data was used with the algorithm to evaluate the enhanced algorithm's performance due to 1) propellant tank venting and repressurization, and 2) repressurization valve opening/closure effects. Moreover, incident test data was also used on the enhanced algorithm to show the improved performance with the modifications. A brief description of the tests and algorithm simulation results for the twelve hot-fire tests simulated during this phase follows.

The tests in (i) through (vi) presented below were selected for simulation because 1) the tests ran for the full planned duration, 2) the tests did not involve any anomalies, 3) venting and/or repressurization of the LOX tank was performed, and 4) venting of the fuel tank was performed. Simulations were made of these nominal tests to establish a set of gain values for the monitored parameters which reflect the nominal signal behavior as a result of tank venting/repressurization procedures.

The tests presented in (vii) through (x) involved both the tank venting/repressurization procedures and engine failures. These simulations were made to evaluate the

algorithm's performance in detecting anomalous behavior under tank venting/repressurization conditions.

Two additional tests were simulated, presented in (xi) and (xii). Neither of these tests involved the tank venting/repressurization procedures. Both tests involved a main injector failure. Since both failures were structural, the failures occurred rapidly. The simulations resulted in algorithm shutdown signals slightly before the redlines.

(i) Test 902-398

The thrust profile for test 902-398 is presented in Figure 11 LOX tank venting was initiated at 80 seconds followed by repressurization at 160 seconds and venting again at 240 seconds. Fuel tank venting was initiated at 10 seconds. The simulation was performed at 104% RPL between 13 and 300 seconds. Figures 12 and 13 show the behavior of the LOX and fuel engine inlet pressures during venting and repressurization, respectively. Figures 14 through 20 show the signal behavior and signal limits of selected parameters during LOX/fuel tank venting and repressurization. Figures 18 and 19 show the HPOTP Boost Pump discharge pressure and LPFTP speed signals and signal limits. The fuel repressurization valve is closed at 250 seconds, at which time these parameters show 20 psi and 90 rpm step drops, respectively. Figure 20 shows the HEX Venturi delta-pressure signal and signal limits. The GOX repressurization valve is closed at 270 seconds, at which time the HEX Venturi delta-pressure drops by 68 psi.

(ii) Test 901-511

The thrust profile for this test is presented in Figure 21. The simulation was performed at 104% RPL between 13 and 410 seconds. Venting/repressurization of the LOX tank was performed twice during this test, at 80 seconds and at 295 seconds. Fuel tank venting was initiated at 10 seconds. The fuel and GOX repressurization valves were closed at 250 and 270 seconds, respectively. Figures 22 and 23 show the behavior of the LOX and fuel engine inlet pressures during venting and repressurization, respectively. Figures 24 through 29 show the signal behavior and signal limits of selected parameters during LOX tank venting/repressurization. In addition, Figures 28 and 29 show the signal limit adjustments made at the time of closing the fuel and GOX repressurization valves.

(iii) Test 901-551

The simulation of this test was performed between 70 and 395 seconds at 104% RPL. The thrust profile, presented in Figure 30 indicates LOX tank venting/repressurization was initiated at 80 seconds. Fuel tank venting was initiated at 10 seconds. The fuel and GOX repressurization valves were closed at 300 and 320 seconds, respectively. Figures 31 and 32 show the LOX and fuel engine inlet pressure signals. Figures 33 through 36 show the simulation results for selected parameters.

(iv) Test 901-683

The simulation of this test was performed between 70 and 330 seconds at 104% RPL. The thrust profile, shown in Figure 37, shows that LOX and fuel tank venting/repressurization was scheduled for 80 seconds and 10 seconds, respectively. The fuel and GOX repressurization valves were closed at 300 and 320 seconds, respectively. Figures 38 and 39 show the LOX and fuel engine inlet pressures. Figures 40, 41, and 43 show the simulation results of three parameters affected by LOX tank venting/repressurization Figures 42 and 43 show the effects on two parameters of closing the fuel and GOX repressurization valves.

(v) Test 902-519

The simulation of this test was performed between 69 and 395 seconds at 104% RPL. The thrust profile is shown in Figure 44. LOX tank venting/repressurization was initiated at 80 seconds. Fuel tank venting was initiated at 10 seconds. The fuel and GOX repressurization valves were scheduled closed at 300 and 320 seconds, respectively. Simulation results of selected parameters are shown in Figures 47 through 50.

(vi) Test 902-532

The thrust profile and venting schedules for this test were the same as for test 902-519 (Figure 51). The simulation was performed beginning at 69 seconds upon throttling to 104% RPL. The simulation results of selected parameters are presented in Figures 54 through 57.

(vii) Test 902-249

Test 902-249 involved failure of the HPFTP. Damage incurred includes HPFTP turbine blade damage and rupture of the volute. The test was shut down at 450.57 seconds due to a HPFTP radial accel redline. The anomaly report indicated that some anomalous behavior was apparent soon after start. Subsequent indicators included a drop in the HPFTP synchronous level at 162.9 seconds and a rise in one of the HPFP radial accels around 250 seconds.

The algorithm simulation was performed beginning at 12 seconds upon throttling to 109% RPL. Figure 58 shows the thrust profile. Figure 59 shows the LOX engine inlet pressure profile indicating initiation of venting at 20 seconds and repressurization at 95 seconds. Venting/repressurization of the fuel tank was not performed during this test.

Figures 60 through 66 present the profiles of the seven parameters for which the algorithm would detect anomalous behavior at the earliest time. By 329 seconds, three parameters exceeded their safety limits: the HPFTP coolant liner pressure (Figure 60), the HPOP intermediate seal purge pressure (Figure 61), and the HPFTP discharge temperature channel B (Figure 62). By 360 seconds, two additional parameters exceeded their safety limits: the HPFT discharge temperature channel A (Figure 63) and the fuel flowmeter (Figure 64). A sixth parameter, the FPOV actuator position, exceeded its safety limits at 374 seconds (Figure 65). A seventh parameter, the HPFP balance cavity pressure, exceeded its safety limits at 395 seconds (Figure 66). The algorithm would signal a shutdown 121 seconds earlier or 90 seconds earlier than the redline due to detection of anomalous behavior in three or five parameters, respectively.

(viii) Test 902-428

Test 902-428 involved failure of the OPB injector. The test was shut down at 204.12 due to a HPFTP discharge temperature redline. The algorithm simulation was performed beginning at 16 seconds upon throttling to 104% RPL. Figure 67 shows the thrust profile. Figures 68 and 69 show the fuel and LOX engine inlet pressure profiles. Fuel tank venting was initiated at 10 seconds. Venting/repressurization of the LOX

tank was initiated at 80 seconds. Closure of the fuel and GOX repressurization valves was scheduled beyond the time of the redline shutdown time. Nine of the algorithm parameters exceeded their safety limits. The HPOT discharge temperature 1 exceeded its limit the earliest at 168 seconds. By 190 seconds, three additional parameters had exceeded their safety limits, fourteen seconds earlier than the HPFTP discharge temperature redline. The profiles of four parameters which exceeded their safety limits that were also affected by LOX tank venting/repressurization are shown in Figures 70 through 73.

(ix) Test 901-364

Test 901-364 involved failure of the HPFTP. The test was shut down at 392.16 seconds due to a PBP radial accel redline. The algorithm simulation was performed beginning at seventy one seconds upon throttling to 109% RPL. Figure 74 shows the thrust profile. Figures 75 and 76 show the fuel and LOX engine inlet pressure profiles. Fuel tank venting was initiated at 100 seconds. Repressurization and venting of the LOX tank was initiated at 200 seconds. The failure occurred suddenly. Four of the algorithm parameters exceeded their safety limits. The HPFP speed exceeded its limit the earliest at 384 seconds. Three additional parameters exceeded their safety limits by 386 seconds, six seconds earlier than the PBP radial accel redline. Only three of the remaining algorithm parameters showed indications of the failure. These did not exceed their safety limits, however. The profiles of the four parameters which exceeded their limits are shown in Figures 77 through 80.

(x) Test 750-175

Test 750-175 involved a high pressure oxidizer duct rupture and was shut down at 116 seconds by a LOX preburner pump accel redline. The failure occurred suddenly and is apparent in only three of the algorithm controller parameters: the LPOP discharge pressure and the OPOV and FPOV actuator positions. Since the test was shut down by the redline shortly following initiation of the failure, the algorithm did not detect the failure earlier than the redline.

The algorithm simulation was performed over two power levels: 1) between 12 and 100 seconds at 109% RPL, and 2) between 102 and 115.6 seconds at 111% RPL. Figure 81 shows the thrust profile. Figures 82 through 87 show the simulation results

at the two consecutive thrust levels, 109% RPL and 111% RPL, for the HPFP speed, the LPOP discharge pressure, and the FPOV actuator position.

Venting/repressurization of the LOX tank was initiated at 10 seconds. The LOX tank venting effects could not be not simulated in the safety limits because data for the LOX tank inlet pressure (facility parameter) was only available at a sampling rate of 16 and 17 msec. This is an unusual sampling rate and is not compatible with the algorithm which requires facility data each 20 msec.

(xi) Test 901-183

A simulation was made of test 901-183 which involved a main injector failure. This test did not involve propellant tank venting procedures. The test was shut down at 51 seconds by a HPFP radial accel redline. The algorithm simulation was performed beginning at 5 seconds upon throttling to 92% RPL. The algorithm signalled a shutdown at 50.35 seconds due to detected anomalies in five parameters, 0.65 seconds earlier than the redline. The thrust profile is shown in Figure 88 The FPOV actuator position signal exceeded its safety limit the earliest at 50.234 seconds followed by the MCC chamber pressure at 50.275 seconds (Figures 89, 90). Three signals exceeded their safety limits at 50.355 seconds: the HPOTP discharge pressure, the PBP discharge pressure, and the fuel flow (Figures 91 through 93).

(xii) Test 901-173

Test 901-173 involved a main injector failure and was shut down at 201.17 seconds due to a HPFT discharge temperature redline. The thrust profile is shown in Figure 94. Pressurization of the fuel tank was performed at 90 seconds. Lox tank venting was scheduled at 460 seconds but was not performed due to the failure. The simulation was performed for both scheduled power levels of 70% RPL and 92% RPL. The simulation at 70% RPL was performed from 5 seconds to 100 seconds. The simulation at 92% was performed from 103 seconds to 201.16 seconds. The simulation resulted in a shutdown at 201.02 seconds due to detected anomalies in four parameters, 0.15 seconds earlier than the redline. Anomalies were first detected in the HPFTP discharge pressure at 165.67 seconds, the HPFTP radial accel at 176.18 seconds, and in the HPOTP discharge pressure and the HPFTP balance cavity pressure at 201.02 seconds. Since the failure was structural, the failure

occurred rapidly and therefore was detected by both the redline system and the algorithm fairly quickly. The four parameters which exceeded their safety limits are shown in Figures 95 through 102, for both power levels.

The gain values characterizing the LOX and fuel tank venting/repressurization effects for ten simulated tests are presented in Tables 4 and 5, respectively. These values represent the expected parameter change per increase in engine inlet pressure. Most of the signal gain values do not vary among the different tests, indicating fairly consistent behavior as a result of these facility processes from test to test. The LOX tank venting/repressurization gain value for the HPOT discharge temperature shows the most variation ranging from -1.0 to -1.8 degrees R per unit inlet increases in LOX tank pressure.

The signal step changes due to closing the GOX and fuel repressurization valves are summarized in Tables 6 and 7, respectively. The opposite effects result if these valves are opened. The resulting signal behavior showed virtually no variation from test to test, as indicated in the values of Tables 6 and 7.

Tables 8 through 13 present data used to compute the signal safety limits for the twelve simulated tests. The tables also indicate the power levels that were simulated for each test. Table 8 presents the estimated mean values used for the first instant check safety limits. Table 9 presents the mean values computed on-line over the first two-second duration of each power level. Tables 10 and 12 present the pre-computed SD values and the N1 factors, respectively, used for the first two-second interval failure detection safety limits. Tables 11 and 13 present the SD values computed on line and the N2 factors, respectively, used for the steady-state interval failure detection safety limits.

6.2.4 RTFC ALGORITHM ENHANCEMENTS

In addition to the code enhancements to model the effects of tank venting/repressurization and repressurization valve closure, several additions have been made to the algorithm code to enhance the safety limits and the shutdown criteria. These include the following:

1. A backup approach to compute, for a given parameter, the safety limit bandwidth during the nominal phase to be 75% of that during the initial two-second phase if (i) the on-line standard deviation value is computed to be near zero (i.e., 0.005 * pre-computed SD), or (II) the safety limit bandwidth is computed to be larger during the nominal phase than during the initial two-second phase;

2. Logic to provide that if a sensor reading is zero or negative for any parameter, that parameter is eliminated from the algorithm computations and will not be a factor in signaling a shut down; and

3. The comparison of the HPFP and the PBP radial accelerometer signals to upper safety limits only since these parameters are not constrained to a minimum value for nominal operating behavior.

6.3 LESSONS LEARNED

During the course of the present contract, several features of the SSME were investigated in detail. Information, useful for future failure detection algorithm development, was analyzed and recorded. Thus, transient effects other than the start and power transients, were found to significantly influence parameter values. If these effects are not compensated for, the failure detection algorithm will lose some of its sensitivity to failures and thus be more sluggish. Nonlinear behavior of several SSME parameters, inherent to engine characteristics, need to be addressed. These effects were termed nonlinear because of the characteristic shape that each parameter takes in time even in the absence of any venting/repressurization or other transient phenomena. For example, it takes over 75 seconds for the HPOT turbine discharge temperature, the MCC liner cavity pressure, and the HPOT secondary seal cavity pressure to reach steady state. The HPOP intermediate seal purge pressure requires nearly 200 seconds to reach steady state (Reference 15). Figures 103 through 106 present some parameters exhibiting this type of behavior.

If these parameters are to be monitored, then it is necessary to develop estimates of their nominal mean values for piecewise linear intervals or define functions representative of the nominal signal behavior. If the signal behavior can be closely represented, then the safety band around it can be made smaller resulting in increased algorithm sensitivity.

Start and power transients are the most difficult areas to be tackled. However, the power transients seem to be relatively easier to track. Hence, the plan for the next phase is to study and modify the power transients.

7. CONCLUSION

Extensive computer simulations with the RTFCA on real SSME incident and nominal test data indicate significantly earlier cutoffs than achieved with the existing redline system. Cutoffs were found to be a function of the kind of failure that occurred, the speed with which it progressed and the location and degree of localization of the anomalies. In fast occurring failures, such as ruptures or breakage of structural areas, the RTFCA resulted in only slight gains over the redlines. For slow occurring failures, however, the RTFCA showed significantly earlier shutdown capability.

Two factors are important in the decision for engine cutoff. Firstly, the performance of the RTFCA depends heavily on the choice of the weighting factor (N) that determines the bandwidth of the safety limits placed around the average value of each monitored signal. Secondly, the algorithm's performance depends on the gain values required for the signal limit adjustments needed in simulating repressurization and venting effects. Moreover, the algorithm has a requirement for multiple anomalous signals prior to signaling an engine cutoff command. This number should be predetermined prior to each test. There is presently no procedure for the selection of these factors other than experience and trial and error. However, work has been performed on finding ways of automatically determining these numbers at the start of the algorithm during a test.

The RTFCA, as it currently stands, can handle steady-state test operating conditions and repressurization and venting conditions. It is turned off during the start transient, as well as during power transients. However, the first instant check that the algorithm is equipped with (that checks the value of each of the first incoming measurement signals against a pre-computed nominal expected value) is for detection of anomalous behavior that might have occurred during a transient. This feature provides some degree of fault detection capability at start or power transients. Moreover, the option of expanding the capability to handle transients, as well as other nonlinear behavior and excursions, are under consideration and plans for such augmentation exist. The algorithm monitors more parameters than the redlines, with the option of expanding the list even further. Also, the RTFCA avoids "false alarms" by the above mentioned requirement for multiple simultaneous anomalous signals prior to a decision for engine shutdown.

The current algorithm does not encompass an approach for sensor failure detection with the exceptions of zero and negative sensor readings. These and other limitations of the RTFC can be addressed and its effectiveness and scope can be enhanced given appropriate planning, analyses, simulations, and judicious approaches.

8. RECOMMENDATIONS

By all means, it is highly desirable to develop a failure detection algorithm for the SSME that can operate under all conditions (steady-state and transient) and that is sensitive enough to detect slow and fast occurring failures at such an early stage that damage to the engine is minimized. There are certain approaches that, if taken, can lead to the above mentioned enhanced and expanded algorithm. In this section a few tasks are outlined that will accomplish some of the enhancements.

8.1 FAILURE DETECTION

The fault detection problem involves a thorough and realistic understanding and specification of the given system. The various failure modes that may occur can be described as either fast occurring and progressing or as incipient (slow developing) faults. Fault detection is approached either via model-based or signal-based techniques. For analytical redundancy purposes some kind of validation of nominal relationships of the given system, using the actual input and the measured output, are carried out and the dynamics of the system are evaluated on-line in a real-time manner.

Most advanced fault detection schemes suffer from complexity and often from inherent weakness in reliability. However, it is usually possible to develop simple fault detection schemes that do not require extensive analytical development and that work reliably and efficiently. Such an approach involves the use of the SSME DTM.

Analytical redundancy, especially when applied to key engine parameters, can provide significant reliability and enhanced performance, especially under sensor failures. A good analytical model of the engine is required that can predict the expected outputs very closely (to that of the actual values) and thus provide analytical values to compare actual outputs with and make a decision regarding the status of the sensor. The SSME DTM is a very effective tool that can be utilized for such analytical redundancy purposes (perhaps piecewise linearization will be required in order to make it real-time on-line applicable). There are many key sensors that need such redundancy and that when implemented can enhance engine performance, avoid engine shutdowns due to false alarms, and that can minimize damage from failures.

8.2 SENSOR FAILURE DETECTION

Throughout the history of the Space Shuttle program, the only SSME in-flight shutdown occurred during flight 51F July 30, 1985, due to the malfunction of the HPFT discharge temperature sensors. This type of failure can be easily avoided given a good (simple) sensor failure detection approach.

Such an approach was evaluated using the information from past engine data as well as simulations via the SSME DTM. It is clearly indicated in the sensor outputs from flight 51F (Reference 15) that the only parameters that showed anomalous behavior were the two HPFT discharge temperature sensors, while all the other parameters were nominal. This is sufficient cause to believe that it is a sensor failure. A change in any one of the SSME parameters, results in a corresponding change in each of the other sensor outputs. Thus, sensor outputs can be correlated in such a manner as to generate useful information regarding the status of sensors.

The implementation of such a scheme is straight forward, does not require extensive computational effort, and can significantly enhance the performance of the SAFD algorithm.

8.3 RTFC PERFORMANCE ENHANCEMENTS

In accordance with the observations made in the previous pages, it is highly recommended that work be continued on the RTFC algorithm development and enhancements directed towards expanding the capabilities of the algorithm. These expansions should address RTFC operation during start and power transients, and accommodations and compensations for nonlinear effects. In addition, sensor failure detection schemes should be simulated that are simple and easy to implement in order to study their feasibility and effectiveness.

The capability exists at Rocketdyne to evaluate the SSME from a systems point of view and develop failure detection schemes based on practical implementation and feasibility issues and formulated on sound mathematical and advanced fault detection knowledge. Advanced observer-based estimation routines can be utilized, using the DTM, that can provide analytical redundancy and enhanced failure detection capability. Various options have already been studied and their feasibility has been evaluated.

This useful effort should continue without the slow-down of unnecessary contractual breaks in order to have the engineers devote their full attention to the important task of SSME failure detection.

9. REFERENCES

1. R. Isermann, "Process Fault Detection Based on Modeling and Estimation Methods. A survey," Automatica, Vol. 20, pp. 387-409, 1984.

2. A. S. Willsky, "A survey of Design Methods for Failure Detection in Dynamic Systems," Automatica, Vol. 12, pp. 601-611, 1976.

3. E. Y. Shapiro, H. V. Panossian, "Analytical Redundancy for Aircraft Flight Control Sensors," NATO/AGARD, 43rd Symposium on Advanced Guidance and Control Systems Technology, pp. 53-1, 53-20, England, October, 1986.

4. H. V. Panossian, "Algorithms for System Fault Detection through Modeling and Estimation Techniques," Control and Dynamics Systems, C. T. Leondes (Ed.), Academic Press, NY, pp. 47-66, 1988.

5. H. L. Jones, "Failure Detection in Linear Systems," Ph.D. Thesis, MIT, Department of Aeronautics and Astronautics, Cambridge, Mass., 1973.

6. T. Weiss, et al, "Robust Detection/Isolation Accommodation for Sensor Failures - Final Report," NASA-CR-164797, NA53-24078, September, 1984.

7. J. J. Gertler, "Survey of Model Based Failure Detection and Isolation in Complex Plants," IEEE Control Systems Magazine, Vol. 8, pp. 3-11, 1988.

8. H. V. Panossian, "Stochastic Optimal Linear Feedback Control Systems Using Available Measurements," Journal of Optimization Theory and Application, Vol. 7, pp. 248-250, 1984.

9. H. Panossian, "State and Parameter Estimation in Electrohydraulic Actuation Systems for Failure Analysis," Proceedings of International Symposium on Test and Failure Analysis, Long Beach, CA, pp. 228-231, 1975

10. J. W. Willsky, "Failure Detection in Dynamic Systems," NATO AGARD-ograph No. 190, 1980.

11. W. C. Merrill, "Sensor Failure Detection for Jet Engines Using Analytical Redundancy," J. Guidance, Vol. 8, No. 6, pp. 517-526, 1988.

12. W. C. Merrill, J. C. DeLaat, and W. M. Bruton, "Advanced Detection, Isolation, and Accommodation of Sensor Failures-Real-Time Evaluation," J. Guidance, Vol. 11, No. 6, pp. 517-526, 1988.

13. M. H. Taniguchi, RI/RD 87-109, "Failure Control Techniques for the SSME," NAS8-36305, Phase II final report, Rockwell International, Rocketdyne Division, Canoga Park, CA, 1988.

14. M. H. Taniguchi, RI/RD 87-109, "SSME Failure Mode and Effects Analysis and Initial Items List," Rockwell International, Rocketdyne Division, Canoga Park, CA, 1988.

15. H.V. Panossian, V.R. Kemp and S.J. Eckerling, "Real-Time Failure Control" Final Report, July 1990, RSS-8826-12, NAS8-4000.

16. H.V. Panossian, V.R. Kemp and S.J. Eckerling, SSME Real-Time Failure Detection Algorithm", NASA< MFSC, Advanced Earth-to-Orbit Propulsion Conference, Huntsville, AL, May 15-17, 1990.

17. H.V. Panossian, V.R. Kemp, R. Nelson and M. Taniguchi, "Real-Time Fault Detection Algor. for the SSME", 26th Joint Propulsion Conference, Orlando, FL., July 16-18, 1990.

18. H.V. Panossian, V.R. Kemp, "A Signal-Based Approach to Failure Detection of the SSME", Int'l Machine Monitoring and Diagnostic Conference, Los Angeles, CA, Oct. 22-25, 1990.

19. H.V. Panossian, V.R. Kemp, "Real-Time Fault Detection of the SSME". IEEE Conference on Decision & Control, Brighton, England, Dec. 1991.

20. H.V. Panossian, V.R. Kemp, "Accommodations of Repressurization and Venting Effects in the SSME Real-Time Failure Control Algorithm", NASA, MFSC, Advanced Earth-to-Orbit Propulsion Conference, May, 1992.

APPENDIX I.

Tables

TABLE 1.
SIMULATED TESTS DURING 1991-1992

1. 902-398	7. 902-249
2. 901-511	8. 902-428
3. 901-551	9. 901-364
4. 901-683	10. 750-175
5. 902-519	11. 901-183
6. 902-532	12. 901-173

TABLE 2.

PRELIMINARY ESTIMATES OF SSME REPRESSURIZATION/VENTING AND VALVE CLOSURE/OPENING EFFECTS ON ENGINE PARAMETERS AT 104% RPL

NO.	PARAMETER NAME	PID NUMBER	FUEL VENTING	LOX VENTING	LOX REPRESS.	FUEL VALVE OPEN	FUEL VALVE CLOSE	GOX VALVE CLOSE
1	HPFTP SPEED	260-261,764	NE	NE	NE	NE	NE	NE
2	HPFTP T. DIS. TEMP	231-232	NE	NEGLIGABLE	0.5	NE	NE	NE
3	HPFTP DIS. PRESS.	52,152	NE	+0.25 PSI/PSI	-0.25 PSI/PSI	NE	NE	NE
4	HPFTP RAD. ACCEL	1981-85	+0.07 g/PSI	NE	NE	NE	NE	NE
5	HPFTP CL. LNR. PR.	53,54	NE	NE	NE	NE	NE	NE
6	HPFTP BAL. CAV. PR.	457	NE	NE	NE	NE	NE	NE
7	HPOTP DIS. PRESS.	90	NE	NE	NE	NE	NE	NE
8	HPOTP T. DIS. TEMP.	233,234	NE	+1.1 °F/PSI	-0.68 °F/PSI	NE	NE	NE
9	HPOTP INT. SEAL PUR. PRESS.	211,212	NE	NE	NE	NE	NE	NE
10	HPOTP SEC. SEAL DR. PRESS.	91-92	NE	NE	NE	NE	NE	NE
11	HPOTP BOOSTPUMP DIS. PR. (PBP DIS. PR.)	59,159,341	NE	+1 PSI/PSI	-1 PSI/PSI	+20PSI	-20PSI	NE
12	HPOTP BOOSTPUMP RAD.ACCEL (PBP RAD ACCEL)	1994-1996	NE	NE	NE	NE	NE	NE
13	HPOTP BOOSTPUMP BRNG COOL. DIS. TEMP.	183,8251,8255	NE	NE	NE	NE	NE	NE
14	LPFTP SPEED	32,754,735	+3.7 RPM/PSI	+0.85 RPM/PSI	-0.6 RPM/PSI	+90RPM	-90RPM	NE
15	LPOTP DIS. PR.	302	NE	-0.83 PSI/PSI	+0.9 PSI/PSI	NE	NE	NE
16	HEX VENT DP	883,8352	NE	+0.07 PSI/PSI	-0.078 PSI/PSI	NE	NE	-68PSI
17	HEX INTERFACE TEMP.	252,8359	NE	NE	-1° F/PSI	NE	NE	NE
18	MCC PRESS	129,130	NE	NE	NE	NE	NE	NE
19	MCC LINK CAV PRESS.	1951	NE	NE	NE	NE	NE	NE
20	OPOV ACT POSIT.	40	NE	+0.022%/PSI	-0.017%/PSI	NE	NE	NE
21	FPOV ACT. POS.	42	NE	-0.015%/PSI	+0.007%/PSI	NE	NE	NE
22	FUEL FLOW	251,253,721 258,133,722	NE	NE	NE	NE	NE	NE

TABLE 3.
POWER BALANCE MODEL GAINS FOR +1 PSI LOX INLET PRESSURE

PID NO.	PARAM. NO.	PARAM. TITLE	GAINS 109%PL	104%PL	100%PL
260,261	4360	HPFP SPEED	-0.1618	-0.1791	-0.1887
231,232	4629	HPFT DIS T	0.0997	0.1068	0.1122
233,234	4638	HPOT DIS T	-0.3945	-0.4135	-0.4253
52	4902	HPFP DIS P	-0.1000	-0.0996	-0.0978
90	4903	HPOP DIS P	0.0015	0.0014	0.0013
59	4915	PBP DIS PR	-0.4435	-0.4406	-0.4439
32	4359	LPFP SPEED	-0.2488	-0.2529	-0.2530
302	4912	LPOP DIS P	0.8833	0.8810	0.8799
40	4798	OPOV POS	-0.0001	-0.0001	-0.0001
42	4799	FPOV POS	0.0001	0.0001	0.0001
129,130	4079	MCC PC	0.0	0.0	0.0
251,253	4542	FUEL VOL F1	0.0	0.0	0.0

Table 4.
LOX Venting/Repressurization Gain Values

TEST NO.		902-398	901-511	901-551	901-683	902-519	902-532	902-428	902-249	901-364	750-175
P.L. (%RPL)		104	104	104	104	104	104	104	109	109	109, 111
I.D. NO.	PARAMETER										
1	HPFP RAD ACCEL (GRMS)	NE	NE	NE	NE	NE	NE	NE	NE	NE	NE
2	HPFP BAL CAV PRES (PSIG)	NE	NE	NE	NE	NE	NE	NE	NE	NE	NE
3	HPOP DIS PRES (PSIA)	NE	NE	NE	NE	NE	NE	NE	NE	NE	NE
4	HPOP IMSL PURGE PRES (PSIA)	NE	NE	NE	NE	NE	NE	NE	NE	NE	NE
5	HPOP SEC SEAL CAV PRES (PSIA)	NE	NE	NE	NE	NE	NE	NE	NE	NE	NE
6	PBP DIS PRES (PSIA)	-2	-1	-1	-1.2	-1	-2	-1	-2	-2	-2
7	PBP RAD ACCEL (GRMS)	NE	NE	NE	NE	NE	NE	NE	NE	NE	NE
8	PBP BEAR CLNT DIS TEMP (DEG R)	NE	NE	NE	NE	NE	NE	NE	NE	NE	NE
9	MCC PRES (PSIA)	NE	NE	NE	NE	NE	NE	NE	NE	NE	NE
10	MCC CAV LNR PRES (PSIG)	NE	NE	NE	NE	NE	NE	NE	NE	NE	NE
11	HPFP SPEED (RPM)	NE	NE	NE	NE	NE	NE	NE	NE	NE	NE
12	HPFT DS T1 A (DEG R)	0.6	0.2	0.5	0.3	0.5	0.3	0.2	0.6	0.4	0.4
13	HPFT DS T1 B (DEG R)	0.6	0.2	0.5	0.3	0.5	0.5	0.2	0.6	0.4	0.4
14	HPOT DS T1 (DEG R)	-1.2	-1	-1	-1.2	-1	-1.8	-0.8	-1.2	-1.2	-1.2
15	HPOT DS T2 (DEG R)	-1.2	-1	-1	-1.2	-1	-1.8	-0.8	-1.2	-1.2	-1.2
16	LPFP SPEED (RPM)	NE	NE	NE	NE	NE	NE	NE	NE	NE	NE
17	LPOP DIS PRES (PSIA)	1.4	1.4	1.4	1.4	1.4	1.2	1.4	1.4	1.4	1.4
18	HPFT DIS PRES (PSIA)	-0.25	-0.25	-0.25	-0.25	-0.25	-0.25	N/A	N/A	N/A	NE
19	HPFP CLNT LNR PRES (PSIA)	NE	NE	NE	NE	NE	NE	NE	NE	NE	NE
20	HEX INT TEMP (DEG F)	-1	-0.4	-1	-1	-1	-1	-1.2	-1.2	-0.6	-0.6
21	HEX VENT DP (PSIG)	-0.078	-0.078	-0.078	-0.078	-0.078	-0.068	-0.02	-0.068	-0.03	NE
22	OPOV ACT POS (PCNT)	-0.022	-0.022	-0.022	-0.022	-0.022	-0.015	-0.001	-0.015	-0.015	-0.015
23	FPOV ACT POS (PCNT)	0.014	0.014	0.014	0.014	0.014	0.014	0.001	0.016	0.016	0.016
24	FUEL FLOW (GPM)	NE	NE	NE	NE	NE	NE	NE	NE	NE	NE

N/A - not available
NE - no effect

Table 5.
Fuel Venting/Repressurization Gain Values

TEST NO.		902-398	901-511	901-551	901-683	902-519	902-532	902-428	902-249	901-364	901-173
P.L. (%RPL)		104	104	104	104	104	104	104	109	109	70, 92
I.D. NO.	PARAMETER										
1	HPFP RAD ACCEL (GRMS)	NE	NE	NE	NE	NE	NE	NE	NE	NE	NE
2	HPFP BAL CAV PRES (PSIG)	NE	NE	NE	NE	NE	NE	NE	NE	NE	NE
3	HPOP DIS PRES (PSIA)	NE	NE	NE	NE	NE	NE	NE	NE	NE	NE
4	HPOP IMSL PURGE PRES (PSIA)	NE	NE	NE	NE	NE	NE	NE	NE	NE	NE
5	HPOP SEC SEAL CAV PRES (PSIA)	NE	NE	NE	NE	NE	NE	NE	NE	NE	NE
6	PBP DIS PRES (PSIA)	NE	NE	NE	NE	NE	NE	NE	NE	NE	NE
7	PBP RAD ACCEL (GRMS)	NE	NE	NE	NE	NE	NE	NE	NE	NE	NE
8	PBP BEAR CLNT DIS TEMP (DEG R)	NE	NE	NE	NE	NE	NE	NE	NE	NE	NE
9	MCC PRES (PSIA)	NE	NE	NE	NE	NE	NE	NE	NE	NE	NE
10	MCC CAV LNR PRES (PSIG)	NE	NE	NE	NE	NE	NE	NE	NE	NE	NE
11	HPFP SPEED (RPM)	NE	NE	NE	NE	NE	NE	NE	NE	NE	NE
12	HPFT DS T1 A (DEG R)	NE	NE	NE	NE	NE	NE	NE	NE	NE	NE
13	HPFT DS T1 B (DEG R)	NE	NE	NE	NE	NE	NE	NE	NE	NE	NE
14	HPOT DS T1 (DEG R)	NE	NE	NE	NE	NE	NE	NE	NE	NE	NE
15	HPOT DS T2 (DEG R)	NE	NE	NE	NE	NE	NE	NE	NE	NE	NE
16	LPFP SPEED (RPM)	-3.7	-3.7	-3.7	-3.7	-3.7	-3.7	-3.7	-3.7	-3.7	-3.7
17	LPOP DIS PRES (PSIA)	NE	NE	NE	NE	NE	NE	NE	NE	NE	NE
18	HPFT DIS PRES (PSIA)	NE	NE	NE	NE	NE	NE	NE	NE	NE	NE
19	HPFP CLNT LNR PRES (PSIA)	NE	NE	NE	NE	NE	NE	NE	NE	NE	NE
20	HEX INT TEMP (DEG F)	NE	NE	NE	NE	NE	NE	NE	NE	NE	NE
21	HEX VENT DP (PSIG)	NE	NE	NE	NE	NE	NE	NE	NE	NE	NE
22	OPOV ACT POS (PCNT)	NE	NE	NE	NE	NE	NE	NE	NE	NE	NE
23	FPOV ACT POS (PCNT)	NE	NE	NE	NE	NE	NE	NE	NE	NE	NE
24	FUEL FLOW (GPM)	NE	NE	NE	NE	NE	NE	NE	NE	NE	NE

N/A - not available
NE - no effect

Table 6.
GOX Repressurization Valve Closure Effects

TEST NO.		902-398	901-511	901-551	901-683	902-519	902-532	902-428	902-249	901-364
P.L. (%RPL)		104	104	104	104	104	104	104	109	109
I.D. NO.	PARAMETER									
1	HPFP RAD ACCEL (GRMS)	NE	NE	NE	NE	NE	NE	NE	NE	NE
2	HPFP BAL CAV PRES (PSIG)	NE	NE	NE	NE	NE	NE	NE	NE	NE
3	HPOP DIS PRES (PSIA)	NE	NE	NE	NE	NE	NE	NE	NE	NE
4	HPOP IMSL PURGE PRES (PSIA)	NE	NE	NE	NE	NE	NE	NE	NE	NE
5	HPOP SEC SEAL CAV PRES (PSIA)	NE	NE	NE	NE	NE	NE	NE	NE	NE
6	PBP DIS PRES (PSIA)	NE	NE	NE	NE	NE	NE	NE	NE	NE
7	PBP RAD ACCEL (GRMS)	NE	NE	NE	NE	NE	NE	NE	NE	NE
8	PBP BEAR CLNT DIS TEMP (DEG R)	NE	NE	NE	NE	NE	NE	NE	NE	NE
9	MCC PRES (PSIA)	NE	NE	NE	NE	NE	NE	NE	NE	NE
10	MCC CAV LNR PRES (PSIG)	NE	NE	NE	NE	NE	NE	NE	NE	NE
11	HPFP SPEED (RPM)	NE	NE	NE	NE	NE	NE	NE	NE	NE
12	HPFT DS T1 A (DEG R)	NE	NE	NE	NE	NE	NE	NE	NE	NE
13	HPFT DS T1 B (DEG R)	NE	NE	NE	NE	NE	NE	NE	NE	NE
14	HPOT DS T1 (DEG R)	NE	NE	NE	NE	NE	NE	NE	NE	NE
15	HPOT DS T2 (DEG R)	NE	NE	NE	NE	NE	NE	NE	NE	NE
16	LPFP SPEED (RPM)	NE	NE	NE	NE	NE	NE	NE	NE	NE
17	LPOP DIS PRES (PSIA)	NE	NE	NE	NE	NE	NE	NE	NE	NE
18	HPFT DIS PRES (PSIA)	NE	NE	NE	NE	NE	NE	NE	NE	NE
19	HPFP CLNT LNR PRES (PSIA)	NE	NE	NE	NE	NE	NE	NE	NE	NE
20	HEX INT TEMP (DEG F)	NE	NE	NE	NE	NE	NE	NE	NE	NE
21	HEX VENT DP (PSIG)	-68	-68	-68	-68	-68	-68	N/A	N/A	N/A
22	OPOV ACT POS (PCNT)	NE	NE	NE	NE	NE	NE	NE	NE	NE
23	FPOV ACT POS (PCNT)	NE	NE	NE	NE	NE	NE	NE	NE	NE
24	FUEL FLOW (GPM)	NE	NE	NE	NE	NE	NE	NE	NE	NE

N/A - not available
NE - no effect

Table 7.
Fuel Repressurization Valve Closure Effects

TEST NO.		902-398	901-511	901-551	901-683	902-519	902-532	902-428	902-249	901-364
P.L. (%RPL)		104	104	104	104	104	104	104	109	109
I.D. NO.	PARAMETER									
1	HPFP RAD ACCEL (GRMS)	NE	NE	NE	NE	NE	NE	NE	NE	NE
2	HPFP BAL CAV PRES (PSIG)	NE	NE	NE	NE	NE	NE	NE	NE	NE
3	HPOP DIS PRES (PSIA)	NE	NE	NE	NE	NE	NE	NE	NE	NE
4	HPOP IMSL PURGE PRES (PSIA)	NE	NE	NE	NE	NE	NE	NE	NE	NE
5	HPOP SEC SEAL CAV PRES (PSIA)	NE	NE	NE	NE	NE	NE	NE	NE	NE
6	PBP DIS PRES (PSIA)	-20	-20	-20	-20	-20	-20	N/A	N/A	N/A
7	PBP RAD ACCEL (GRMS)	NE	NE	NE	NE	NE	NE	NE	NE	NE
8	PBP BEAR CLNT DIS TEMP (DEG R)	NE	NE	NE	NE	NE	NE	NE	NE	NE
9	MCC PRES (PSIA)	NE	NE	NE	NE	NE	NE	NE	NE	NE
10	MCC CAV LNR PRES (PSIG)	NE	NE	NE	NE	NE	NE	NE	NE	NE
11	HPFP SPEED (RPM)	NE	NE	NE	NE	NE	NE	NE	NE	NE
12	HPFT DS T1 A (DEG R)	NE	NE	NE	NE	NE	NE	NE	NE	NE
13	HPFT DS T1 B (DEG R)	NE	NE	NE	NE	NE	NE	NE	NE	NE
14	HPOT DS T1 (DEG R)	NE	NE	NE	NE	NE	NE	NE	NE	NE
15	HPOT DS T2 (DEG R)	NE	NE	NE	NE	NE	NE	NE	NE	NE
16	LPFP SPEED (RPM)	-90	-90	-90	-90	-90	-90	N/A	N/A	N/A
17	LPOP DIS PRES (PSIA)	NE	NE	NE	NE	NE	NE	NE	NE	NE
18	HPFT DIS PRES (PSIA)	NE	NE	NE	NE	NE	NE	NE	NE	NE
19	HPFP CLNT LNR PRES (PSIA)	NE	NE	NE	NE	NE	NE	NE	NE	NE
20	HEX INT TEMP (DEG F)	NE	NE	NE	NE	NE	NE	NE	NE	NE
21	HEX VENT DP (PSIG)	NE	NE	NE	NE	NE	NE	NE	NE	NE
22	OPOV ACT POS (PCNT)	NE	NE	NE	NE	NE	NE	NE	NE	NE
23	FPOV ACT POS (PCNT)	NE	NE	NE	NE	NE	NE	NE	NE	NE
24	FUEL FLOW (GPM)	NE	NE	NE	NE	NE	NE	NE	NE	NE

N/A - not available
NE - no effect

Table 8.
Pre-Computed Average Values

TEST NO.		902-398	901-511	901-551	901-683	902-519	902-532	902-428	902-249	901-364	750-175	750-175	901-183	901-173	901-173
P.L. (%RPL)		104	104	104	104	104	104	104	109	109	109	111	92	70	92
LD. NO.	PARAMETER														
1	HPFP RAD ACCEL (GRMS)	4.91	4.91	4.91	4.91	4.91	4.91	4.91	5.12	5.12	5.12	5.12	3.04	1.5	5.1
2	HPFP BAL CAV PRES (PSIG)	4975	4810	4810	4810	4880	4880	4810	5078				4203	3160	4070
3	HPOP DIS PRES (PSIA)	4090	4090	4090	4090	4090	4090	4090	4300	4300	4300	4300	3800	2895	3700
4	HPOP IMSL PURGE PRES (PSIA)	230	230	230	230	230	230	230	246	246	246	246	228	449	448
5	HPOP SEC SEAL CAV PRES (PSIA)	23	23	23	23	23	23	23	20.5	20.5	20.5	20.5	N/A	N/A	N/A
6	PBP DIS PRES (PSIA)	7489	7489	7489	7489	7489	7489	7489	7757	7757	7757	7757	6300	4850	6260
7	PBP RAD ACCEL (GRMS)	2.2	2.2	2.2	2.2	2.2	2.2	2.2	2.68	2.68	2.68	2.68	1.44	2.5	3.15
8	PBP BEAR CLNT DIS TEMP (DEG R)	N/A	N/A	N/A	N/A	N/A	N/A	N/A	N/A	N/A	N/A	N/A	N/A	N/A	N/A
9	MCC PRES (PSIA)	3127	3127	3127	3127	3127	3127	3127	3260	3260	3260	3260	2700	2070	2720
10	MCC CAV LNR PRES (PSIG)	-5	7.8	7.8	-5	-10	-10	7.8	-5	-5	-5	-5	N/A	N/A	N/A
11	HPFP SPEED (RPM)	35100	35320	35320	35320	35100	35100	35320	36800	36800	36800	36800	33500	28800	33150
12	HPFT DS T1 A (DEG R)	1702	1702	1702	1702	1702	1702	1702	1800	1800	1800	1800	1600	1550	1730
13	HPFT DS T1 B (DEG R)	1665	1665	1665	1665	1665	1665	1665	1850	1900	1900	1900	1600	1780	1880
14	HPOT DS T1 (DEG R)	1300	1426	1426	1426	1300	1450	1426	1293	1293	1293	1293	1142	1290	1370
15	HPOT DS T2 (DEG R)	1500	1500	1500	1500	1350	1450	1500	1368	1368	1368	1368	1194	1240	1280
16	LPFP SPEED (RPM)	16120	16120	16120	16120	15900	15400	16120	15500	15900	15900	15900	15600	13250	14400
17	LPOP DIS PRES (PSIA)	348	348	348	348	348	348	348	381	325	325	325	364	340	360
18	HPFT DIS PRES (PSIA)	6150	6150	6150	6150	6150	6000	6150	6800	6800	6800	6800	5550	4140	5360
19	HPFP CLNT LNR PRES (PSIA)	3442	3442	3442	3442	3442	3442	3442	3648	3648	3648	3648	N/A	N/A	N/A
20	HEX INT TEMP (DEG F)	820	205	205	205	800	800	N/A	800	800	800	800	650	660	780
21	HEX VENT DP (PSIG)	115	115	115	115	115	115	115	60	130	N/A	N/A	100	68	88
22	OPOV ACT POS (PCNT)	66	66	66	66	66	66	66	69.1	69.1	69.1	69.1	64	61	73
23	FPOV ACT POS (PCNT)	78	78	78	78	78	78	78	85.49	85.49	85.49	85.49	79.26	71	81.25
24	FUEL FLOW (GPM)	16220	16220	16220	16220	16220	16220	16220	16960	16960	16960	16960	14500	10700	14150

N/A - not available

Table 9.
On-Line Computed Average Values

TEST NO.		902-398	901-511	901-551	901-683	902-519	902-532	902-428	902-249	901-364	750-175	750-175	901-183	901-173	901-173
P.L. (%RPL)		104	104	104	104	104	104	104	109	109	109	111	92	70	92
LD. NO.	PARAMETER														
1	HPFP RAD ACCEL (GRMS)	1.04	2.13	2.59	3.65	0.721	1.41	4.914	10.62	3.36	N/A	N/A	6.5	1.3	4.5
2	HPFP BAL CAV PRES (PSIG)	4971	4924	4880	4787	4920	4861	4812	5041	N/A	N/A	N/A	4165	3172	4065
3	HPOP DIS PRES (PSIA)	4100	4075	4075	4015	4045	4130	4089	4407	4322	4305	4400	3662	2891	3708
4	HPOP IMSL PURGE PRES (PSIA)	221.5	235	245	229	236	224	231	218	303	231	274	277	448	448
5	HPOP SEC SEAL CAV PRES (PSIA)	22.3	24.9	20	20	16.5	16.02	22.2	33	21	25.9	16.8	N/A	N/A	N/A
6	PBP DIS PRES (PSIA)	7327	7225	7377	7225	7380	7267	7487	7929	7807	7881	8078	6413	4905	6243
7	PBP RAD ACCEL (GRMS)	2.1	2.34	2.43	1.82	1.65	3.14	2.16	4.96	5.43	N/A	N/A	2.2	2.5	2.9
8	PBP BEAR CLNT DIS TEMP (DEG R)	n/a	n/a	n/a	n/a	n/a	n/a	n/a	n/a	n/a	N/A	N/A	N/A	N/A	N/A
9	MCC PRES (PSIA)	3127	3129	3136	3122	3123	3123	3128	3290	3272	3270	3330	2756	2078	2717
10	MCC CAV LNR PRES (PSIG)	-5.9	-5.7	-8.3	-9.07	-10.1	-9.9	-7.28	-5	-11.1	N/A	N/A	N/A	N/A	N/A
11	HPFP SPEED (RPM)	35003	34951	35001	35089	34977	34945	35323	37209	36876	36454	36888	33320	28564	33117
12	HPFT DS T1 A (DEG R)	1616	1650	1677	1738	1713	1673	1697	1606	1779	1631	1860	1624	1537	1736
13	HPFT DS T1 B (DEG R)	1689	1673	1711	1765	1743	1691	1661	1672	1911	1751	1773	1588	1753	1874
14	HPOT DS T1 (DEG R)	1309	1367	1293	1396	1294	1357	1421	1344	1306	758	760	1151	1345	1364
15	HPOT DS T2 (DEG R)	1414	1406	1301	1365	1316	1378	1502	1344	1368	762	762	1082	1300	1285
16	LPFP SPEED (RPM)	16086	15819	15472	15708	15843	15882	16120	15460	15919	16230	16407	15535	13248	14388
17	LPOP DIS PRES (PSIA)	334	353	342	344	343	350	348	380	321	333	296	354	339	359
18	HPFT DIS PRES (PSIA)	6165	6134	6163	6038	6192	6115	6149	6829	6722	6599	6757	5552	4149	5360
19	HPFP CLNT LNR PRES (PSIA)	3417	3409	3427	3382	3448	3426	3435	3700	3699	N/A	N/A	N/A	N/A	N/A
20	HEX INT TEMP (DEG F)	827	801	908	897	800	835	n/a	788	781	N/A	N/A	671	657	777
21	HEX VENT DP (PSIG)	112	121	121	124	117	121	115	58.7	127	N/A	N/A	97	67.9	87
22	OPOV ACT POS (PCNT)	65.5	66.6	64.8	66.8	65.6	67.9	65.79	66.8	72	72	73	64	62.1	74.2
23	FPOV ACT POS (PCNT)	80.2	80.3	80.7	80.02	79.3	79.2	78.44	86.4	85.5	82	83	77	70.4	81.5
24	FUEL FLOW (GPM)	16054	16031	16017	16158	16032	16084	16216	17065	17085	16787	17071	14660	10650	14155

N/A - not available

Table 10.
Pre-Computed Standard Deviation Values

TEST NO.		902-398	901-511	901-551	901-683	902-519	902-532	902-428	902-249	901-364	750-175	750-175	901-183	901-173	901-173
P.L. (%RPL)		104	104	104	104	104	104	104	109	109	109	111	92	70	92
I.D. NO.	PARAMETER														
1	HPFP RAD ACCEL (GRMS)	3	3	3	3	3	3	3	3	3	3	3	1	3	3
2	HPFP BAL CAV PRES (PSIG)	15.07	15.07	15.07	15.07	15.07	15.07	15.07	15.07	15.07	15.07	15.07	15.07	70	70
3	HPOP DIS PRES (PSIA)	24.53	24.53	24.53	24.53	24.53	24.53	24.53	24.53	24.53	24.53	24.53	24.53	37	37
4	HPOP IMSL PURGE PRES (PSIA)	29.46	29.46	29.46	29.46	29.46	29.46	29.46	29.46	29.46	20	20	15	10	10
5	HPOP SEC SEAL CAV PRES (PSIA)	20	20	20	20	20	20	20	10	10	5	5	N/A	N/A	N/A
6	PBP DIS PRES (PSIA)	46.5	46.5	46.5	46.5	46.5	46.5	46.5	46.5	46.5	46.5	46.5	46.5	96	96
7	PBP RAD ACCEL (GRMS)	20	31.6	31.6	31.6	10	10	10	10	10	10	10	5	1	1
8	PBP BEAR CLNT DIS TEMP (DEG R)	N/A	N/A	N/A	N/A	N/A	N/A	N/A	N/A	N/A	N/A	N/A	N/A	N/A	N/A
9	MCC PRES (PSIA)	21.2	21.2	21.2	21.2	21.2	21.2	21.2	21.2	21.2	21.2	21.2	21.2	21.2	21.2
10	MCC CAV LNR PRES (PSIG)	6.3	6.3	6.3	6.3	3	2	6.3	2	2	2	2	N/A	N/A	N/A
11	HPFP SPEED (RPM)	184.2	184.2	184.2	184.2	184.2	184.2	184.2	184.2	184.2	184.2	184.2	184.2	184.2	184.2
12	HPFT DS T1 A (DEG R)	38.78	38.78	38.78	38.78	38.78	38.78	38.78	38.78	38.78	38.78	38.78	38.78	38.78	38.78
13	HPFT DS T1 B (DEG R)	30.56	30.56	30.56	30.56	30.56	30.56	30.56	30.56	30.56	30.56	30.56	30.56	30.56	30.56
14	HPOT DS T1 (DEG R)	18.39	18.39	18.39	18.39	18.39	18.39	18.39	18.39	18.39	18.39	18.39	18.39	50	50
15	HPOT DS T2 (DEG R)	32.3	32.3	32.3	32.3	32.3	32.3	32.3	32.3	32.3	25	25	32.3	32.3	32.3
16	LPFP SPEED (RPM)	5.88	5.88	5.88	5.88	5.88	50	150	50	50	50	50	50	221	221
17	LPOP DIS PRES (PSIA)	4.75	4.75	4.75	4.75	4.75	4.75	20.94	4.75	4.75	4.75	4.75	4.75	8.2	8.2
18	HPFT DIS PRES (PSIA)	20.94	20.94	20.94	20.94	20.94	20.94	21	20.94	20.94	20.94	20.94	20.94	52	52
19	HPFP CLNT LNR PRES (PSIA)	27.95	27.95	27.95	27.95	27.95	27.95	27.95	27.95	27.95	27.95	27.95	N/A	N/A	N/A
20	HEX INT TEMP (DEG F)	0.67	0.67	0.67	0.67	1	1	N/A	1	1	1	1	1	47	47
21	HEX VENT DP (PSIG)	1.83	1.83	1.83	1.83	1.83	1.83	11.8	1.83	1.83	1.83	1.83	1.83	1.83	1.83
22	OPOV ACT POS (PCNT)	0.76	0.76	0.76	0.76	0.76	0.76	0.76	0.76	0.76	0.76	0.76	0.76	1.4	1.4
23	FPOV ACT POS (PCNT)	1.2	1.2	1.2	1.2	1.2	1.2	1.2	1.2	1.2	1.2	1.2	1.2	1.2	1.2
24	FUEL FLOW (GPM)	50	50	50	50	50	50	50	50	50	50	50	50	74	74

N/A - not available

Table 11.
On-Line Computed Standard Deviation Values

TEST NO.		902-398	901-511	901-551	901-683	902-519	902-532	902-428	902-249	901-364	750-175	750-175	901-183	901-173	901-173
P.L. (%RPL)		104	104	104	104	104	104	104	109	109	109	111	92	70	92
I.D. NO.	PARAMETER														
1	HPFP RAD ACCEL (GRMS)	0.12	0.281	0.247	0.564	0.077	0.217	0.265	0.1369	0.28	N/A	N/A	0.28	0.09	0.23
2	HPFP BAL CAV PRES (PSIG)	4.162	9.052	7.422	4.917	5.918	7.21	2.62	7.023	1.532	N/A	N/A	7.6	5.1	5.7
3	HPOP DIS PRES (PSIA)	10.108	10.189	4.605	8.423	8.832	8.83	11.12	12.464	6.75	11.5	10.3	7.1	5.7	5
4	HPOP IMSL PURGE PRES (PSIA)	0.51	0.407	N/A	0.303	0.391	0.57	0.373	0.728	0.779	0.56	0.71	0.8	0.18	0.18
5	HPOP SEC SEAL CAV PRES (PSIA)	0.23	0.298	0.043	0.065	0.314	0.18	0.224	0.2497	0.337	0.18	0.25	N/A	N/A	N/A
6	PBP DIS PRES (PSIA)	17.07	10.586	20.908	17.88	13.18	11.7	13.47	16.425	12.32	13.7	23.5	20.4	16.2	18
7	PBP RAD ACCEL (GRMS)	0.21	0.208	0.389	0.137	0.123	0.32	0.308	0.3235	1.517	N/A	N/A	0.12	0.2	0.16
8	PBP BEAR CLNT DIS TEMP (DEG R)	N/A	N/A	N/A	N/A	N/A	N/A	N/A	N/A	N/A	N/A	N/A	N/A	N/A	N/A
9	MCC PRES (PSIA)	2.236	3.51	4.222	4.218	2.352	2.82	3.536	5.103	3.018	5.2	5.1	5.1	2.3	4.1
10	MCC CAV LNR PRES (PSIG)	0.02	0.024	0.006	0.009	0.027	0.03	0.013	0.0146	0.0097	N/A	N/A	N/A	N/A	N/A
11	HPFP SPEED (RPM)	391.76	186.13	391.33	40.54	545.57	25.3	10.886	350.36	133.05	257	401	227	115	182
12	HPFT DS T1 A (DEG R)	1.94	2.246	1.747	1.986	1.803	1.58	2.143	1.82	3.62	2.9	0	5.6	6.6	13.4
13	HPFT DS T1 B (DEG R)	1.63	1.425	1.89	1.641	1.368	2.37	2.716	2.45	2.24	1.8	2.9	5.3	4.2	6.9
14	HPOT DS T1 (DEG R)	1.003	1.366	0.754	1.271	1.508	8.2	1.72	2.188	1.749	0.23	1.6	3.5	4.2	4.7
15	HPOT DS T2 (DEG R)	0.674	1.491	1.131	1.312	1.687	4.2	0.85	1.996	2.6	0.23	1	3.4	4.7	4.4
16	LPFP SPEED (RPM)	23.66	23.56	20.63	17.46	28.615	10.6	9.56	15.629	15.313	14	24.7	17.4	25.3	49.5
17	LPOP DIS PRES (PSIA)	1.283	1.013	1.374	1.099	1.153	0.83	1.613	0.8096	1.008	0.89	0.7	2.2	3.8	2.6
18	HPFT DIS PRES (PSIA)	8.857	13.803	10.761	9.327	10.408	8.3	10.67	9.89	5.473	11.2	8	3.7	6.3	8.4
19	HPFP CLNT LNR PRES (PSIA)	1.424	4.204	3.178	2.843	6.231	3.2	3.56	3.918	3.518	N/A	N/A	N/A	N/A	N/A
20	HEX INT TEMP (DEG F)	1.125	0.782	0.211	0.511	0.844	7.6	N/A	1.035	1.33	N/A	N/A	7.1	10.5	4.8
21	HEX VENT DP (PSIG)	0.058	0.046	0.062	0.09	0.064	0.23	0.053	0.031	0.095	N/A	N/A	0.15	0.25	0.13
22	OPOV ACT POS (PCNT)	0.087	0.036	N/A	0.037	0.12	0.06	0.096	0.1339	0.109	0.08	0.11	0.11	0.4	0.15
23	FPOV ACT POS (PCNT)	0.128	0.075	0.111	0.074	0.149	0.12	0.095	0.1385	0.056	0.13	0.15	0.14	0.14	0.08
24	FUEL FLOW (GPM)	89.537	72.259	47.172	87.504	29.292	93.1	16.724	54.813	42.24	120	102	26.2	32.9	27.1

N/A - not available

Table 12.
First Two-Second Interval Signal Limit (N1) Factors

TEST NO.		902-398	901-511	901-551	901-683	902-519	902-532	902-428	902-249	901-364	750-175	750-175	901-183	901-173	901-173
P.L. (%RPL)		104	104	104	104	104	104	104	109	109	109	111	92	70	92
I.D. NO.	PARAMETER														
1	HPFP RAD ACCEL (GRMS)	1.5	3	3	3	1.5	1.5	3	3	3	3	3	2	1.5	1.5
2	HPFP BAL CAV PRES (PSIG)	5.5	5.5	5.5	5.5	8.5	8.5	15	6	4	4	4	15	2	2
3	HPOP DIS PRES (PSIA)	4.5	4.5	4.5	4.5	4.5	4.5	10	3	6	4	4	3	3	3
4	HPOP IMSL PURGE PRES (PSIA)	3	3	3	3	1.5	2	4	1.5	4	4	1	1	1	1
5	HPOP SEC SEAL CAV PRES (PSIA)	2	3	3	3	1	0.7	2	2	1.5	5	1	N/A	N/A	N/A
6	PBP DIS PRES (PSIA)	4	4	4	4	4	4	12	5	4	4	4	7	2	2
7	PBP RAD ACCEL (GRMS)	1.5	1.5	1.5	1.5	1	1	0.3	0.3	1.2	1.2	1.2	0.3	2	2
8	PBP BEAR CLNT DIS TEMP (DEG R)	N/A	N/A	N/A	N/A	N/A	N/A	N/A	N/A	N/A	N/A	N/A	N/A	N/A	N/A
9	MCC PRES (PSIA)	3	3	3	3	1.5	1.5	6	2	3	2	2	2	2	2
10	MCC CAV LNR PRES (PSIG)	1.5	3	3	3	1.5	1	1	3	0.5	0.5	0.5	N/A	N/A	N/A
11	HPFP SPEED (RPM)	9	3	3	3	9	5	5	13	7	20	20	10	5	5
12	HPFT DS T1 A (DEG R)	3	3	3	3	1.5	2	3	3.5	4.5	8	8	3.5	2	2
13	HPFT DS T1 B (DEG R)	3	3	3	3	1.5	2	3	2.5	2.5	2	2	2	3	3
14	HPOT DS T1 (DEG R)	10	5	5	5	9	9	7	7	7	0.5	4	7	3	3
15	HPOT DS T2 (DEG R)	5	3	3	3	3	5	3	3	5	0.5	1	3	4	4
16	LPFP SPEED (RPM)	65	9	9	9	65	10	6	6	6	5	5	6	4	4
17	LPOP DIS PRES (PSIA)	14	3	3	3	25	35	3	18	15	13	8	12	3	3
18	HPFT DIS PRES (PSIA)	15	15	15	15	8	8	13	5	4	5	5	6	2	2
19	HPFP CLNT LNR PRES (PSIA)	3	3	3	3	1.5	3	7	4.5	2	2	2	N/A	N/A	N/A
20	HEX INT TEMP (DEG F)	200	100	100	100	225	225	N/A	150	150	150	150	150	4	4
21	HEX VENT DP (PSIG)	15	10	10	10	15	15	3	5	6	6	6	3	3	3
22	OPOV ACT POS (PCNT)	3	3	3	3	5	5	5	5	5	5	3	5	4	4
23	FPOV ACT POS (PCNT)	3	3	3	3	3	3	3	3	5	2	2	2	2	2
24	FUEL FLOW (GPM)	12	3	3	3	12	12	12	12	12	18	15	12	6	6

N/A - not available

Table 13.
Steady-State Interval Signal Limit (N2) Factors

TEST NO.		902-398	901-511	901-551	901-683	902-519	902-532	902-428	902-249	901-364	750-175	750-175	901-183	901-173	901-173
P.L. (%RPL)		104	104	104	104	104	104	104	109	109	109	111	92	70	92
I.D. NO.	PARAMETER														
1	HPFP RAD ACCEL (GRMS)	12	13	12	7	45	8	9	50	20	20	20	5	12	12
2	HPFP BAL CAV PRES (PSIG)	16	8	10	8	18	9	45	8	7	7	7	25	9	9
3	HPOP DIS PRES (PSIA)	6	7	10	10	7	8	10	4	8	6	6	6	7	7
4	HPOP IMSL PURGE PRES (PSIA)	80	160	200	105	80	140	160	40	70	85	20	7	14	14
5	HPOP SEC SEAL CAV PRES (PSIA)	70	40	70	20	20	65	60	70	20	70	10	N/A	N/A	N/A
6	PBP DIS PRES (PSIA)	10	10	6	7	10	15	16	10	10	10	4	5	11	5
7	PBP RAD ACCEL (GRMS)	12	8	5	10	11	12	4	5	3	2	2	20	8	6
8	PBP BEAR CLNT DIS TEMP (DEG R)	N/A	N/A	N/A	N/A	N/A	N/A	N/A	N/A	N/A	N/A	N/A	N/A	N/A	N/A
9	MCC PRES (PSIA)	9	7	5	5	10	6	18	6	9	5	7	6	12	4
10	MCC CAV LNR PRES (PSIG)	200	200	100	60	50	20	250	250	50	50	50	N/A	N/A	N/A
11	HPFP SPEED (RPM)	3	4	3	7	3	10	22	4	7	6	4	4	7	7
12	HPFT DS T1 A (DEG R)	40	40	25	25	25	18	25	50	35	15	15	13	8	4
13	HPFT DS T1 B (DEG R)	40	40	25	25	25	45	20	23	23	15	15	18	16	7
14	HPOT DS T1 (DEG R)	150	85	50	80	40	15	30	40	40	25	25	12	26	13
15	HPOT DS T2 (DEG R)	150	85	50	60	40	30	40	30	30	18	18	8	24	14
16	LPFP SPEED (RPM)	13	16	14	16	10	25	35	12	12	9	7	12	18	18
17	LPOP DIS PRES (PSIA)	40	80	50	50	50	100	18	50	50	50	20	8	5	5
18	HPFT DIS PRES (PSIA)	18	8	8	9	8	9	12	7	9	9	9	14	5	5
19	HPFP CLNT LNR PRES (PSIA)	25	8.5	16	10	5	24	25	25	10	10	10	N/A	N/A	N/A
20	HEX INT TEMP (DEG F)	80	80	140	80	175	300	N/A	125	100	100	100	50	12	12
21	HEX VENT DP (PSIG)	400	500	400	200	300	350	280	200	90	90	90	100	25	25
22	OPOV ACT POS (PCNT)	25	85	50	50	18	25	15	20	25	42	12	30	25	25
23	FPOV ACT POS (PCNT)	20	40	20	35	18	10	13	18	70	8	8	8	10	0
24	FUEL FLOW (GPM)	5	7	8	7	16	31	24	8	8	6	5	8	7	7

N/A - not available

APPENDIX II.

Figures

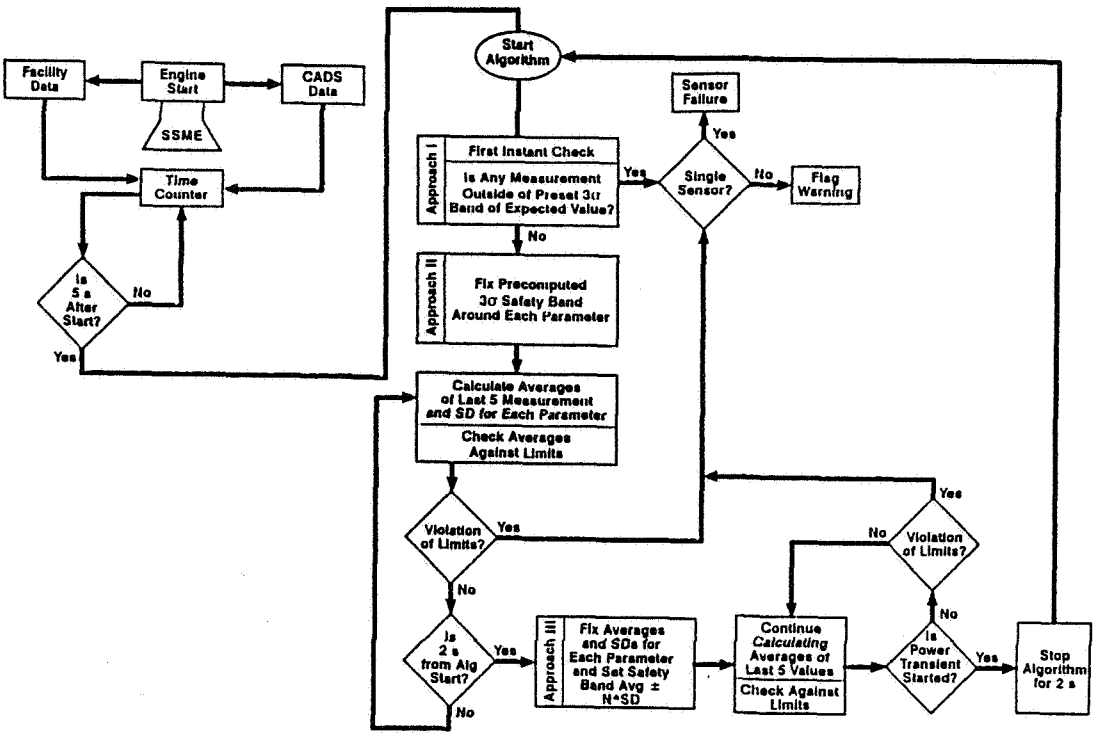

Figure 1. RTFC Algorithm Software Structure

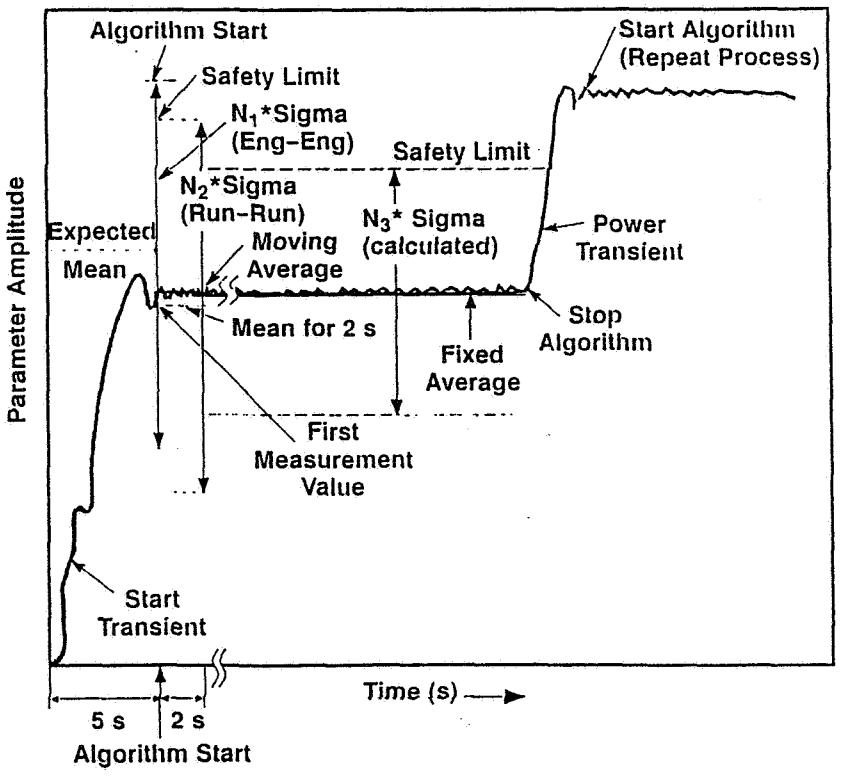

Figure 2. RTFC Algorithm Schematic

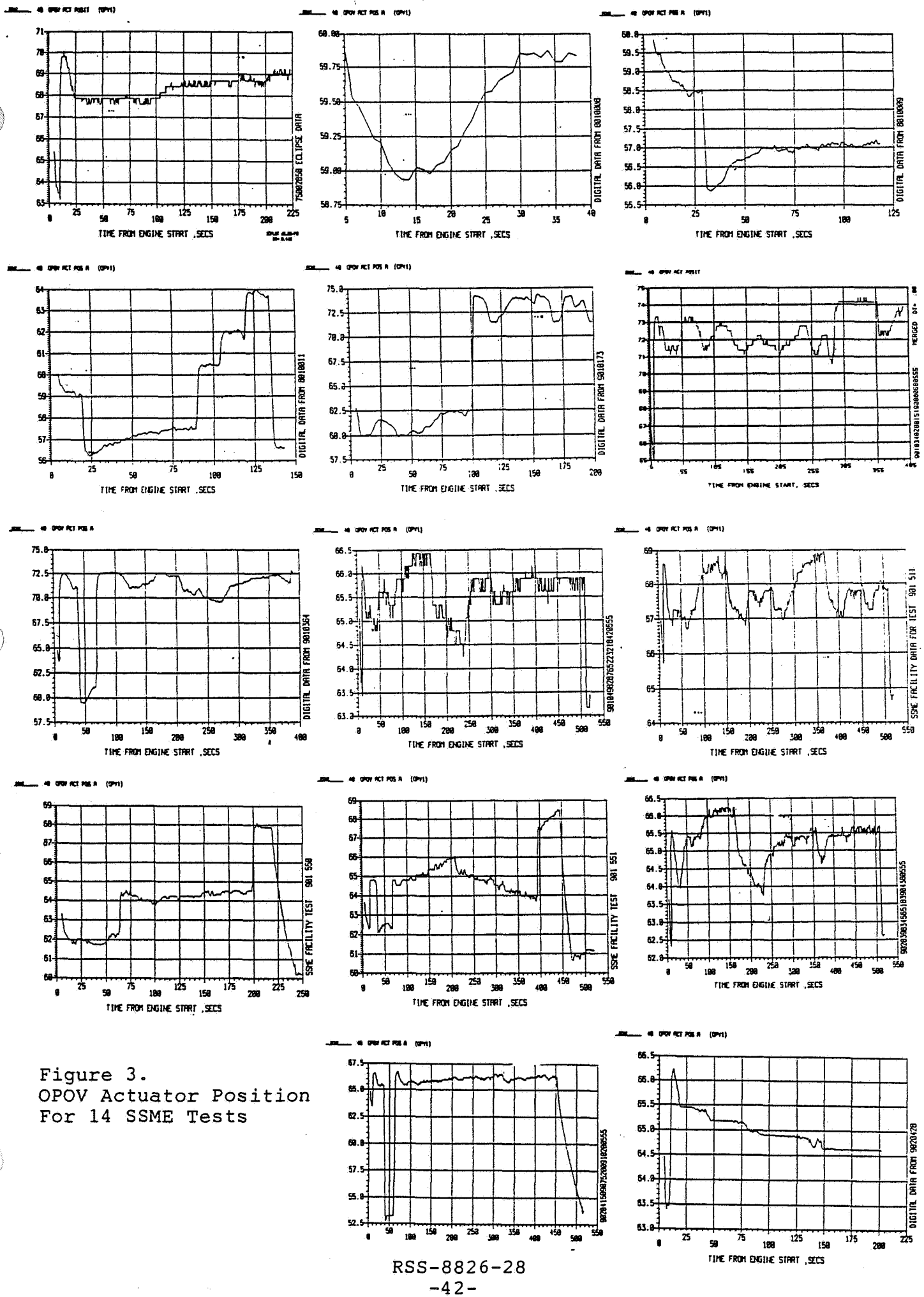

Figure 3.
OPOV Actuator Position
For 14 SSME Tests

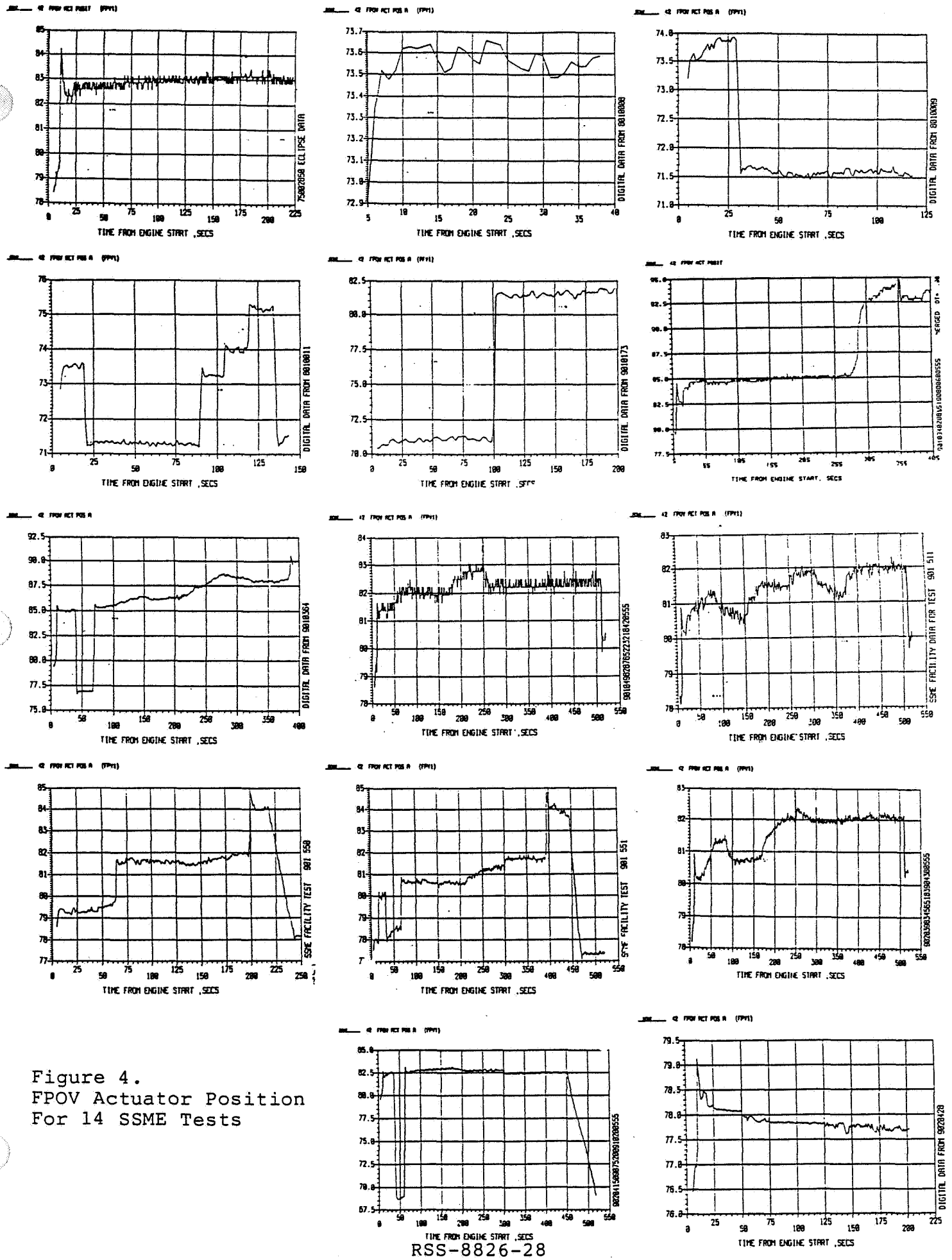

Figure 4.
FPOV Actuator Position
For 14 SSME Tests

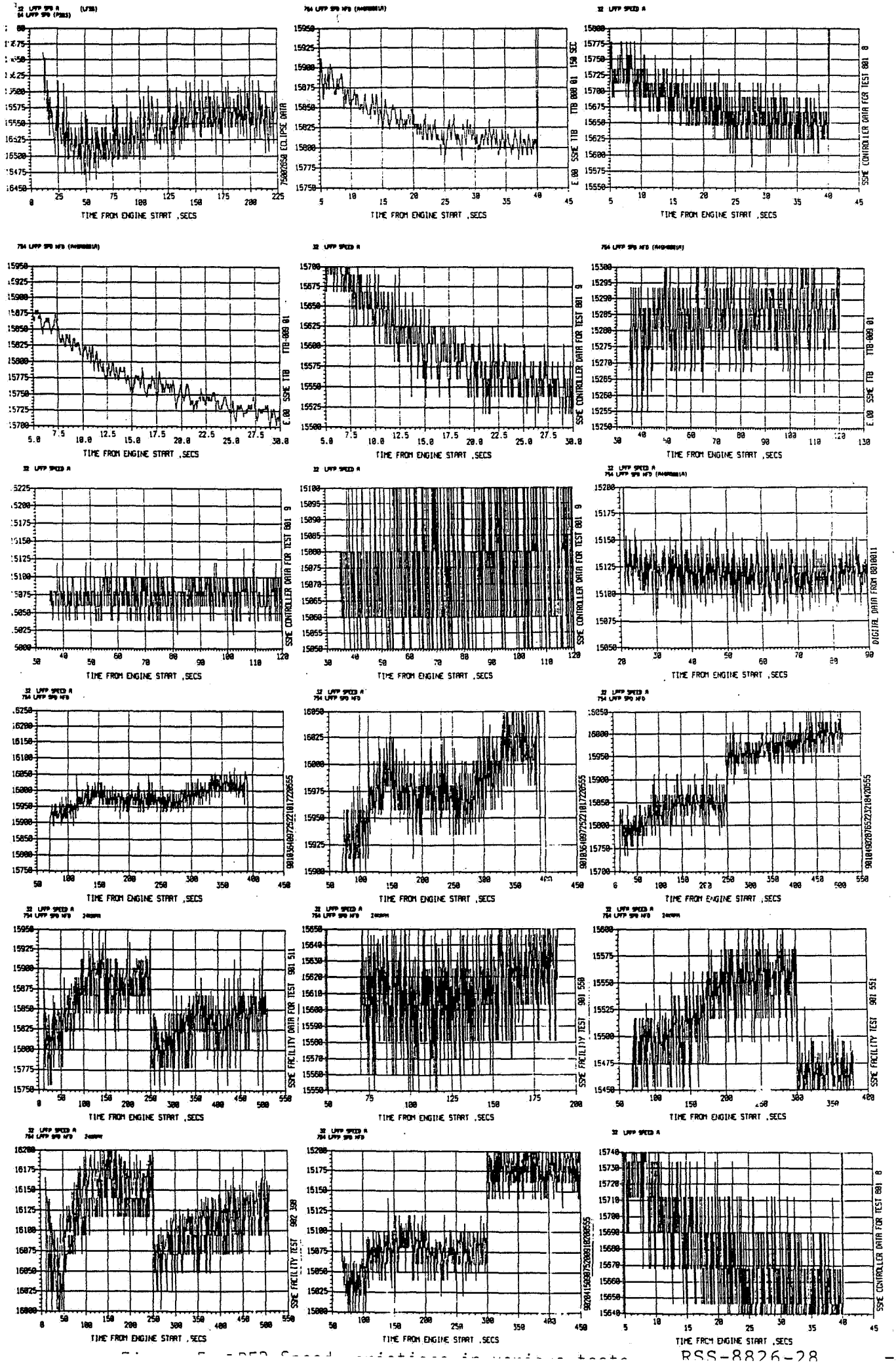

Figure 5.- RFP Speed variations in various tests RSS-8826-28 -44-

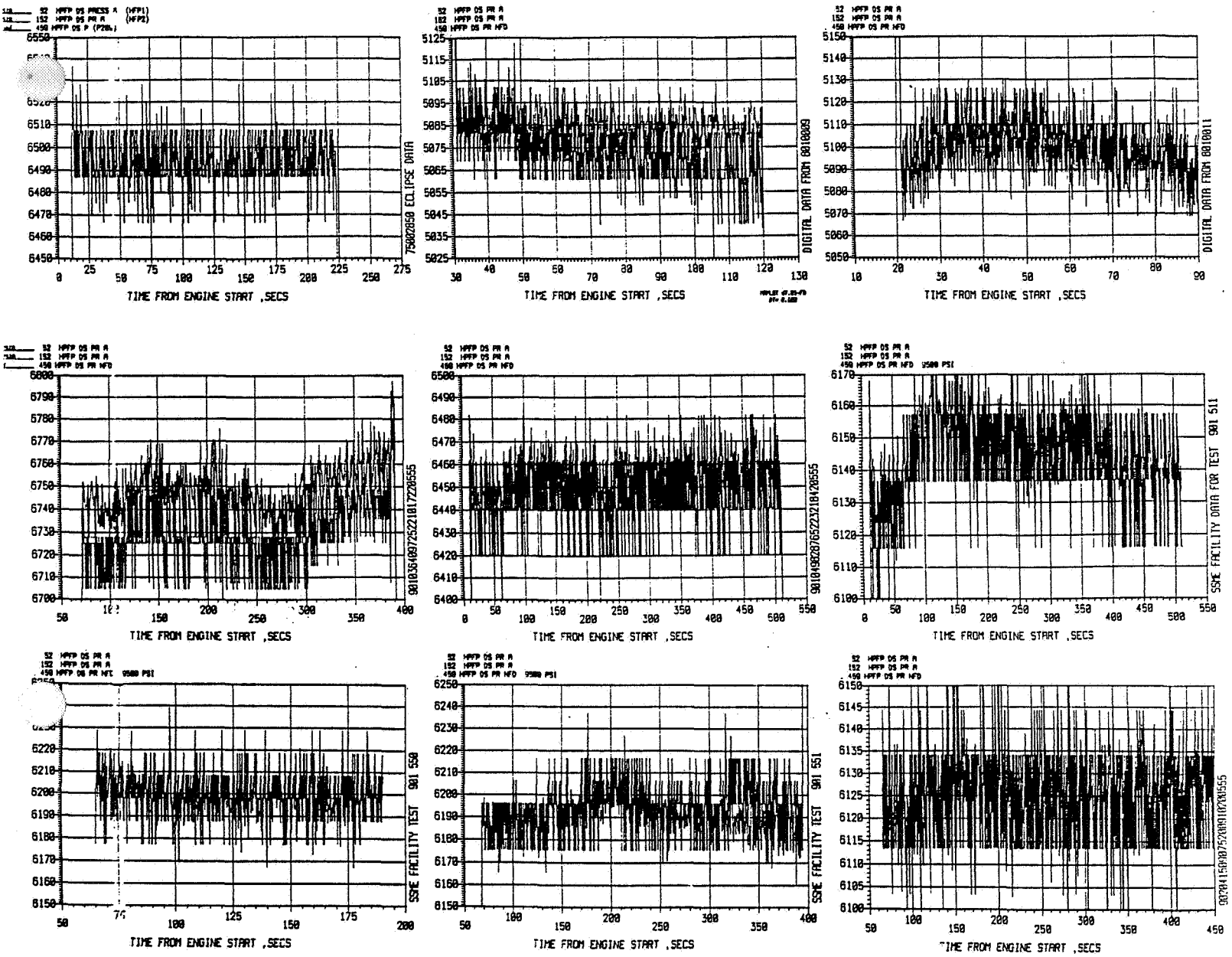

Figure 6. HPFP Discharge Pressure Variations Under Various Conditions

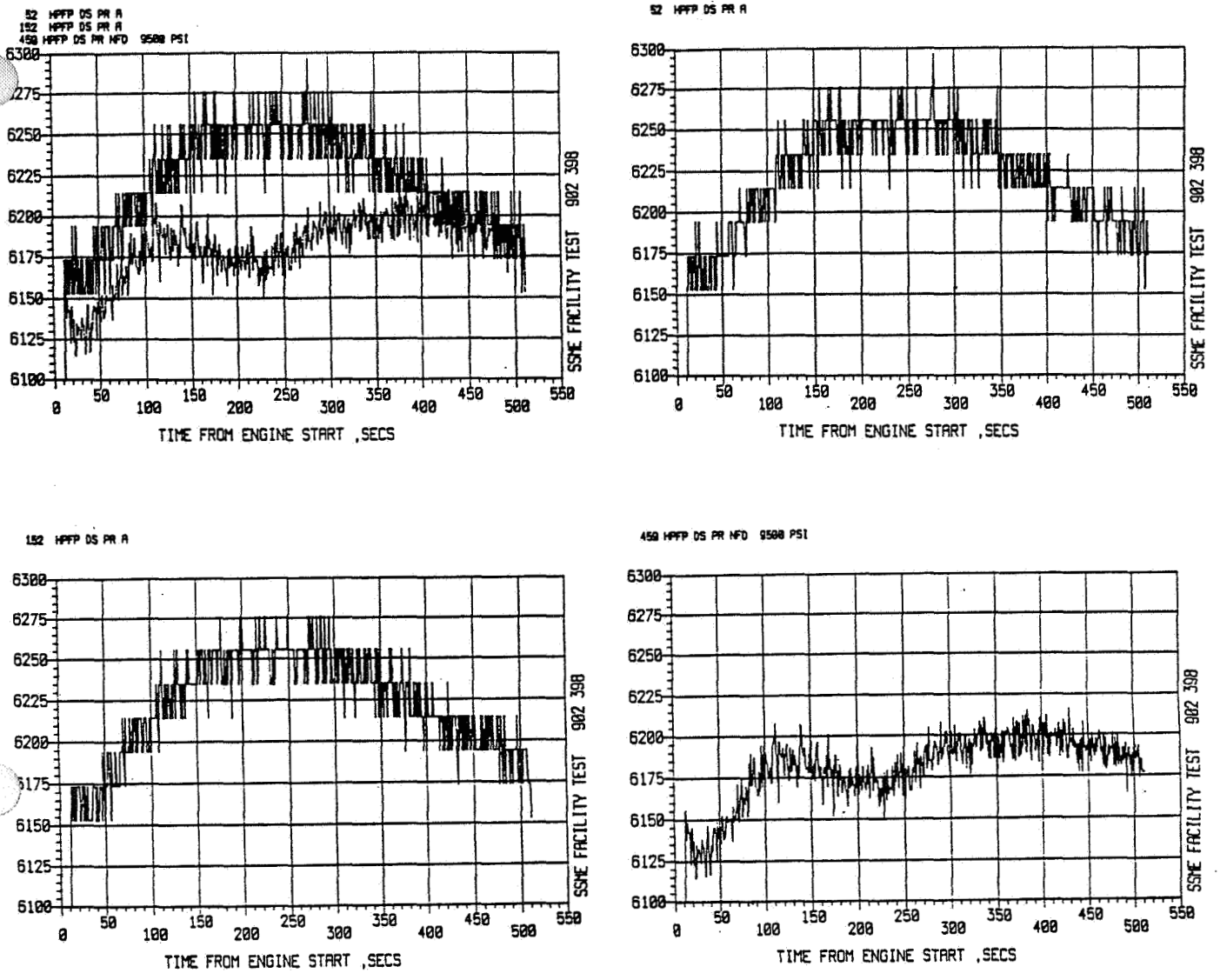

Figure 7. HPFP Discharge Pressure Variations In Test 902-398

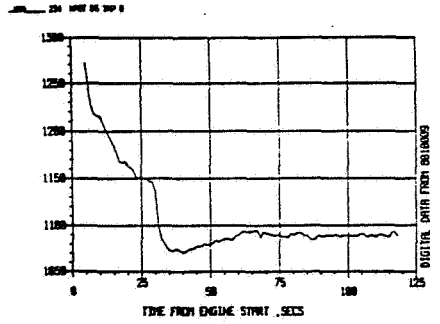
TIME FROM ENGINE START ,SECS
DIGITAL DATA FROM 8018009

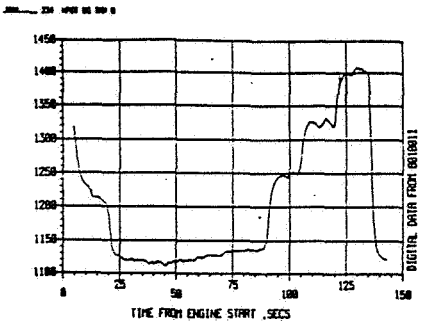
TIME FROM ENGINE START ,SECS
DIGITAL DATA FROM 8018011

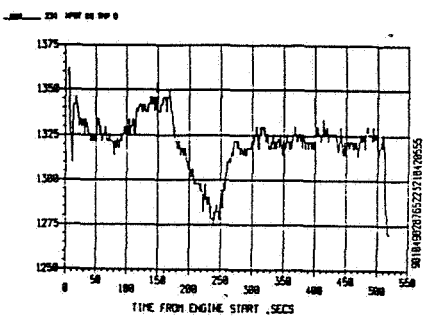
TIME FROM ENGINE START ,SECS

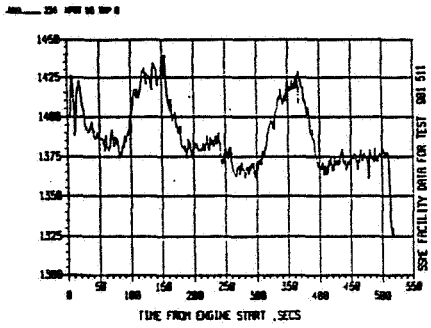
TIME FROM ENGINE START ,SECS
SSME FACILITY DATA FOR TEST 901 511

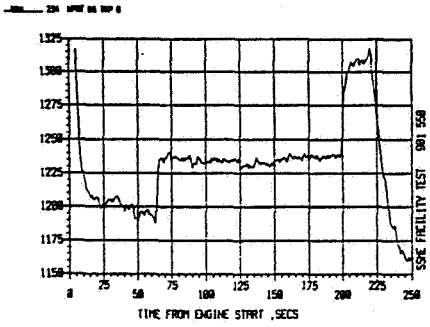
TIME FROM ENGINE START ,SECS
SSME FACILITY TEST 901 550

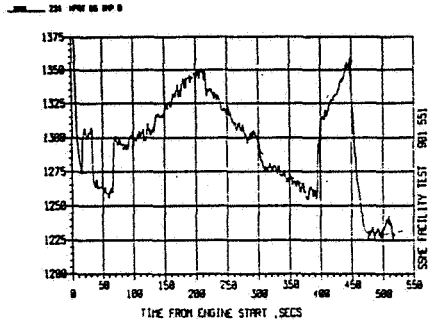
TIME FROM ENGINE START ,SECS
SSME FACILITY TEST 901 551

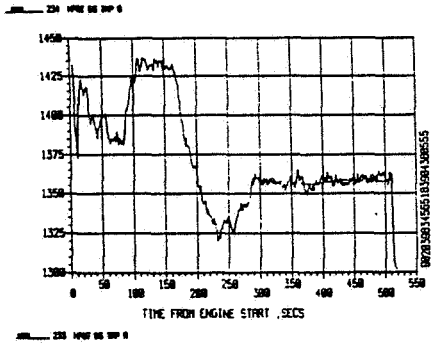
TIME FROM ENGINE START ,SECS

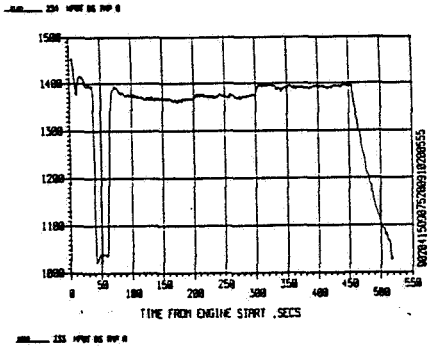
TIME FROM ENGINE START ,SECS

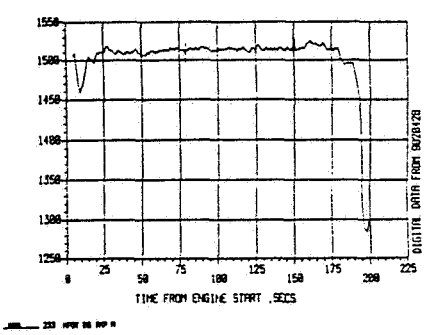
TIME FROM ENGINE START ,SECS
DIGITAL DATA FROM 8020128

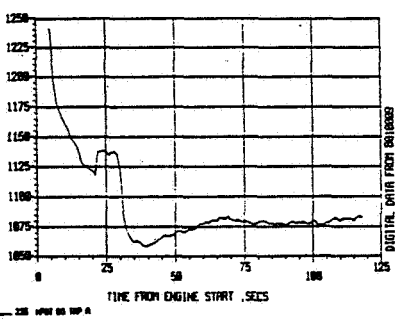
TIME FROM ENGINE START ,SECS
DIGITAL DATA FROM 8018009

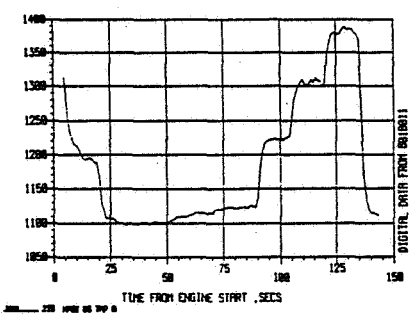
TIME FROM ENGINE START ,SECS
DIGITAL DATA FROM 8018011

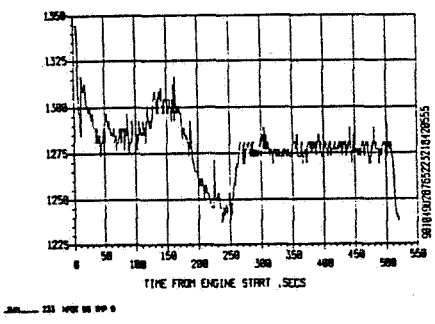
TIME FROM ENGINE START ,SECS

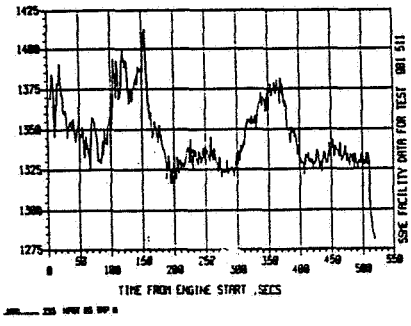
TIME FROM ENGINE START ,SECS
SSME FACILITY DATA FOR TEST 901 511

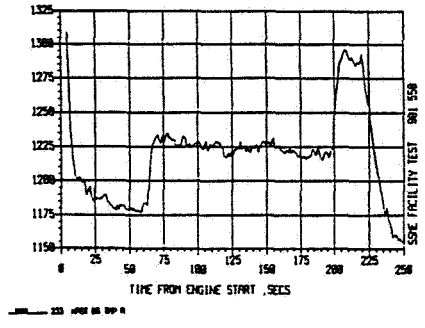
TIME FROM ENGINE START ,SECS
SSME FACILITY TEST 901 550

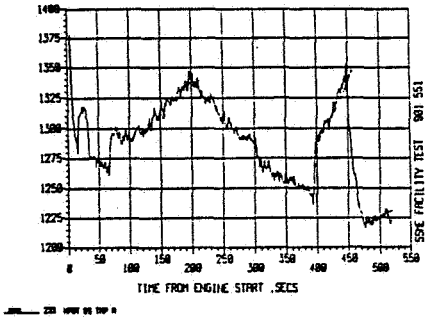
TIME FROM ENGINE START ,SECS
SSME FACILITY TEST 901 551

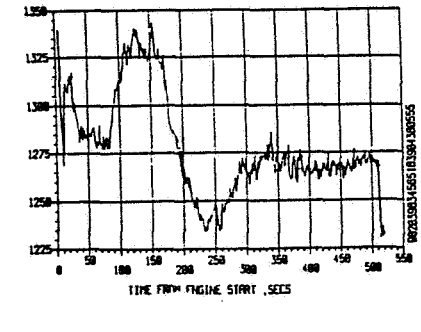
TIME FROM ENGINE START ,SECS

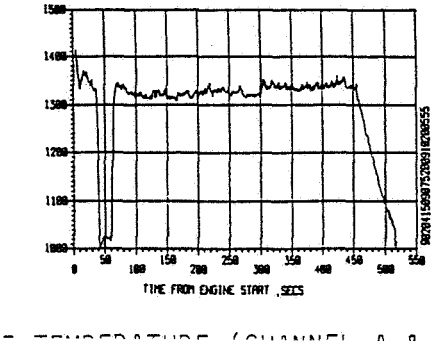
TIME FROM ENGINE START ,SECS

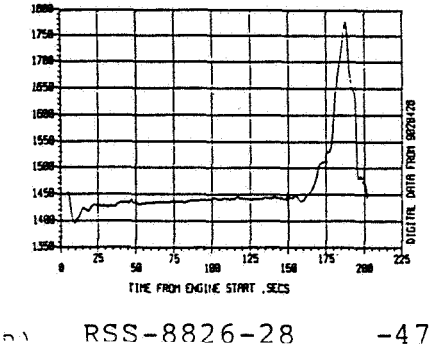
TIME FROM ENGINE START ,SECS
DIGITAL DATA FROM 8020128

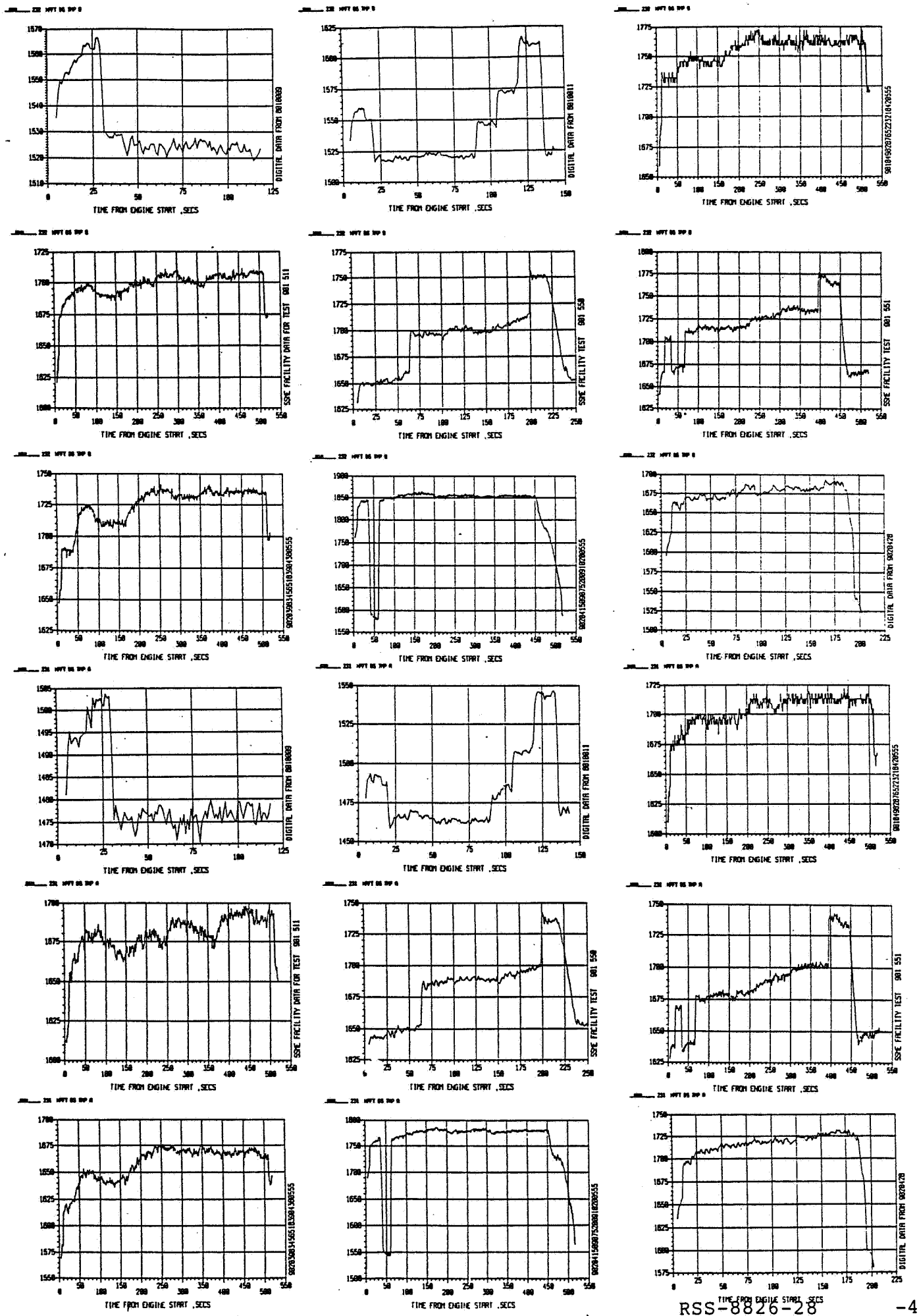

FIGURE 9. HPFT DISCHARGE TEMPERATURE (CHANNEL A & B)

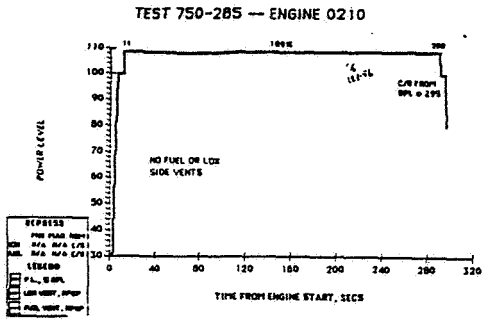

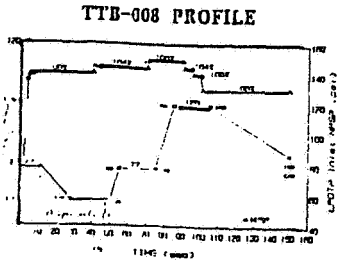

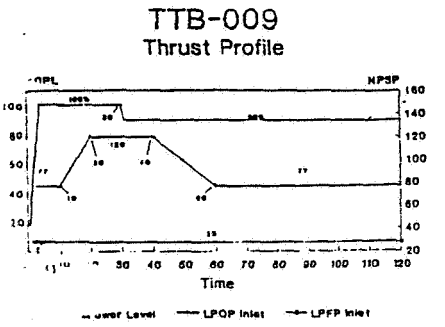

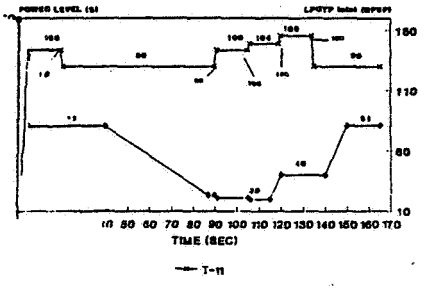

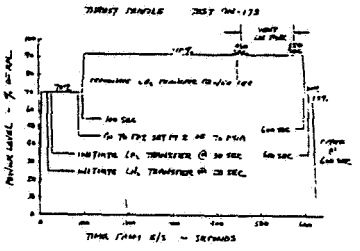

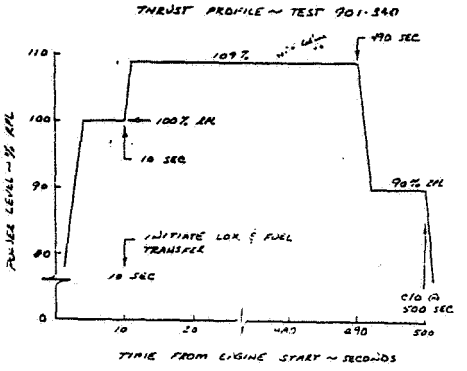

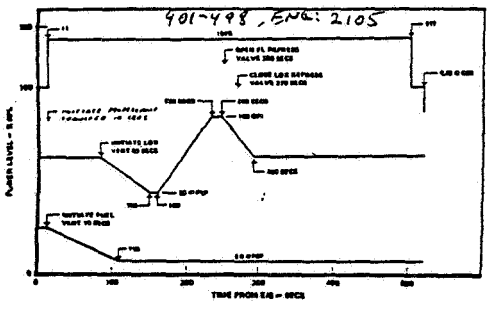

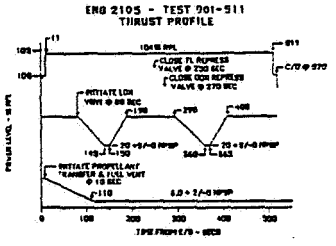

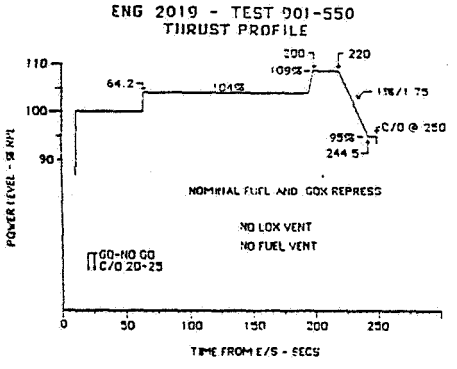

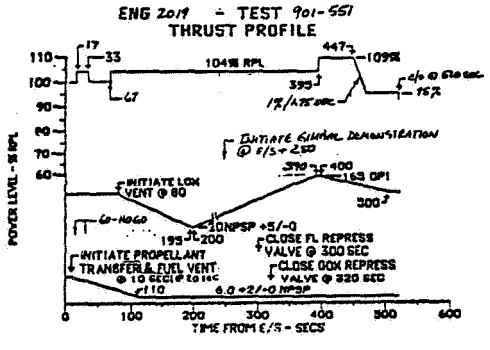

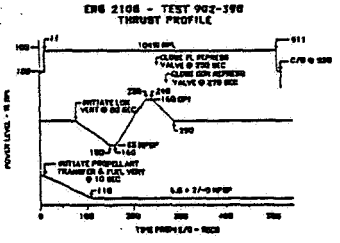

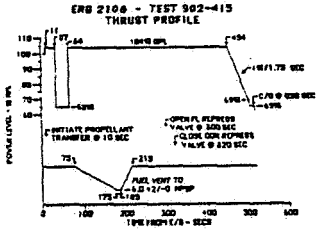

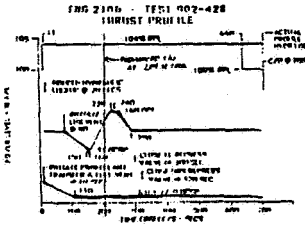

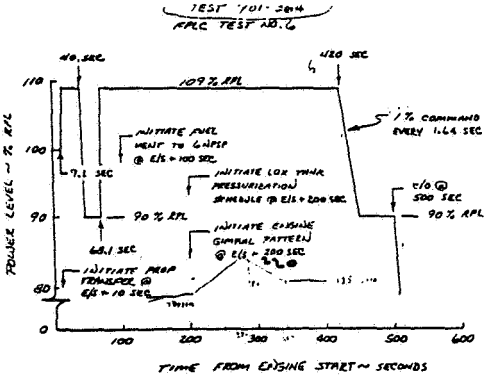

Figure 10.
Thrust Profiles For
Various SSME Tests

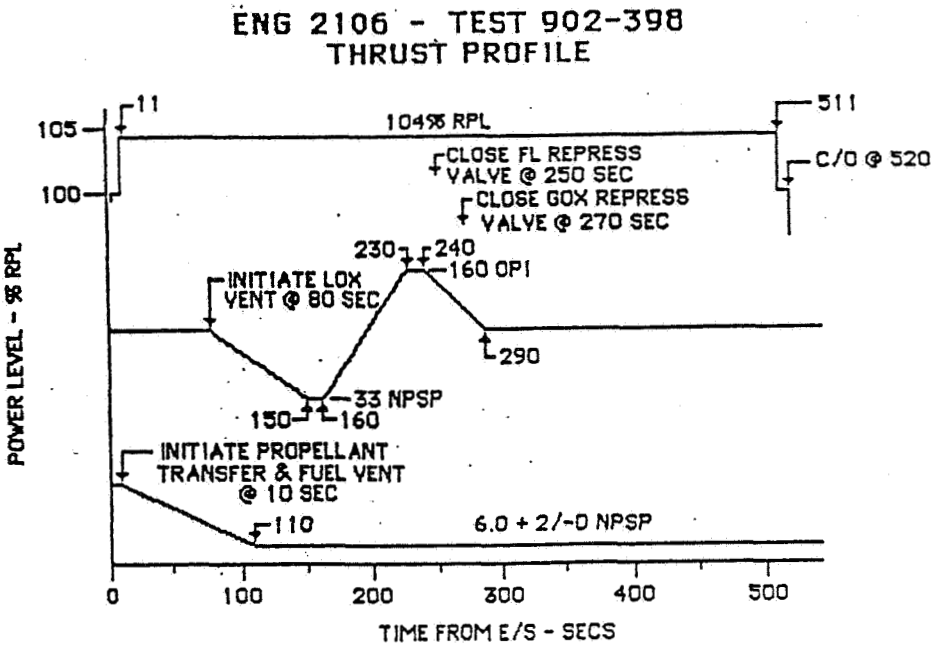

Figure 11.

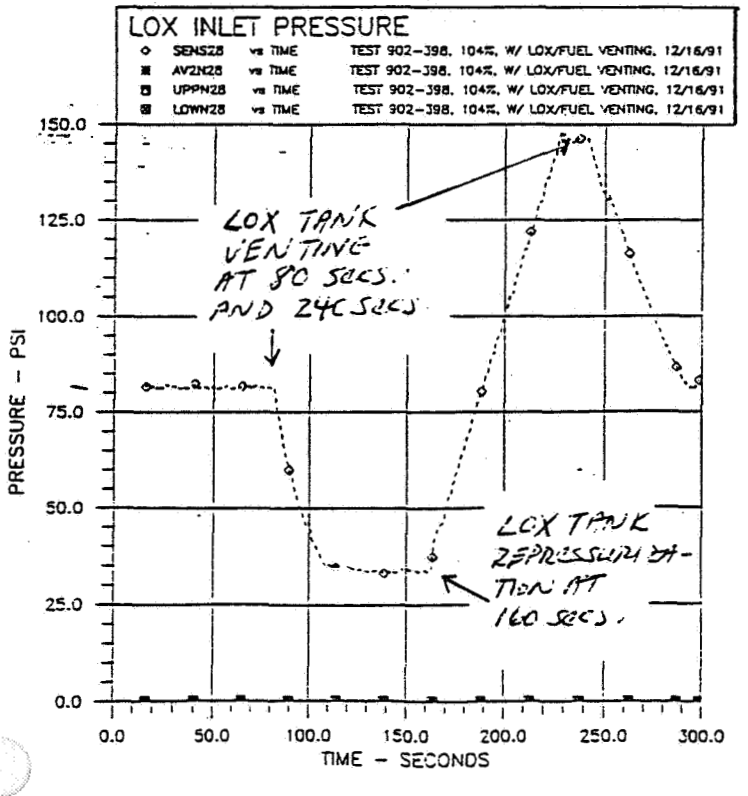

Figure 12.

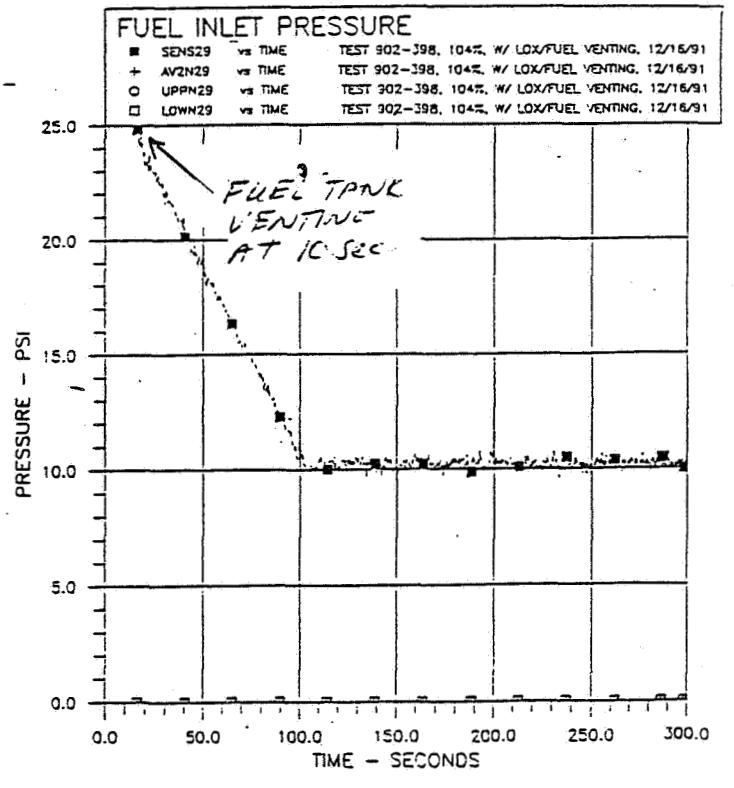

Figure 13.

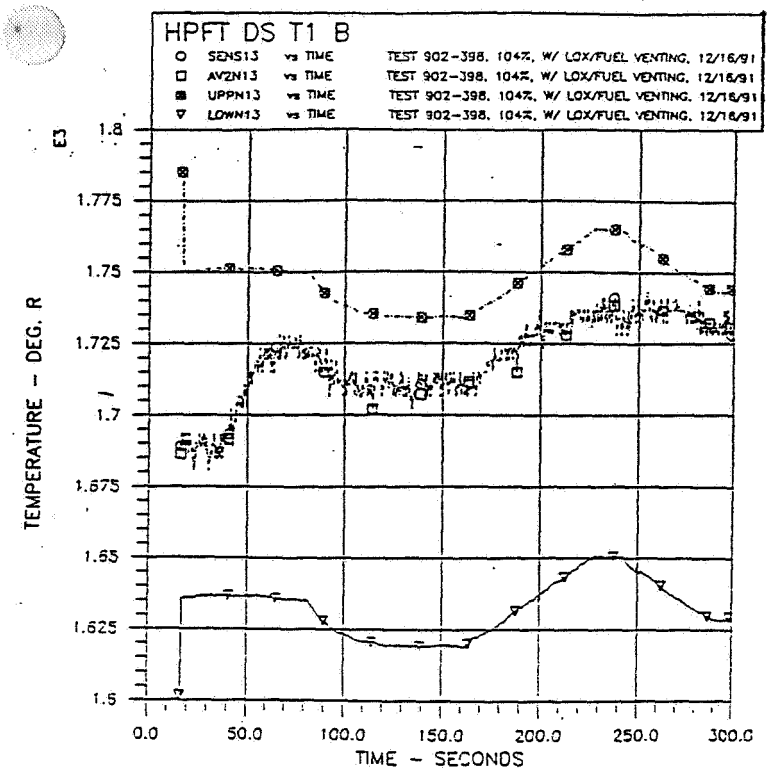

Figure 14.

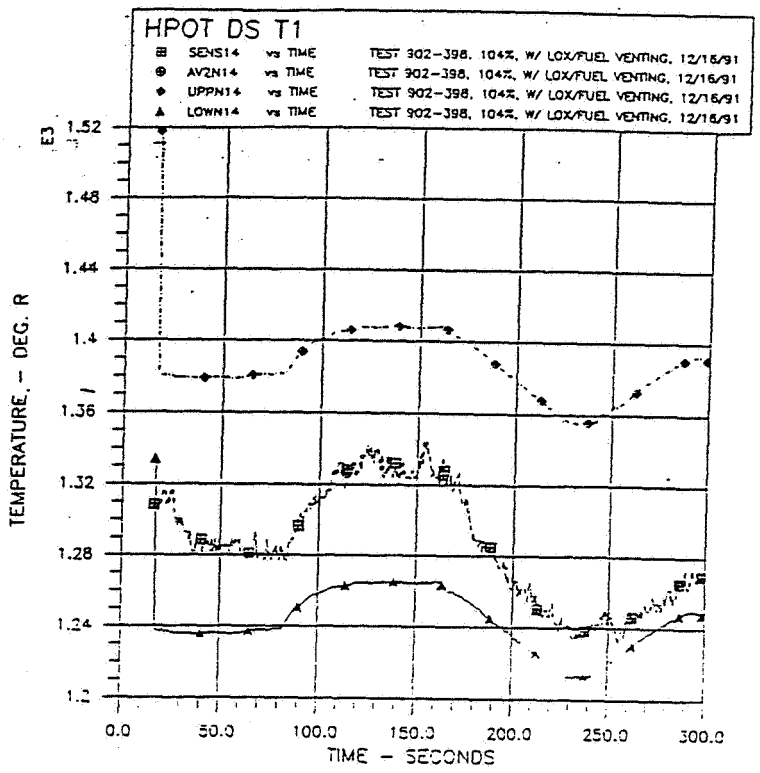

Figure 15.

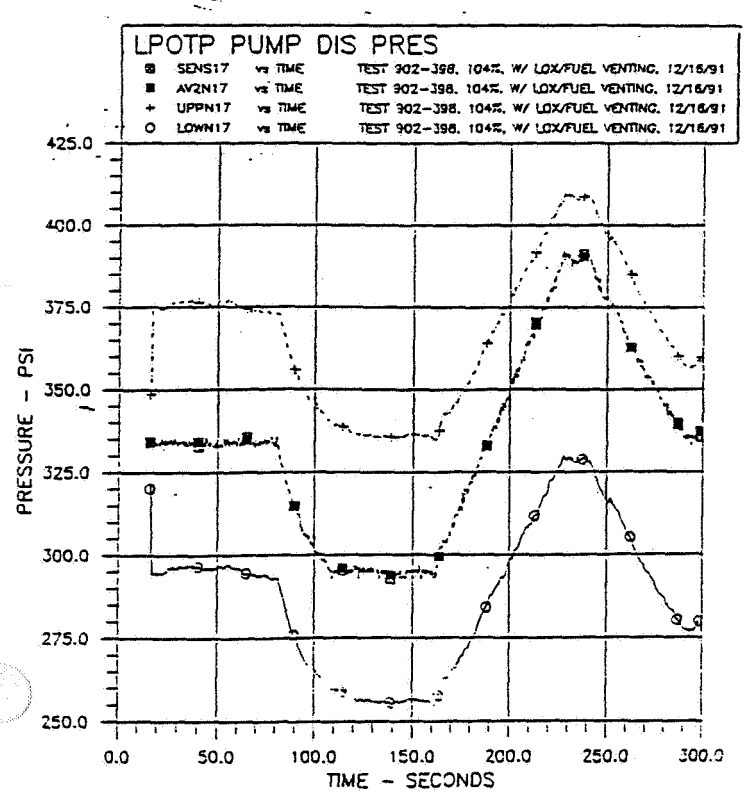

Figure 16.

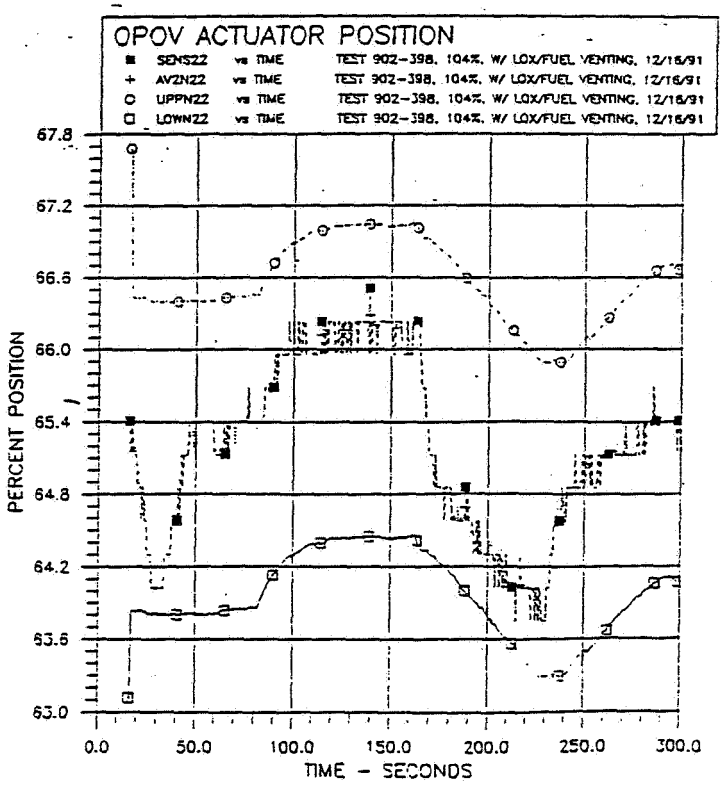

Figure 17.

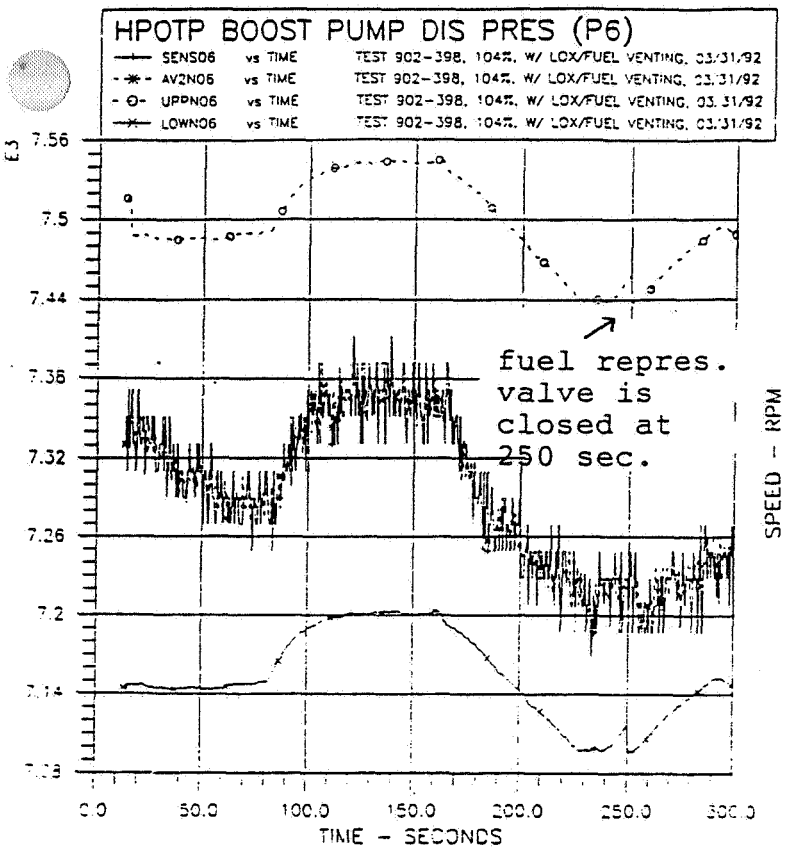

Figure 18.

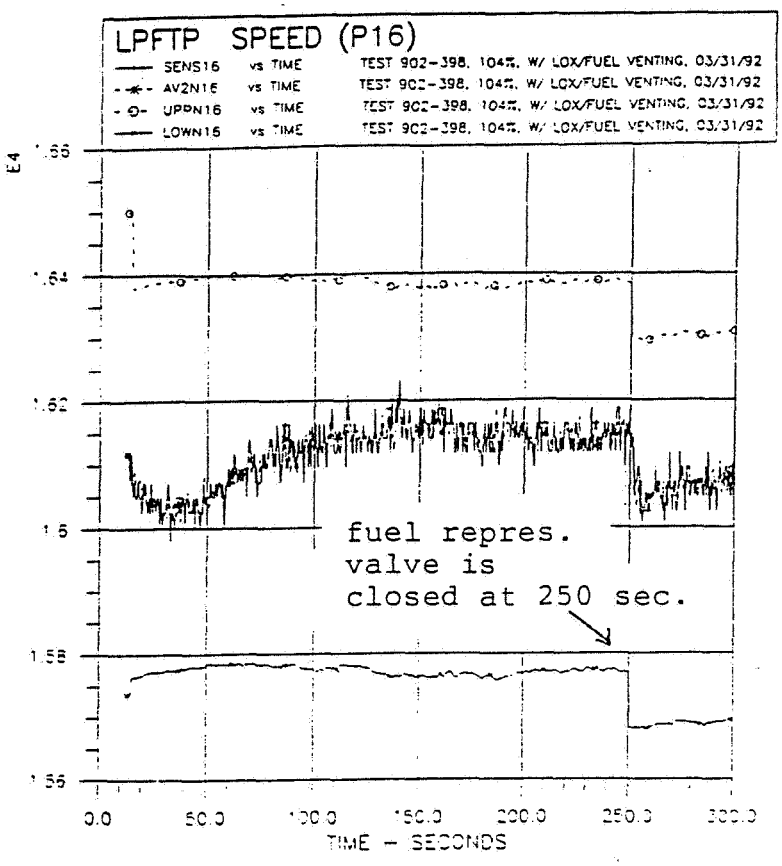

Figure 19.

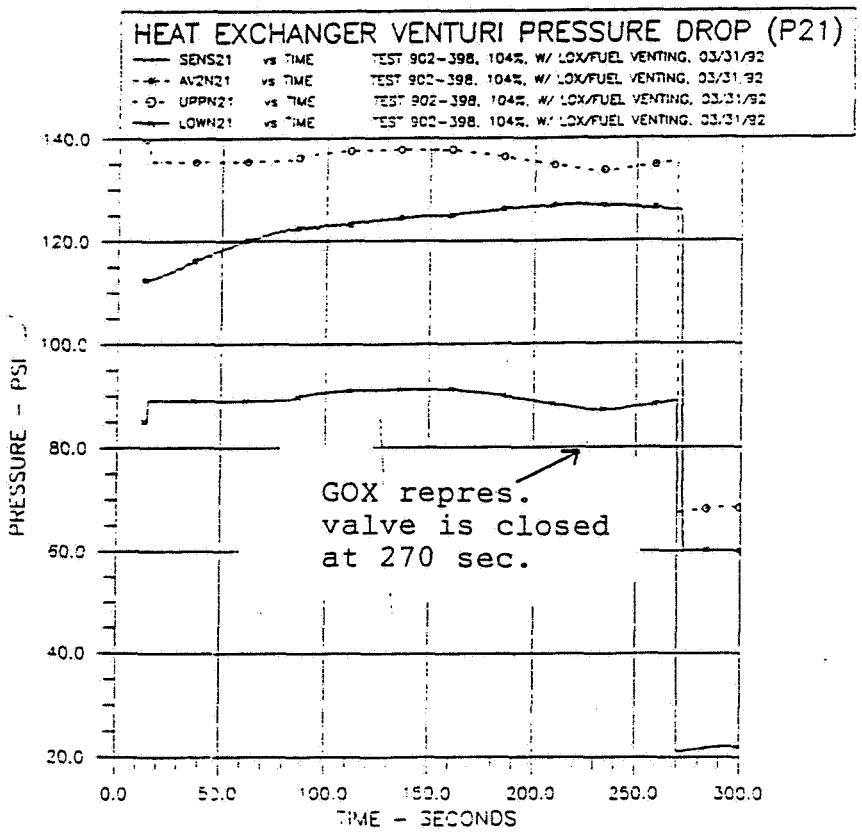

Figure 20.

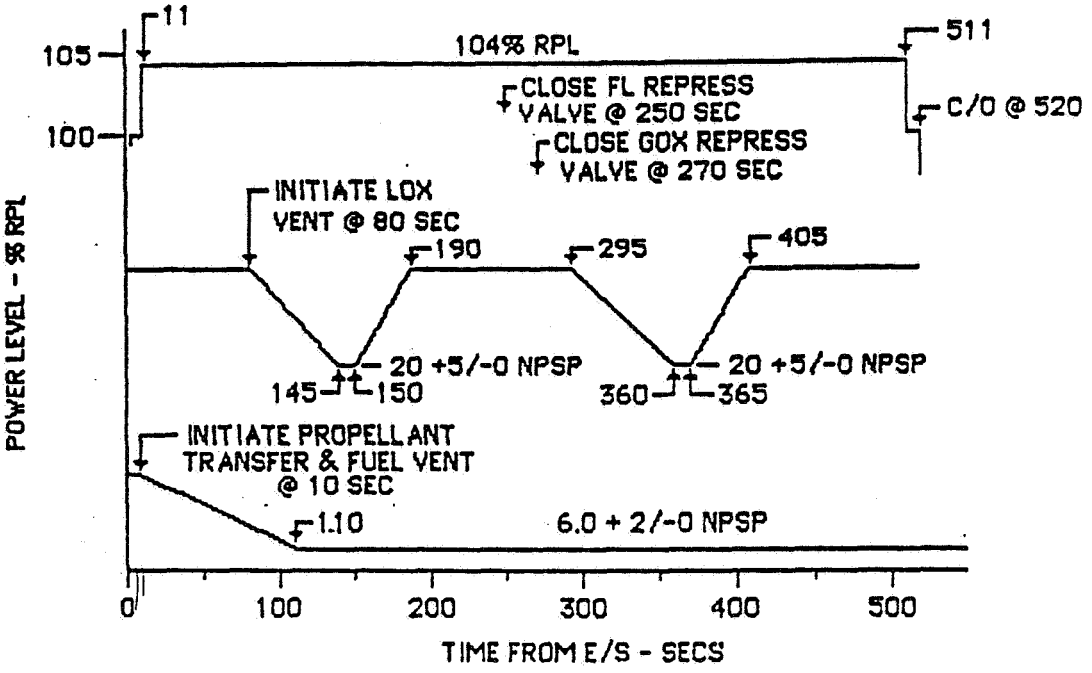

Figure 21.

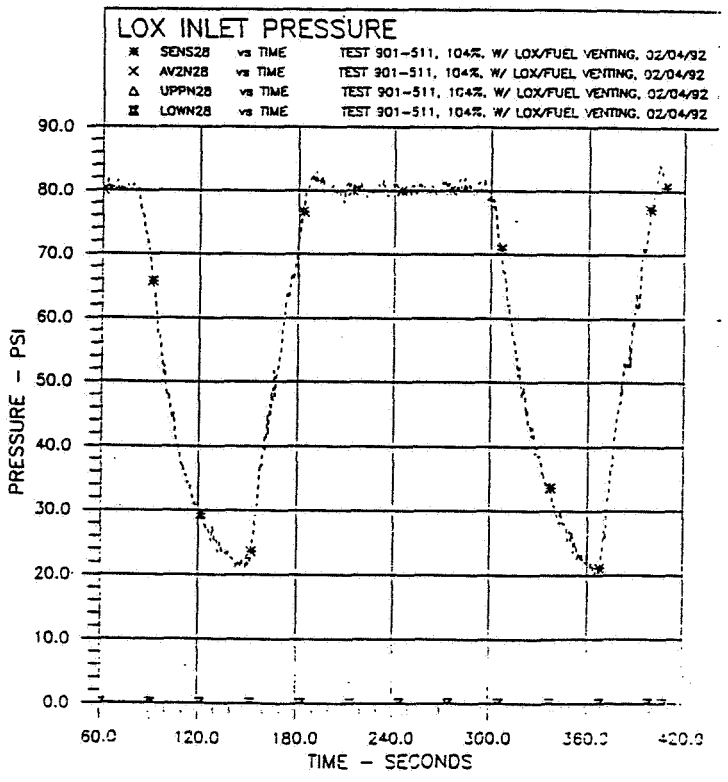

Figure 22.

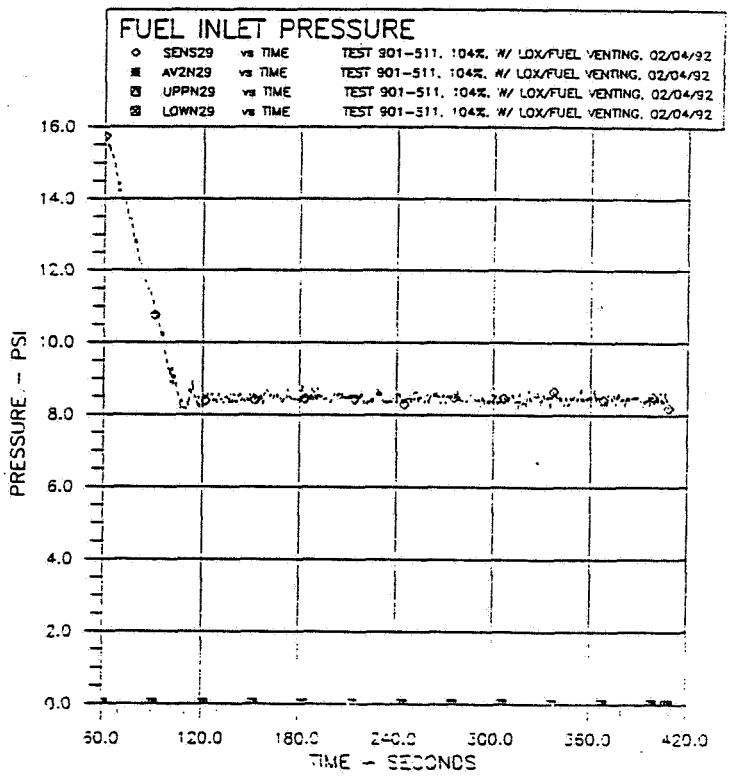

Figure 23.

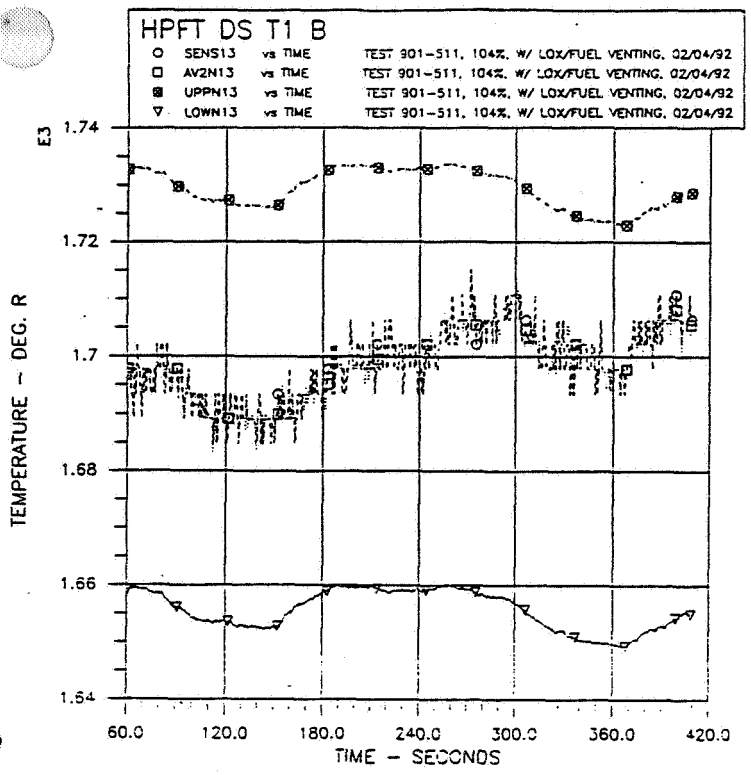

Figure 24.

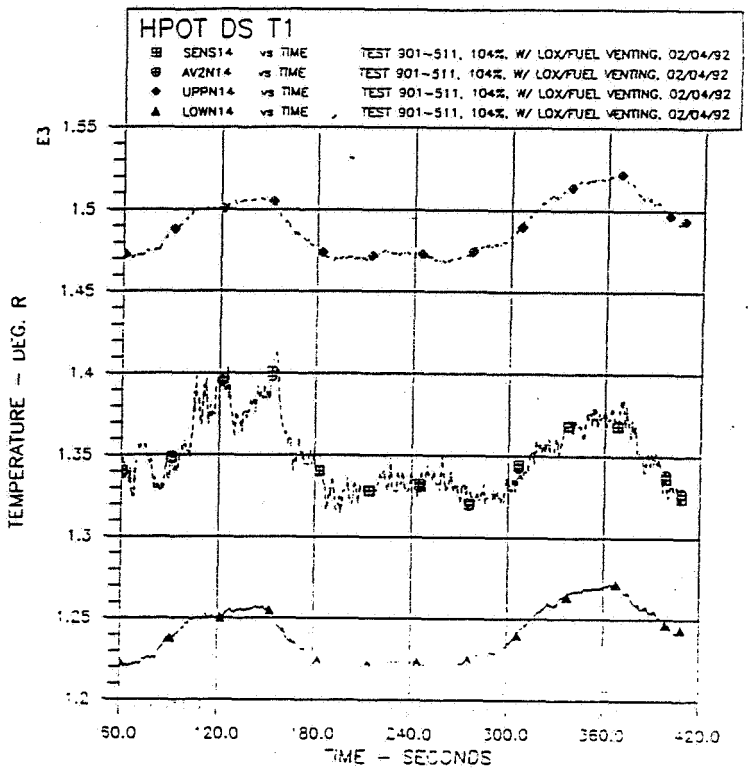

Figure 25.

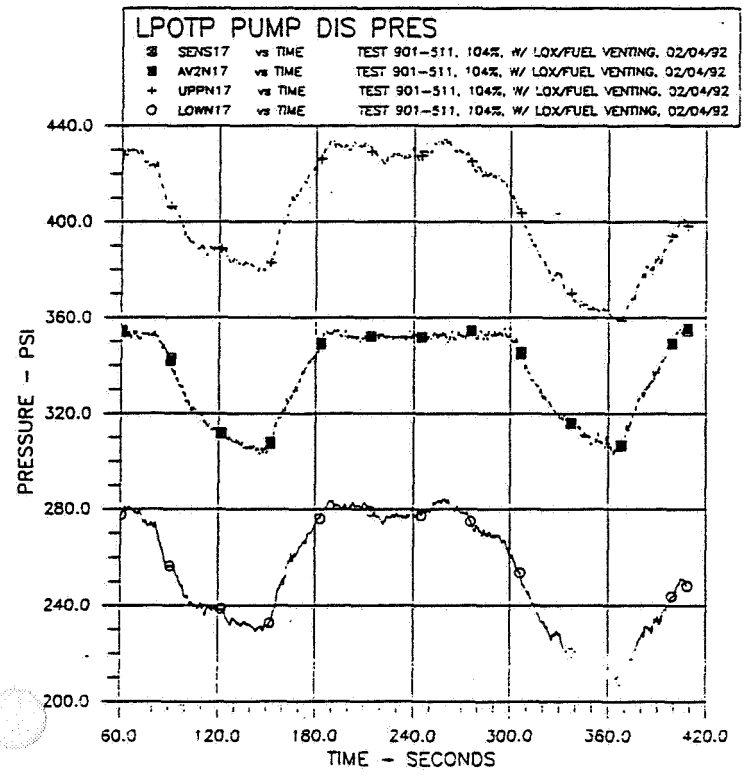

Figure 26.

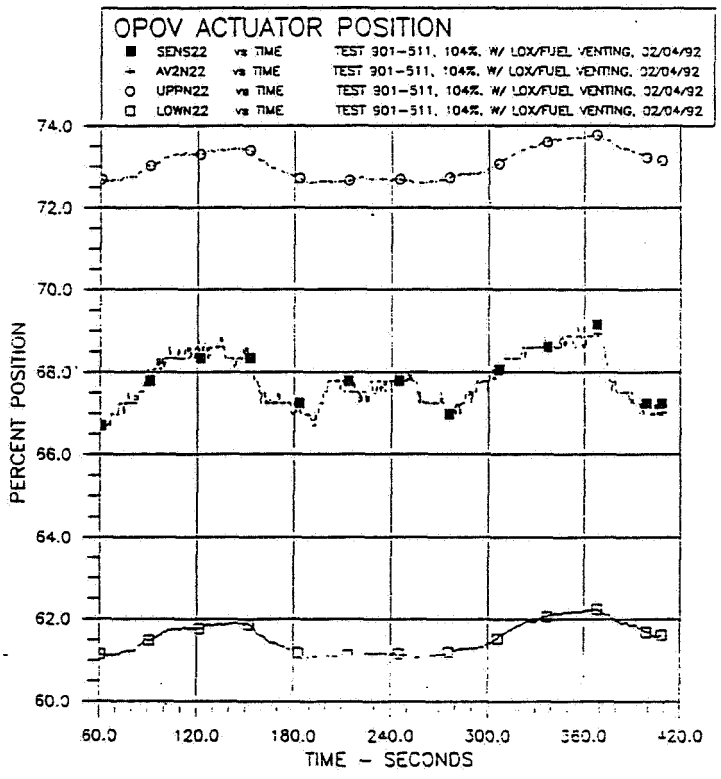

Figure 27.

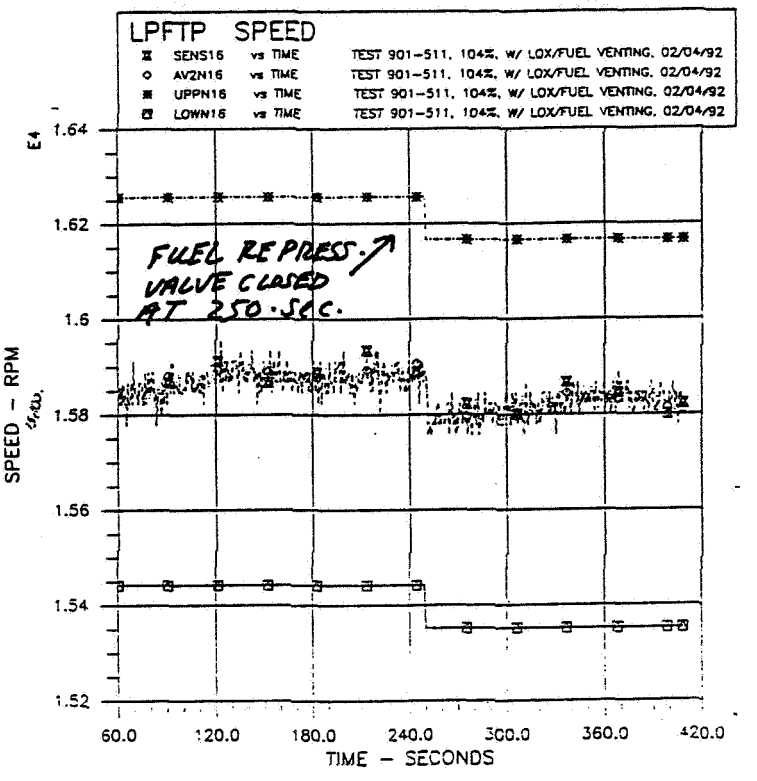

Figure 28.

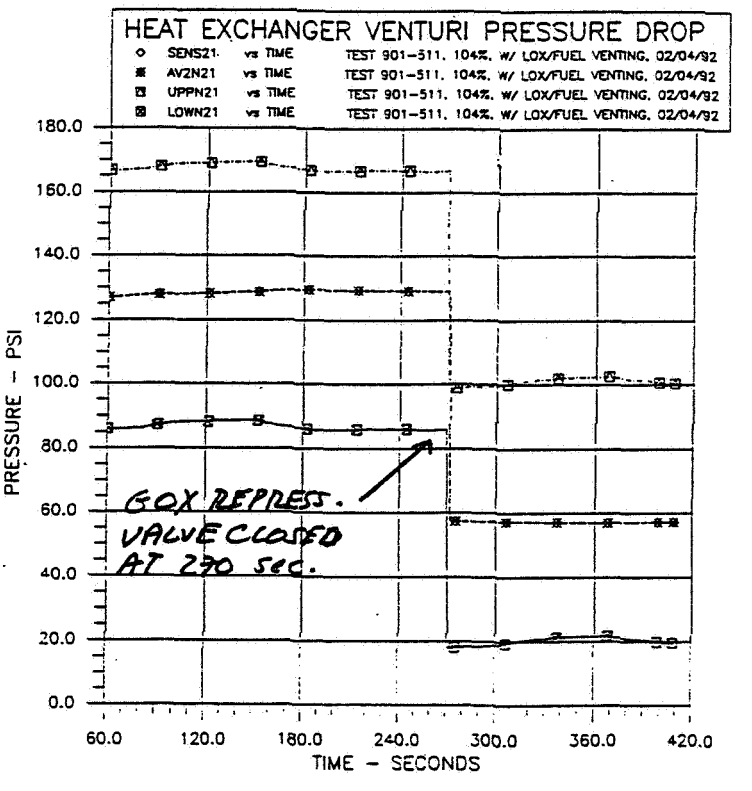

Figure 29.

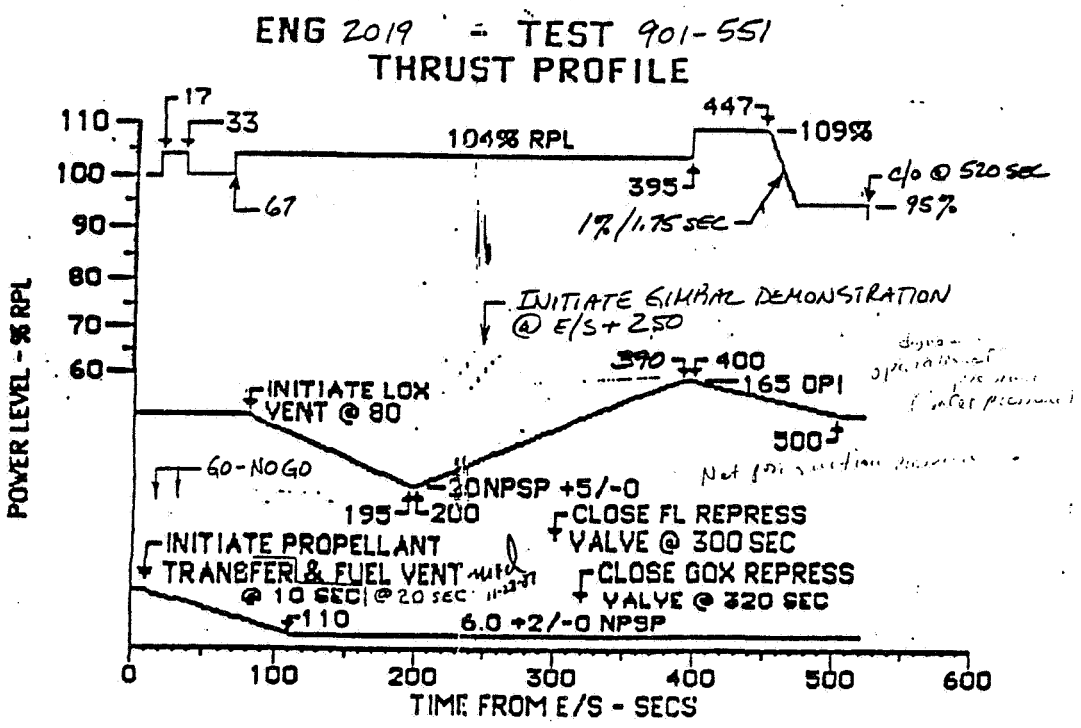

Figure 30.

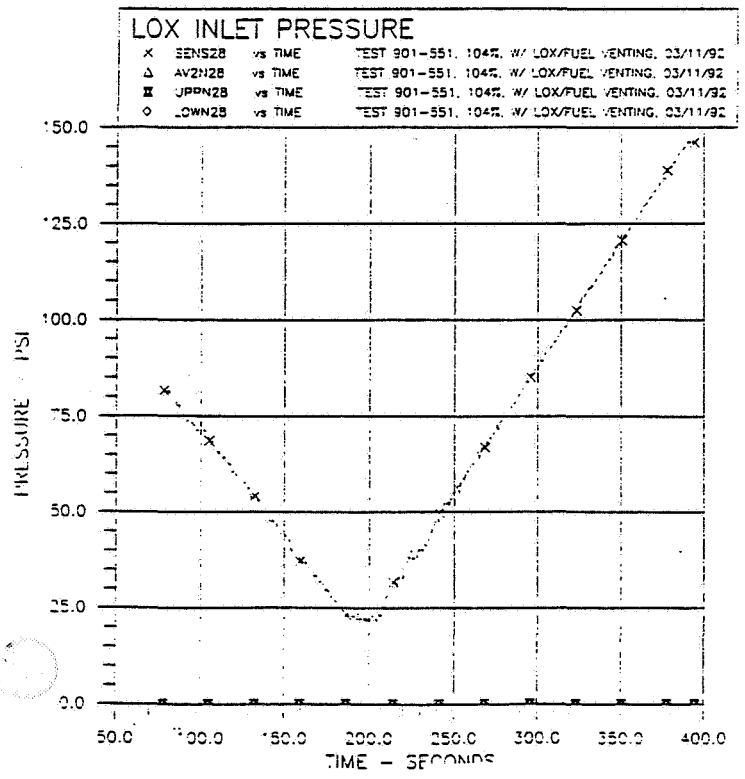

Figure 31.

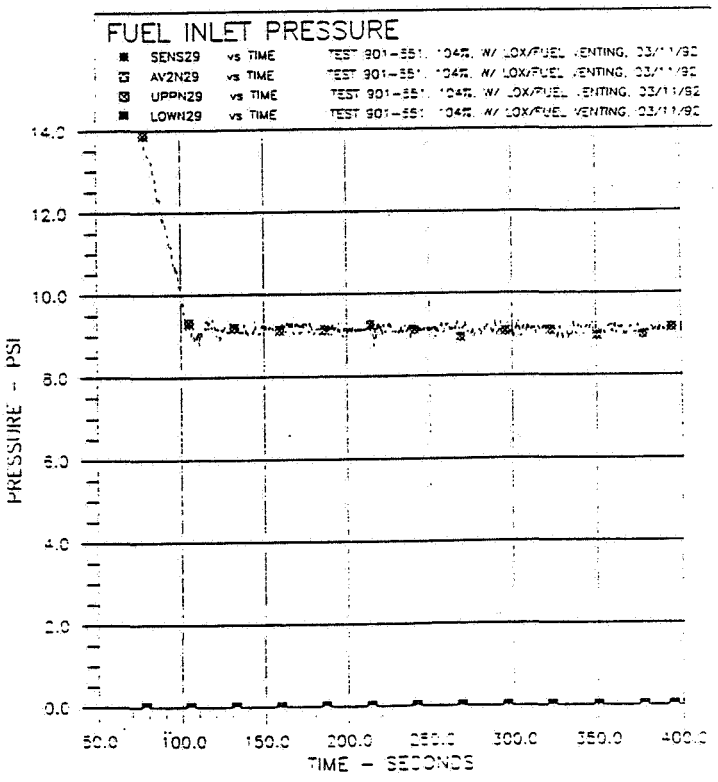

Figure 32.

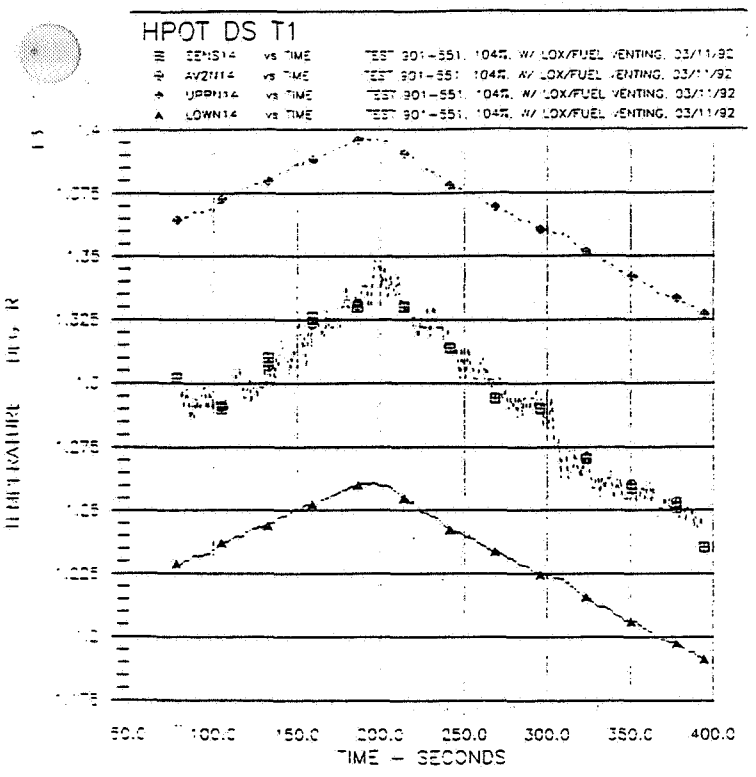

Figure 33.

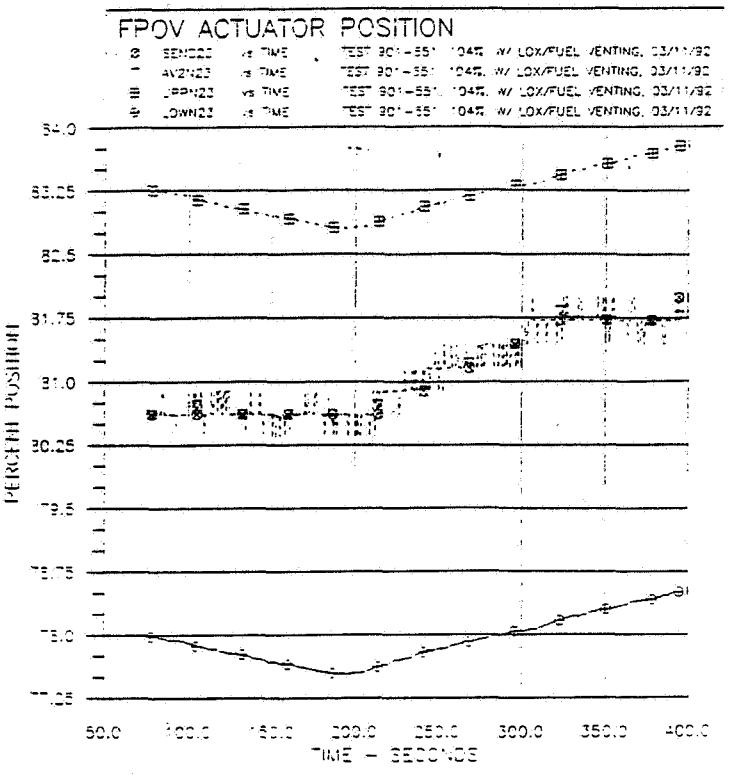

Figure 34.

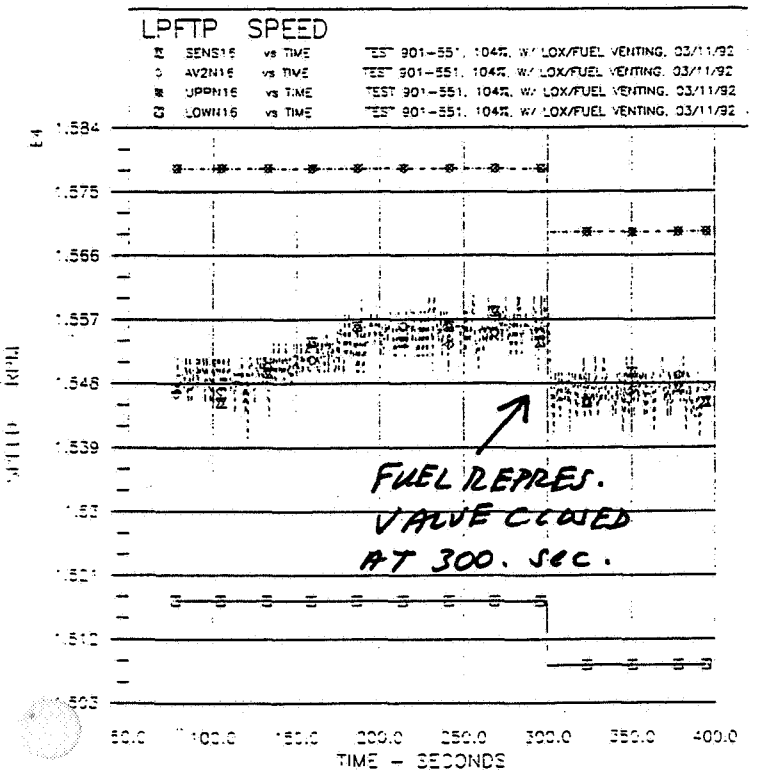

Figure 35.

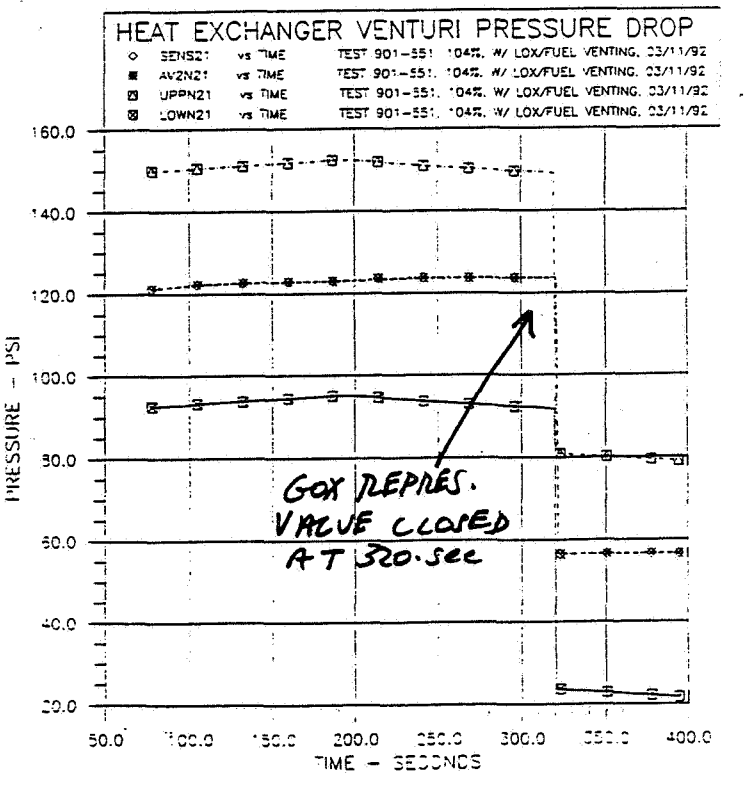

Figure 36.

ENG 0219 - TEST 901-683
THRUST PROFILE

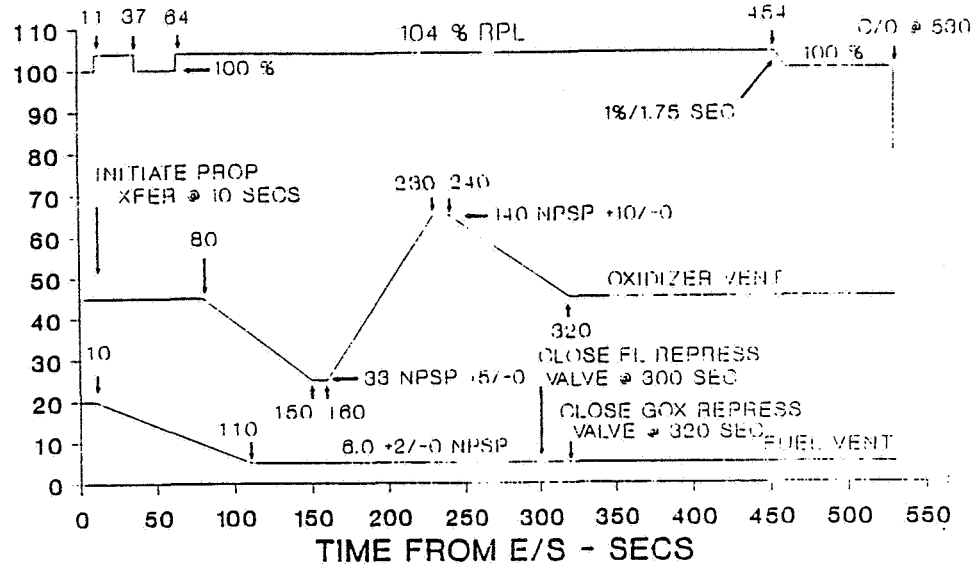

Figure 37.

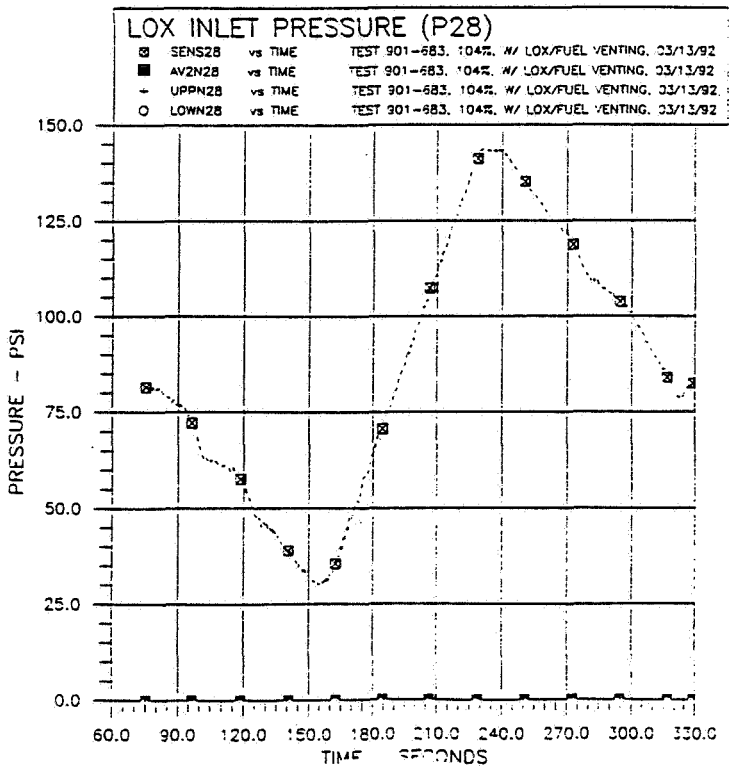

Figure 38.

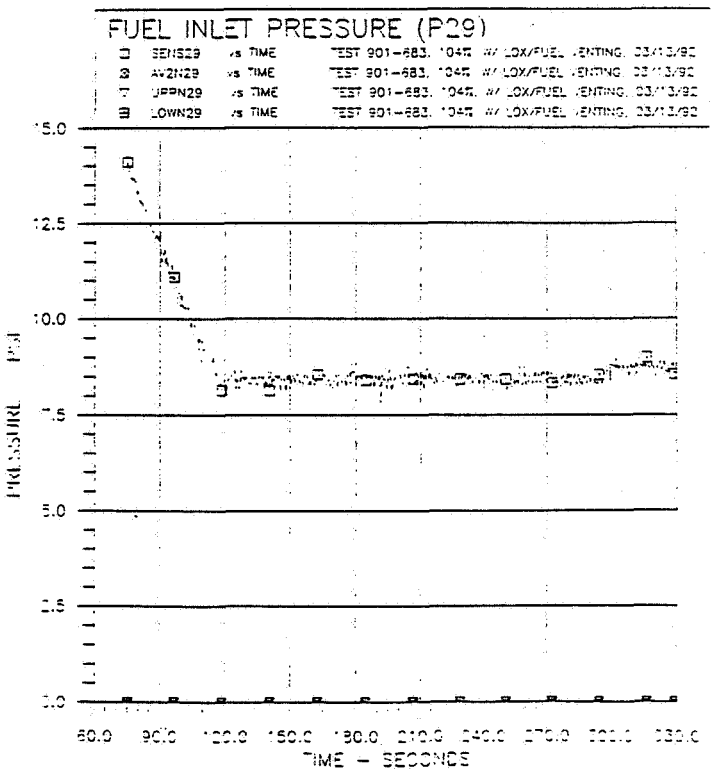

Figure 39.

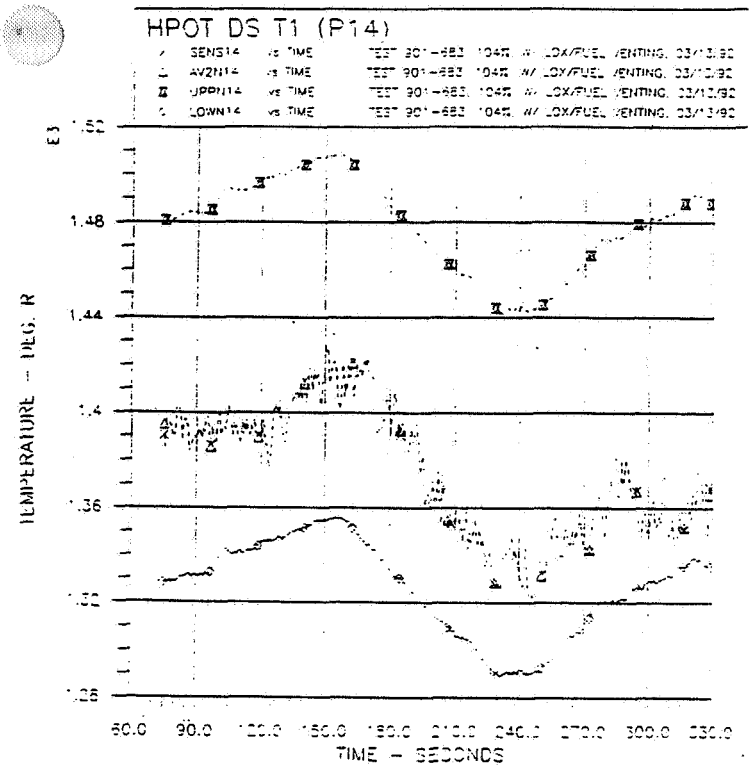

Figure 40.

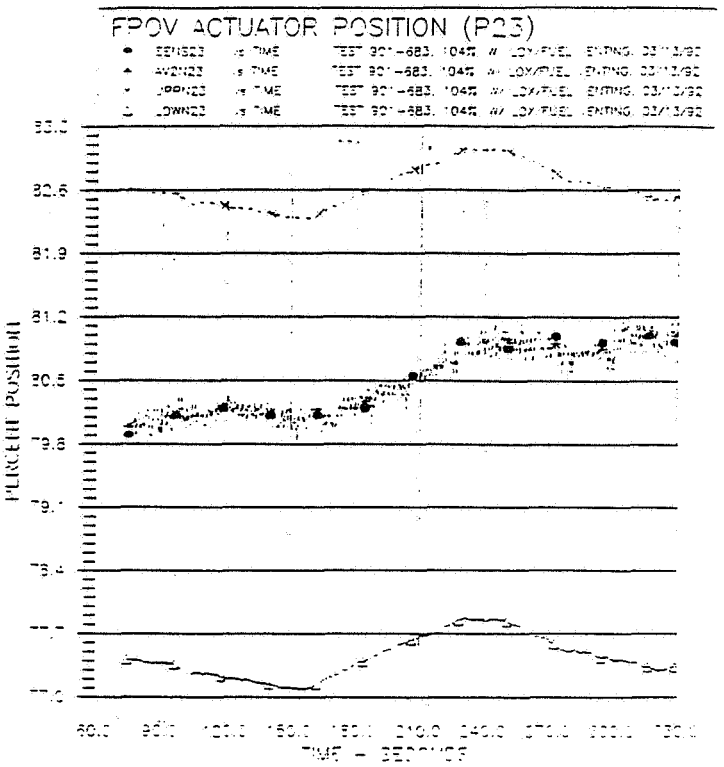

Figure 41.

ORIGINAL PAGE IS
OF POOR QUALITY

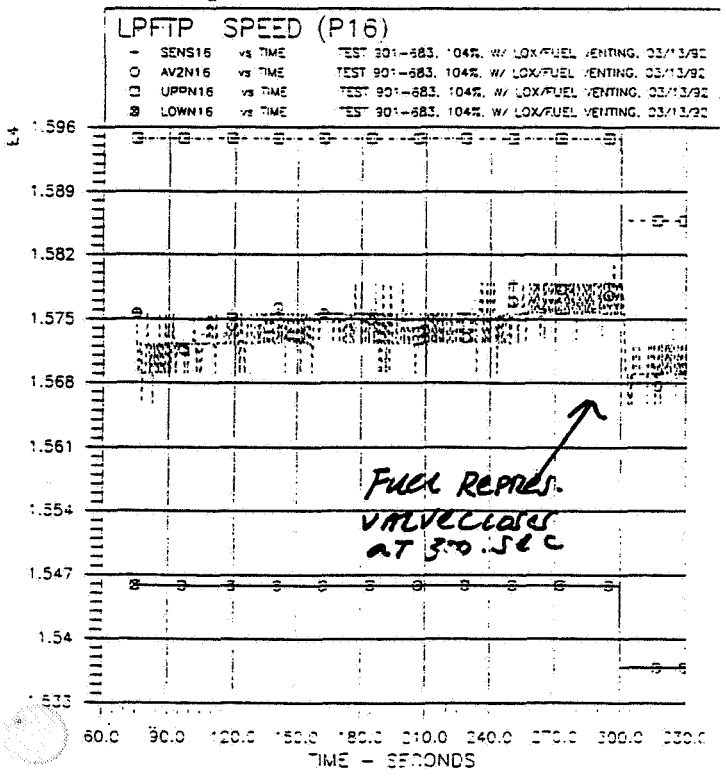

Figure 42.

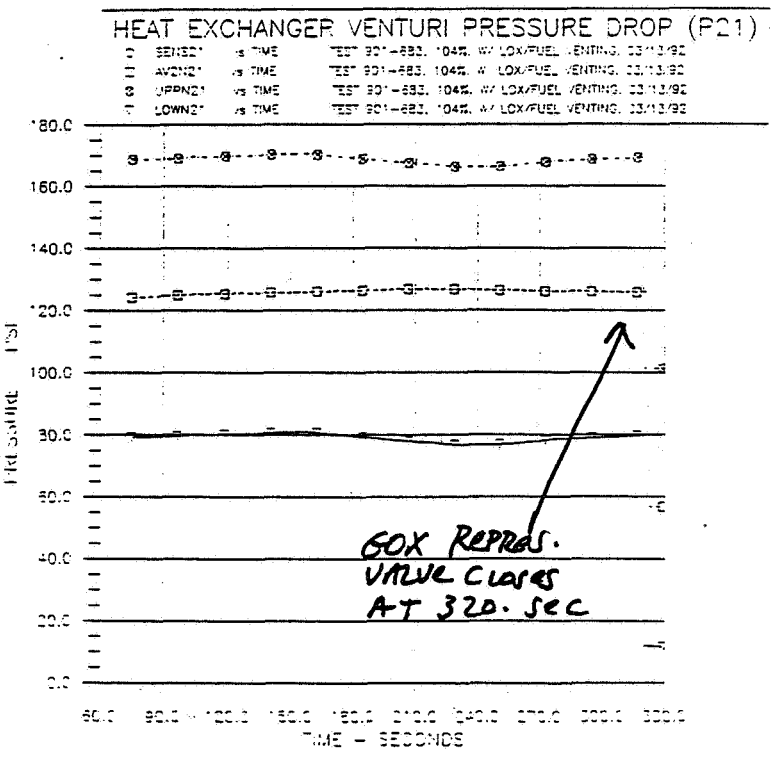

Figure 43.

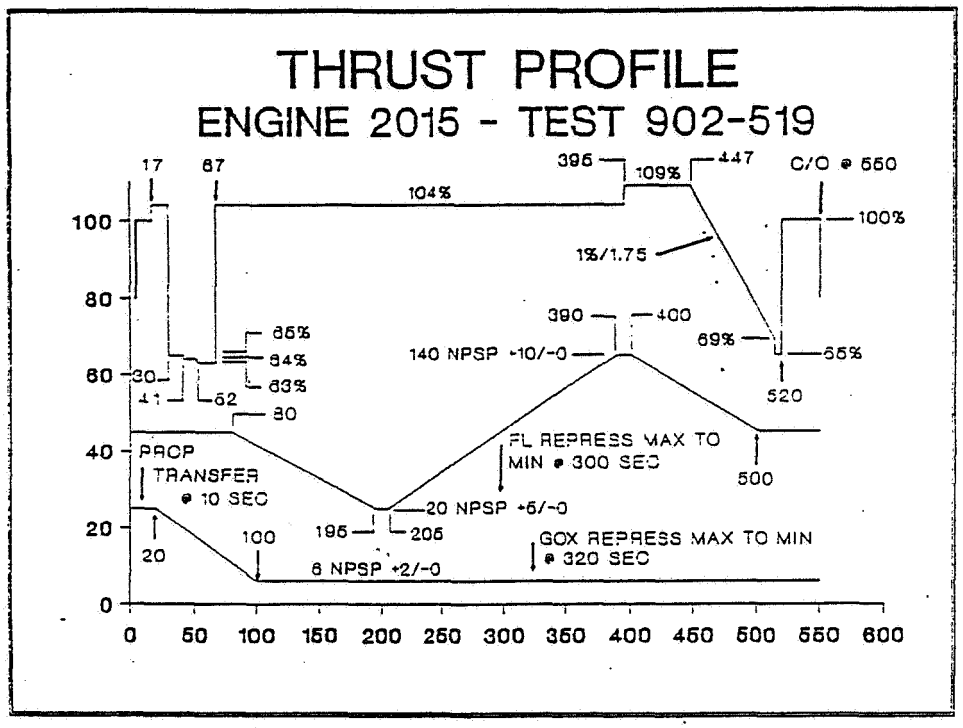

Figure 44.

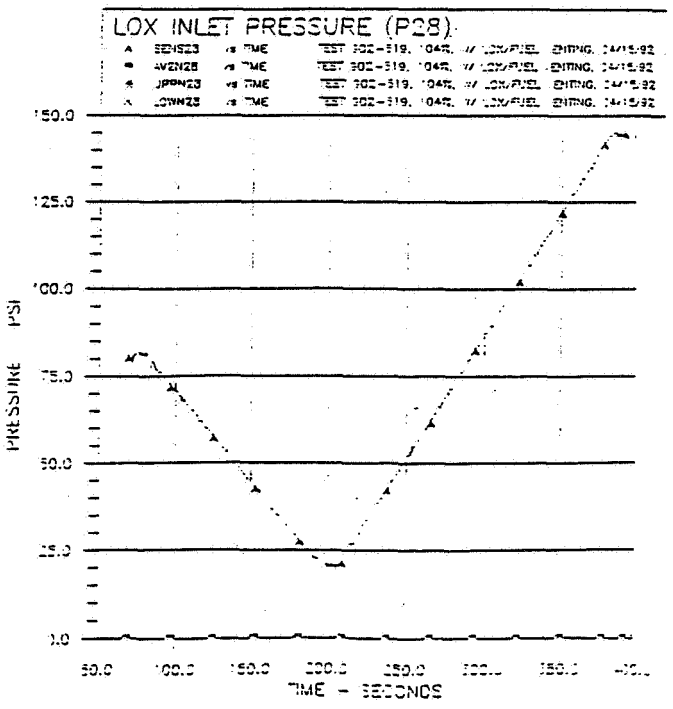

Figure 45.

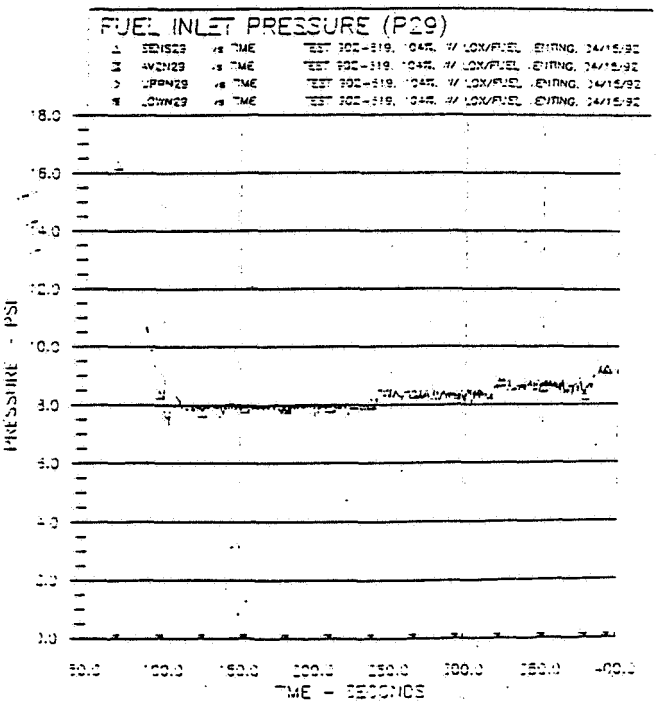

Figure 46.

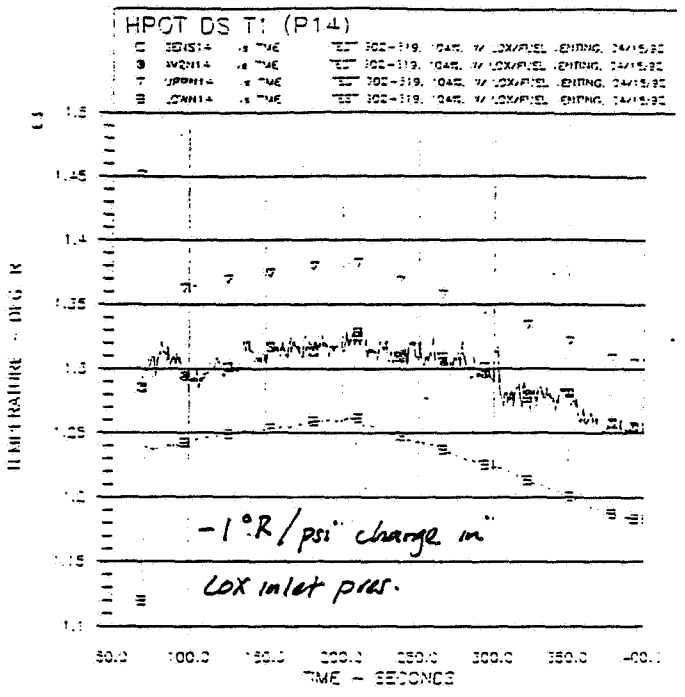

Figure 47.

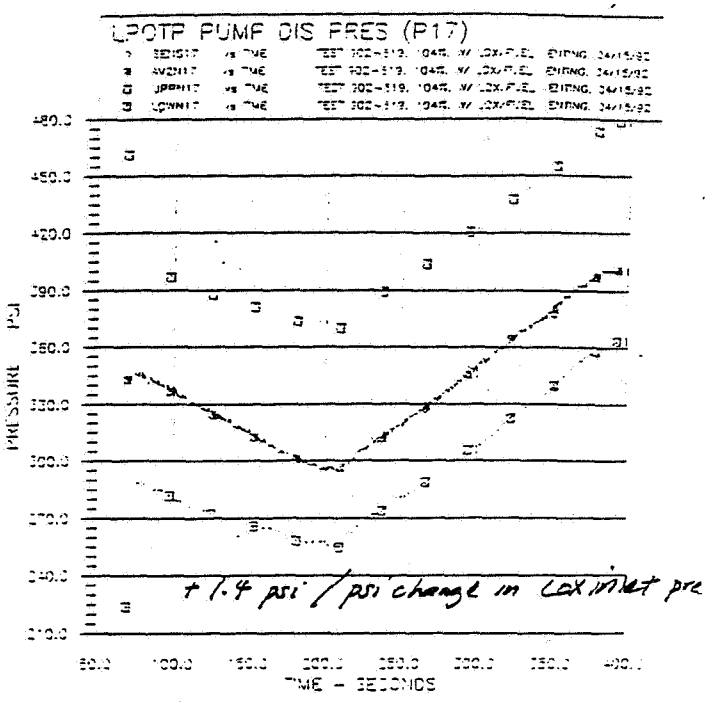

Figure 48.

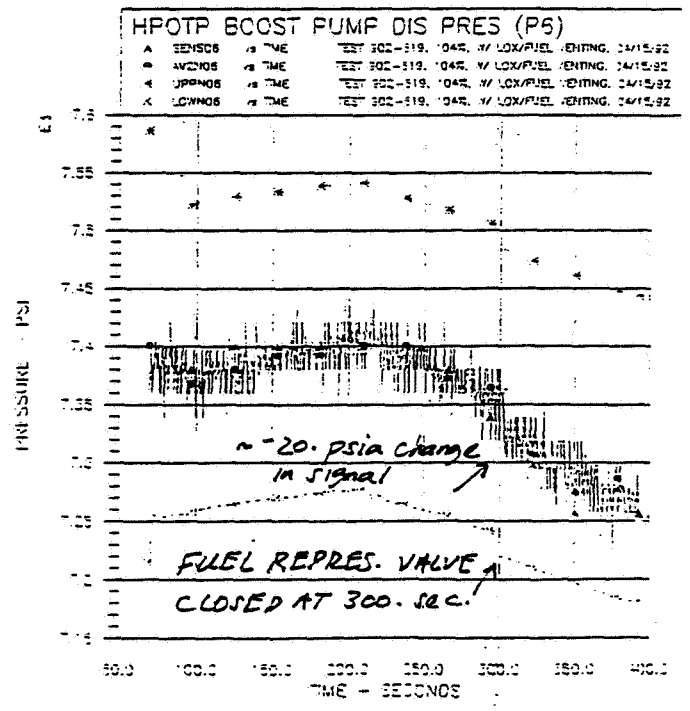

Figure 49.

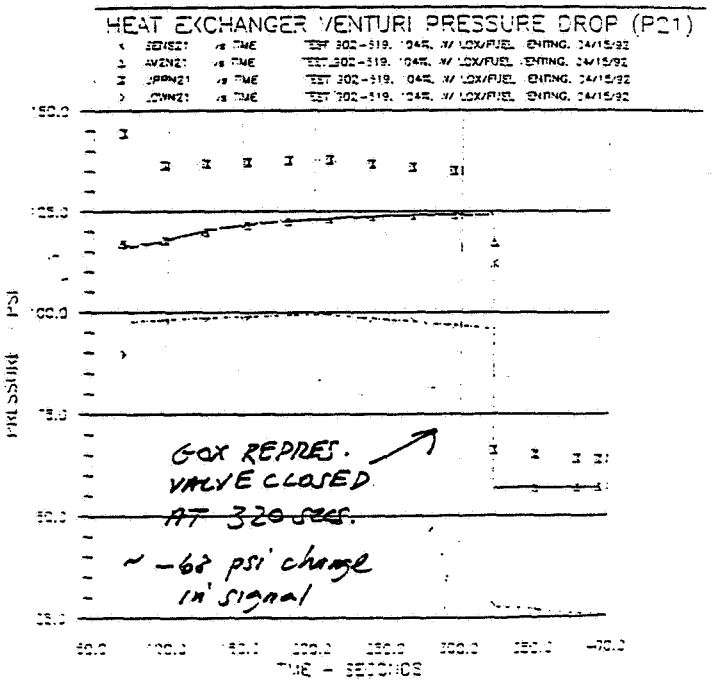

Figure 50.

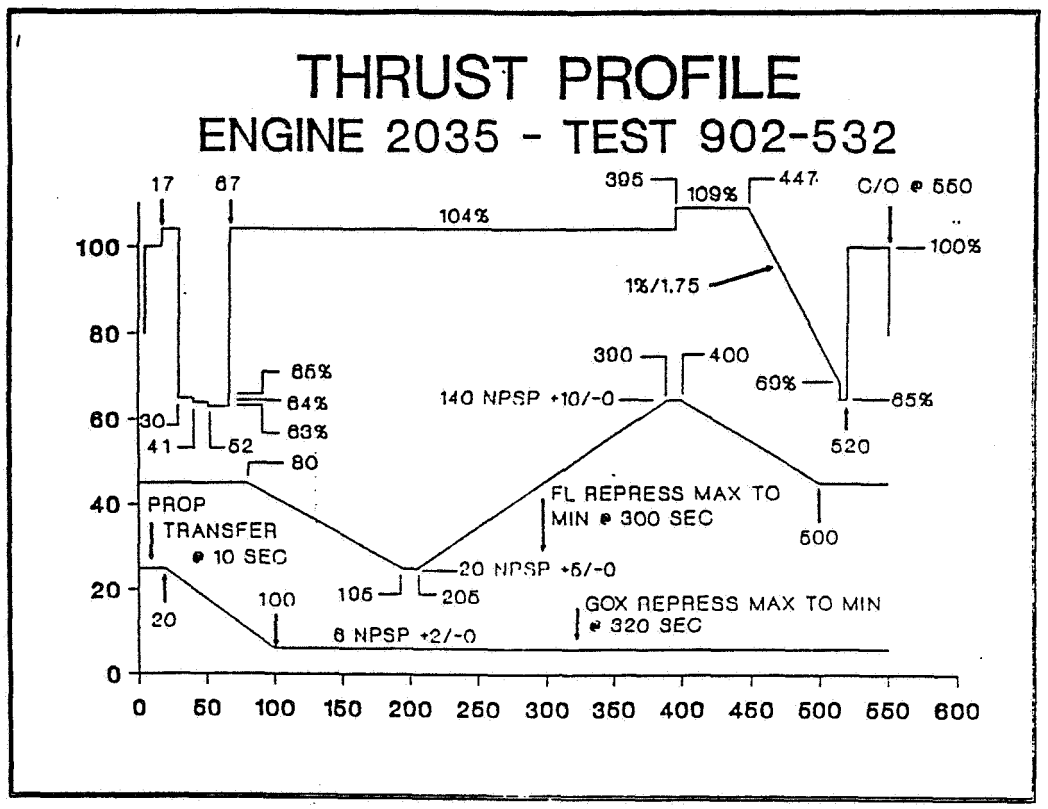

Figure 51.

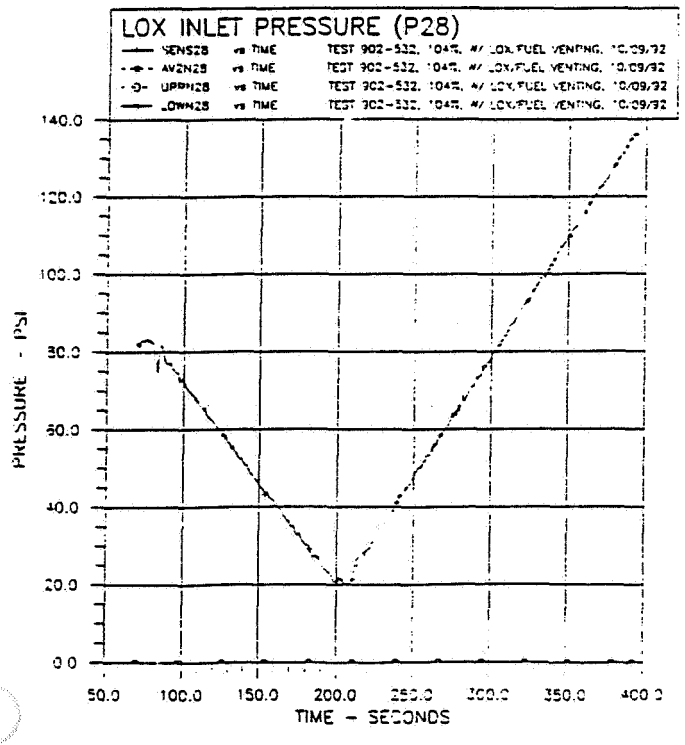

Figure 52.

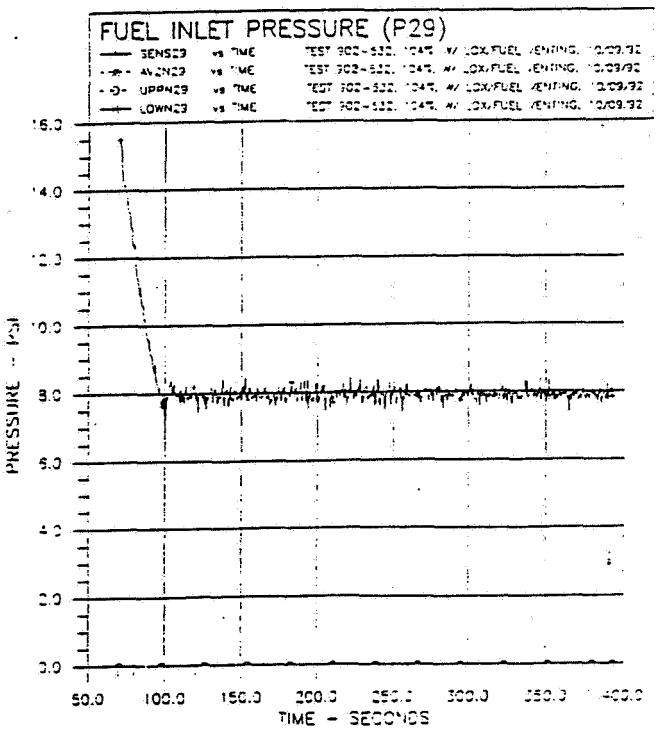

Figure 53.

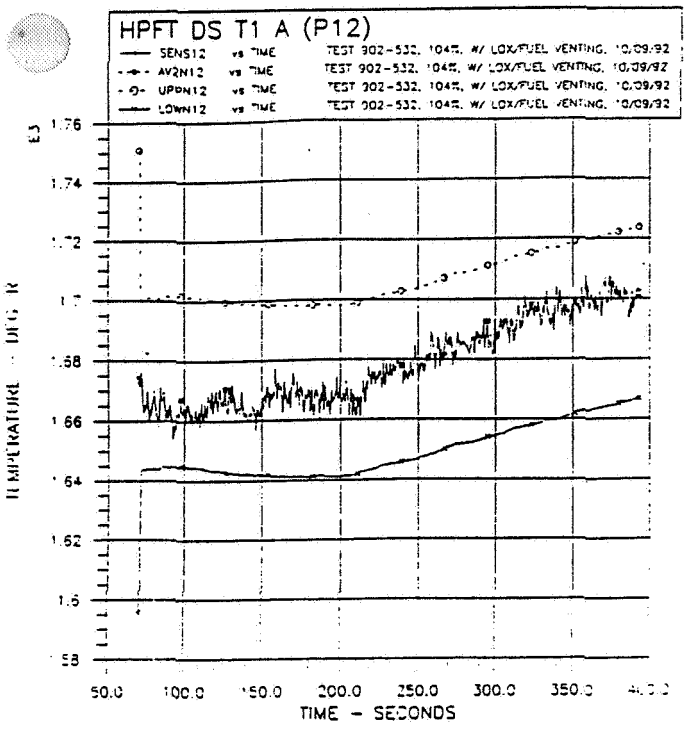

Figure 54.

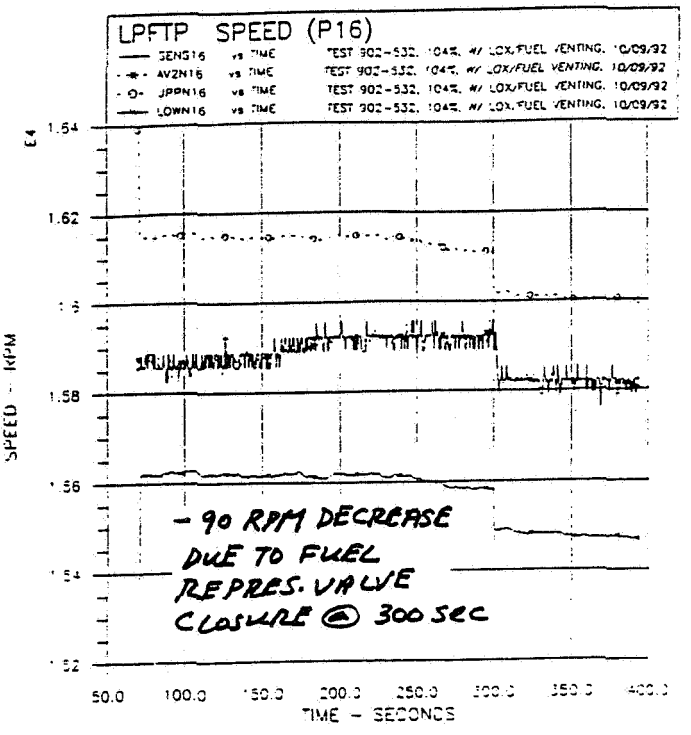

Figure 55.

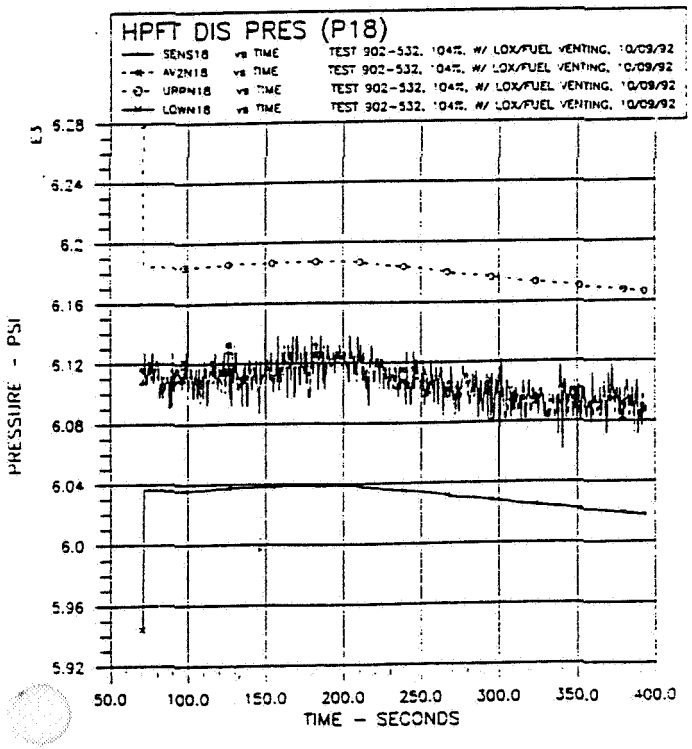

Figure 56.

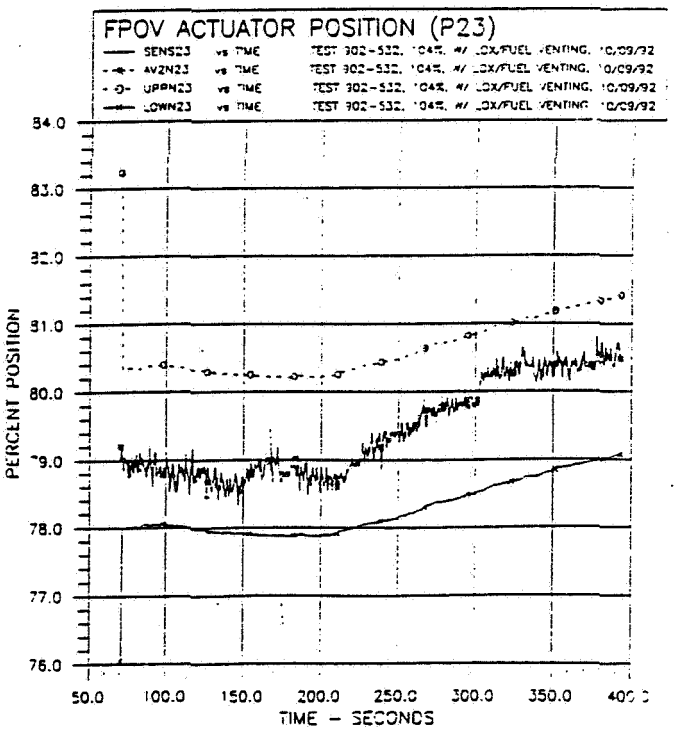

Figure 57.

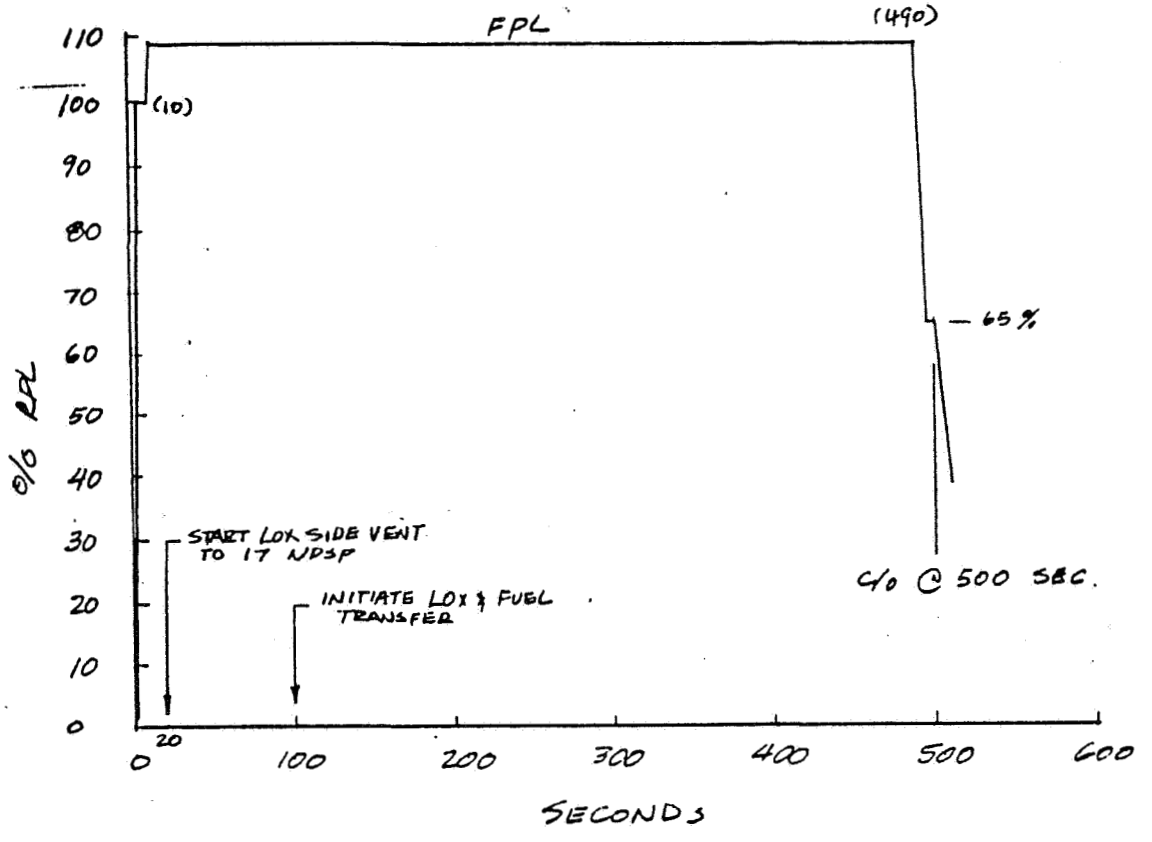

Figure 58. Thrust Profile, Test 902-249

ORIGINAL PAGE IS
OF POOR QUALITY

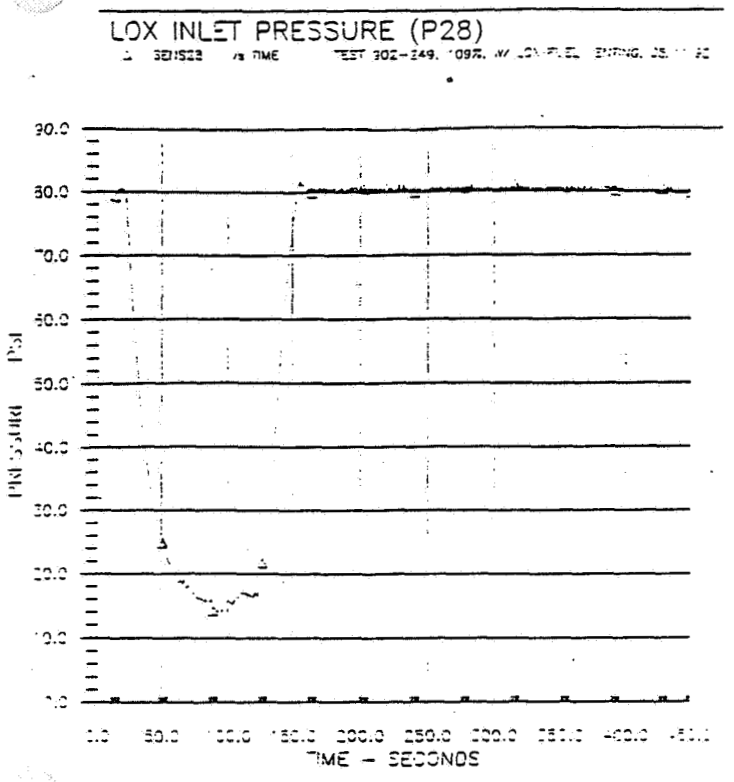

Figure 59.

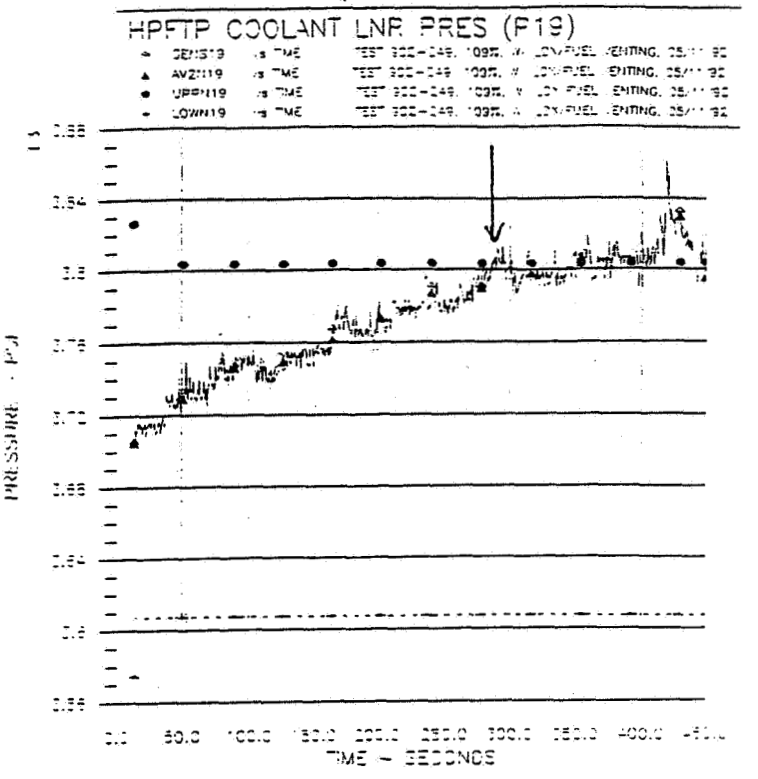

Figure 60.

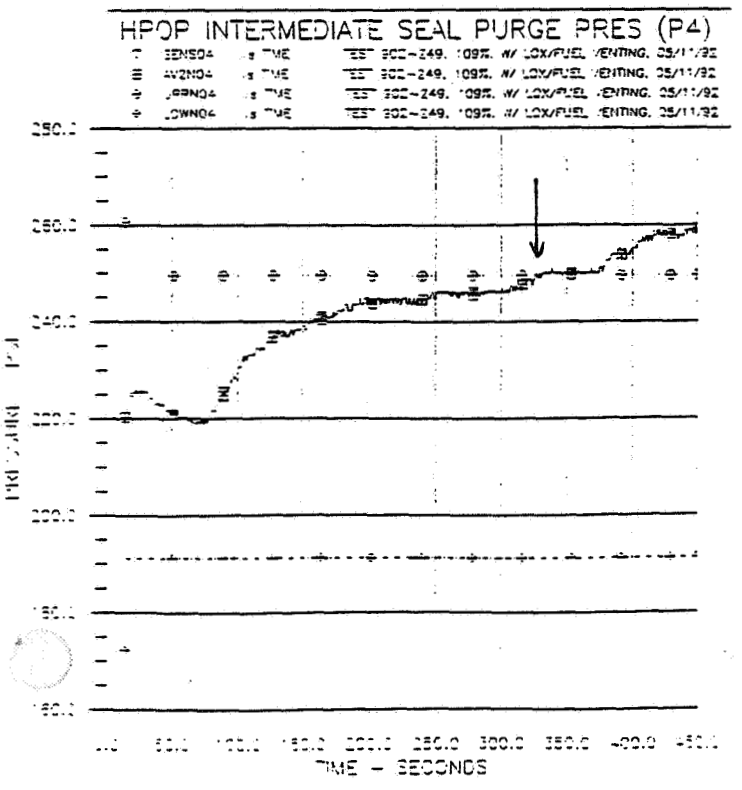

Figure 61.

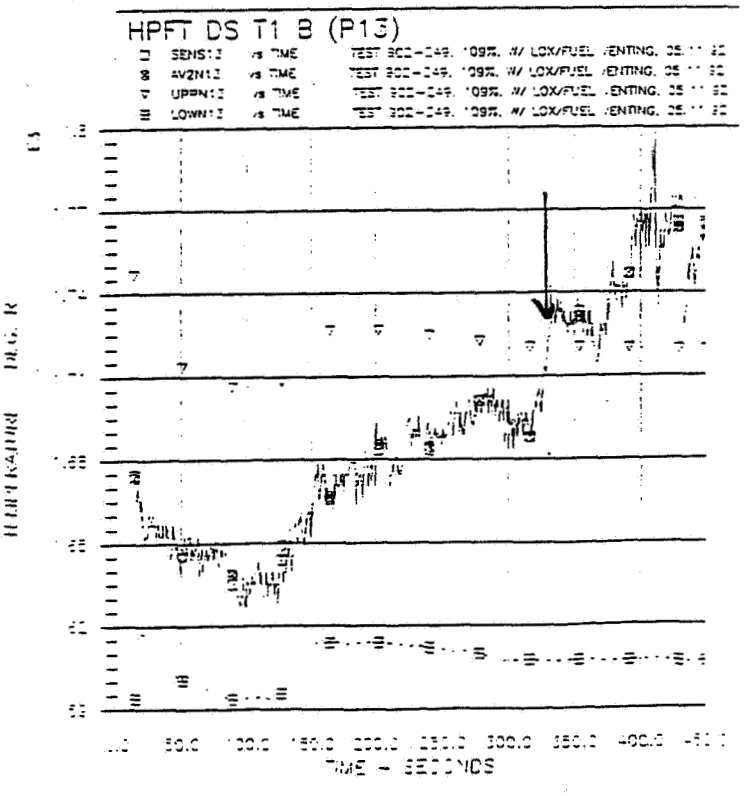

Figure 62.

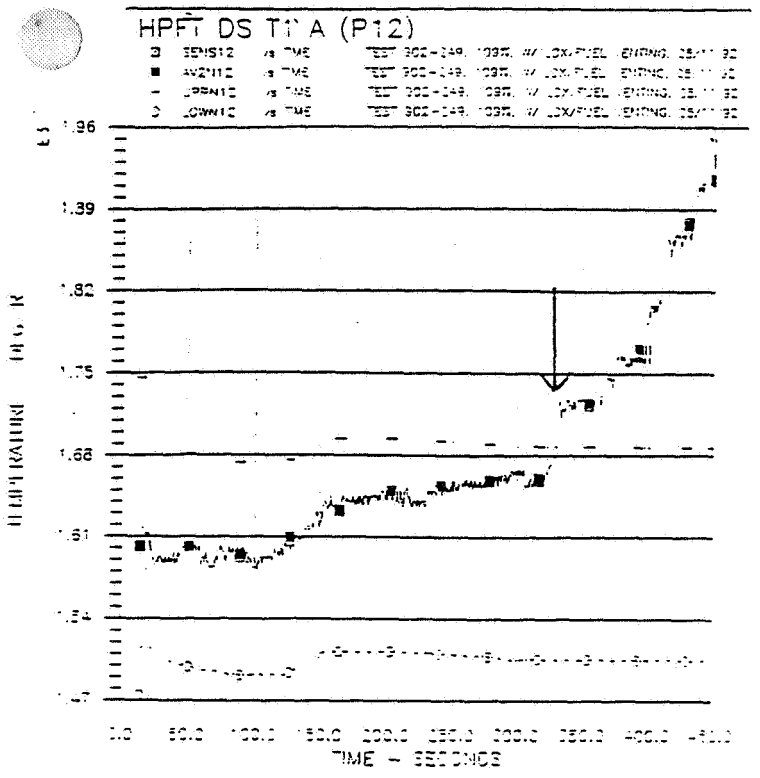

Figure 63.

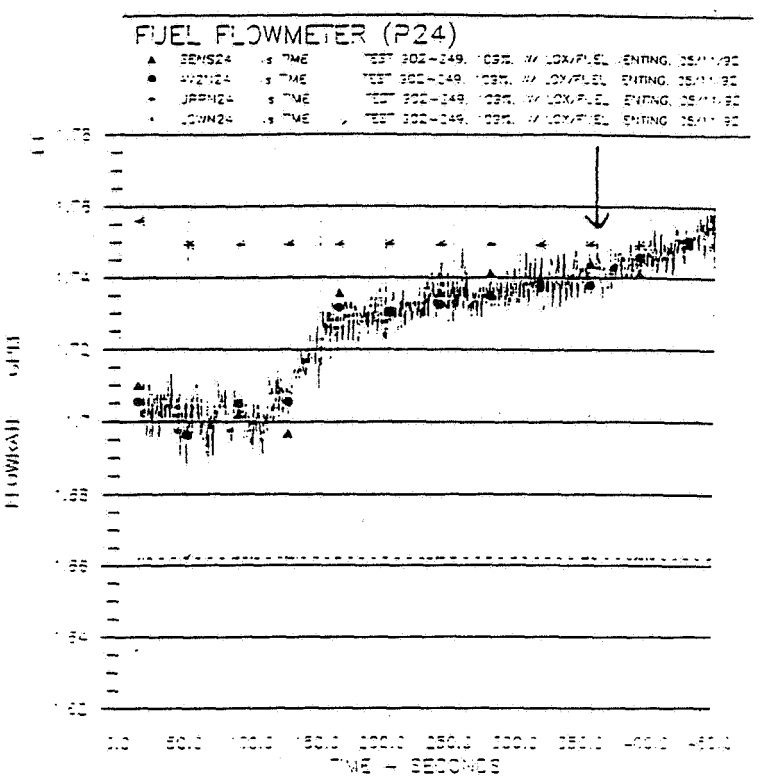

Figure 64.

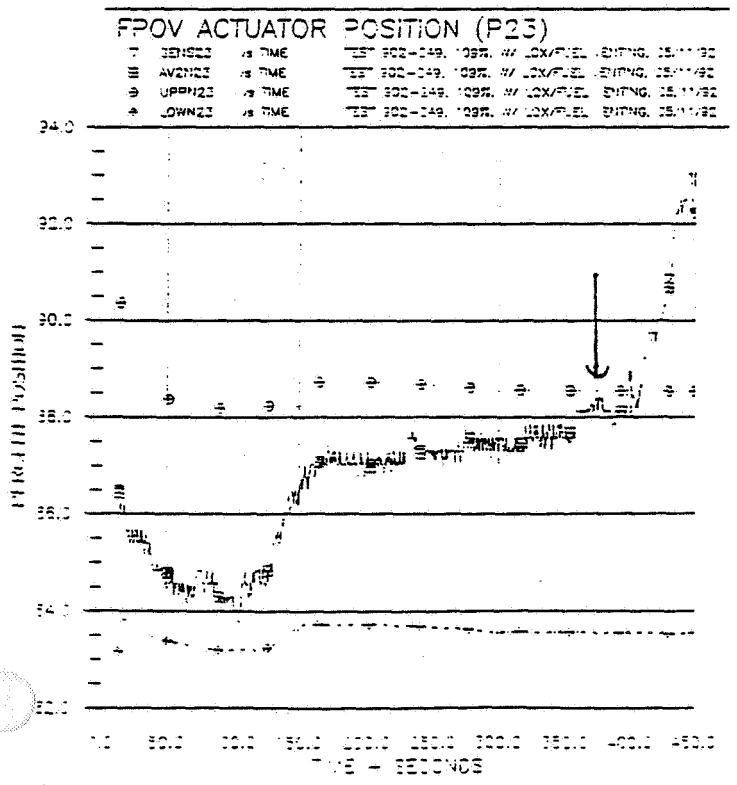

Figure 65.

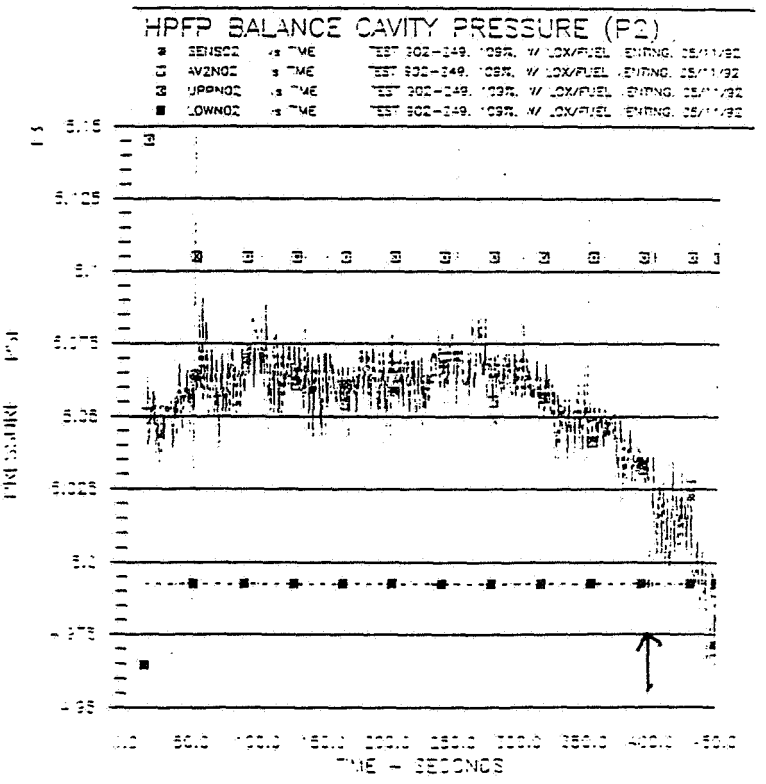

Figure 66.

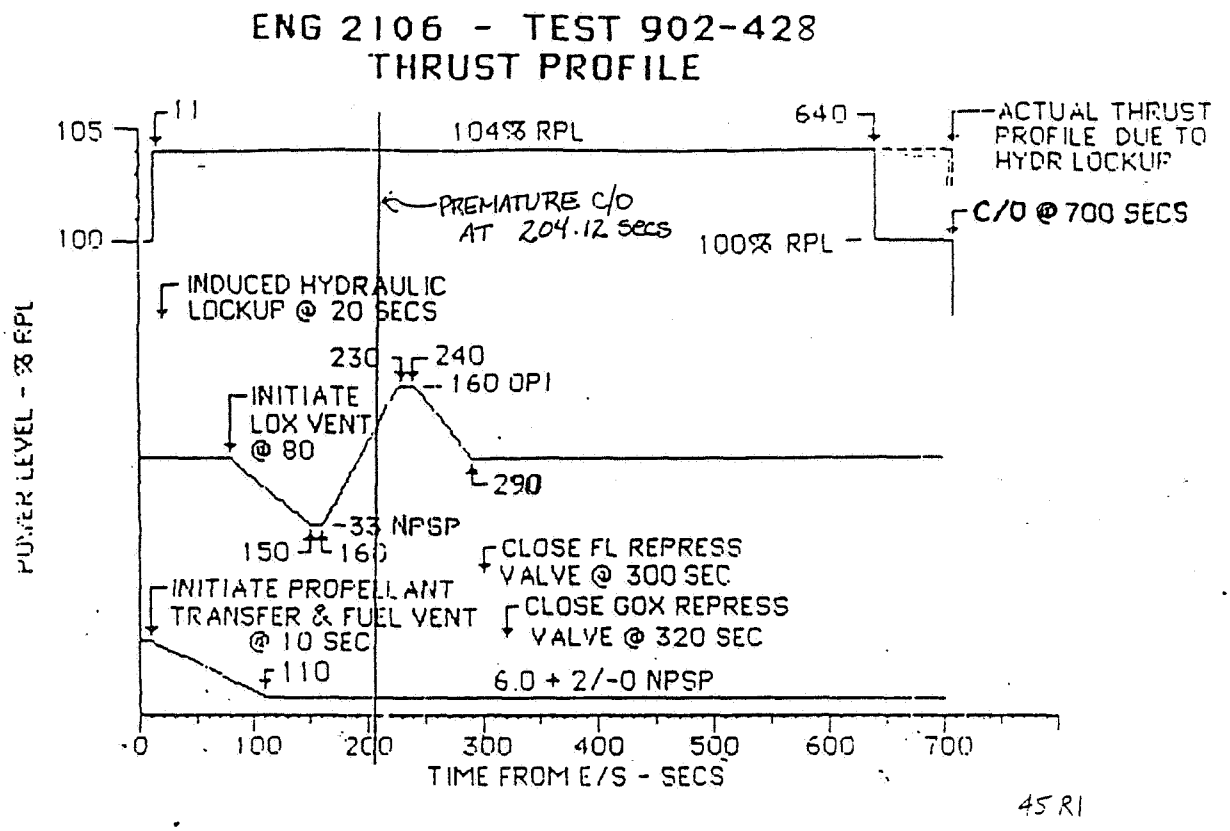

Figure 67.

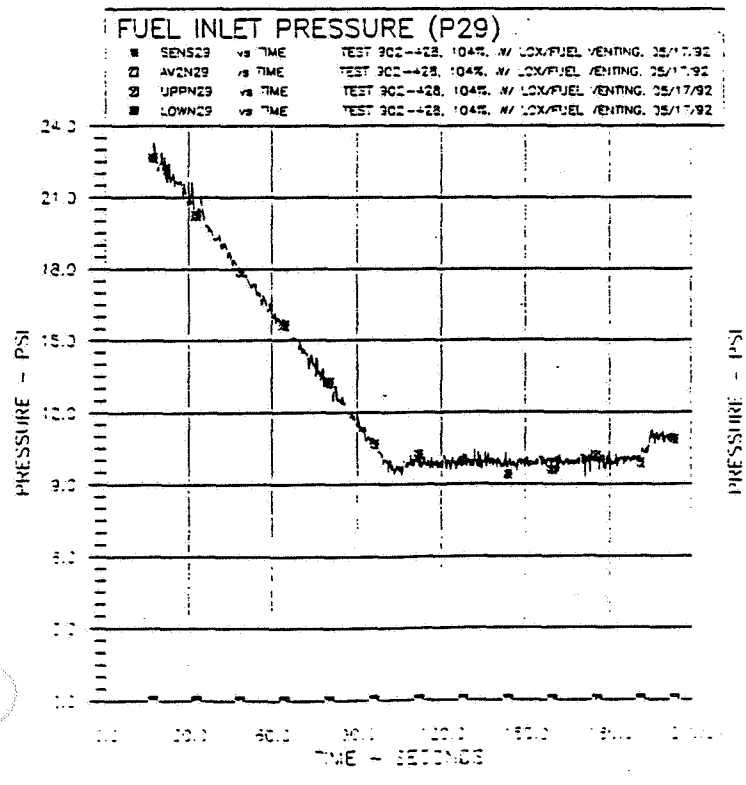

Figure 68.

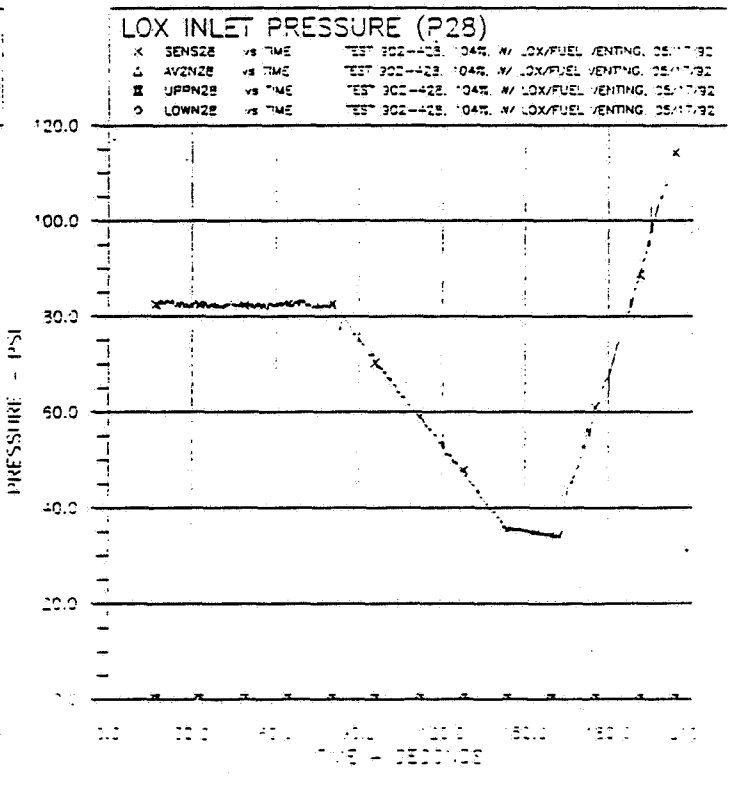

Figure 69.

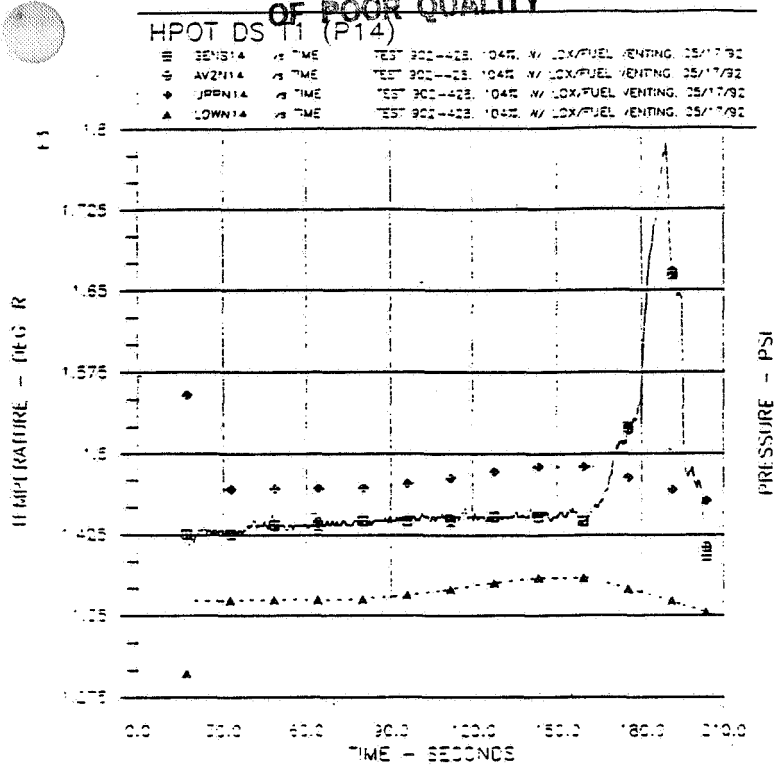

Figure 70.

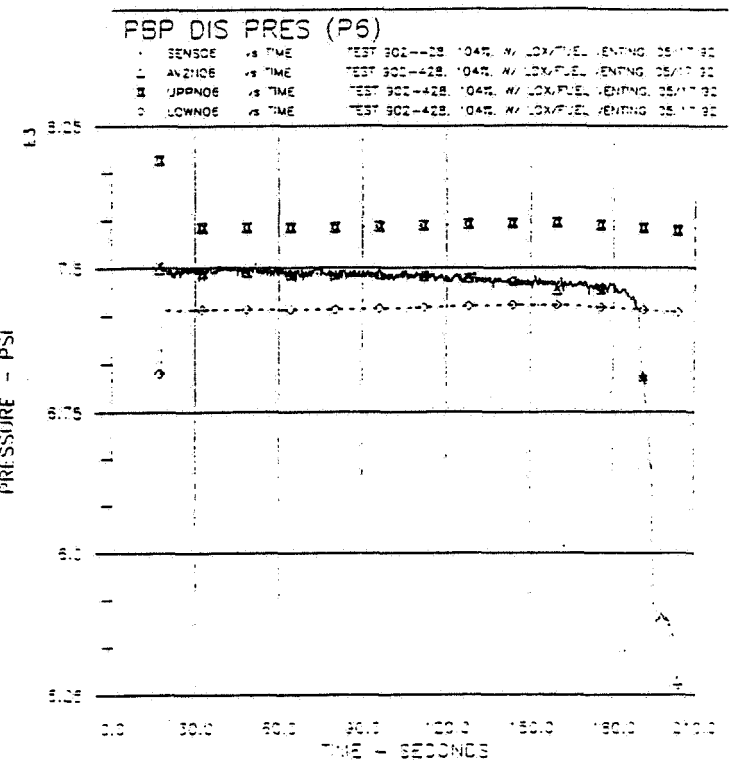

Figure 71.

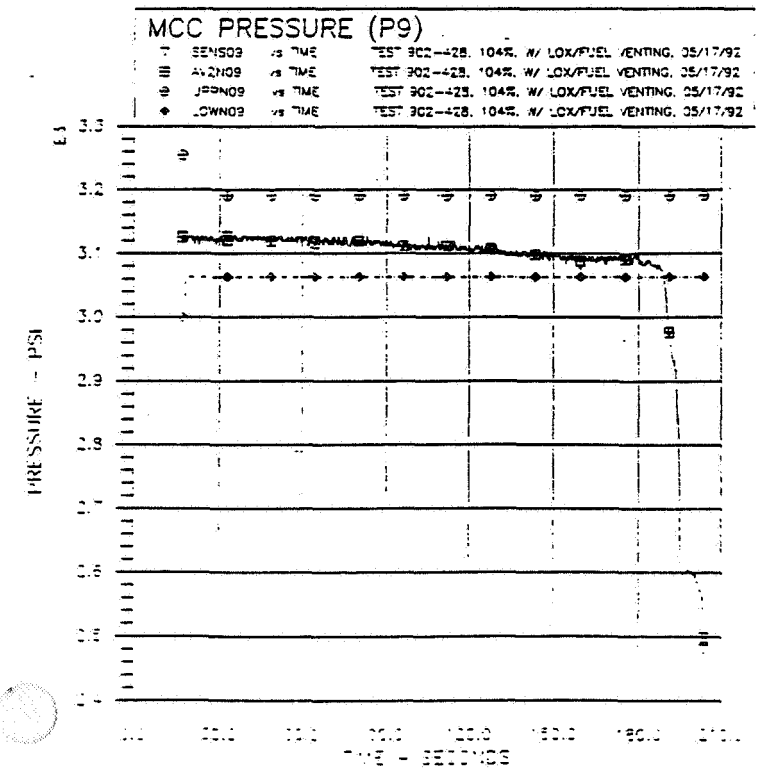

Figure 72.

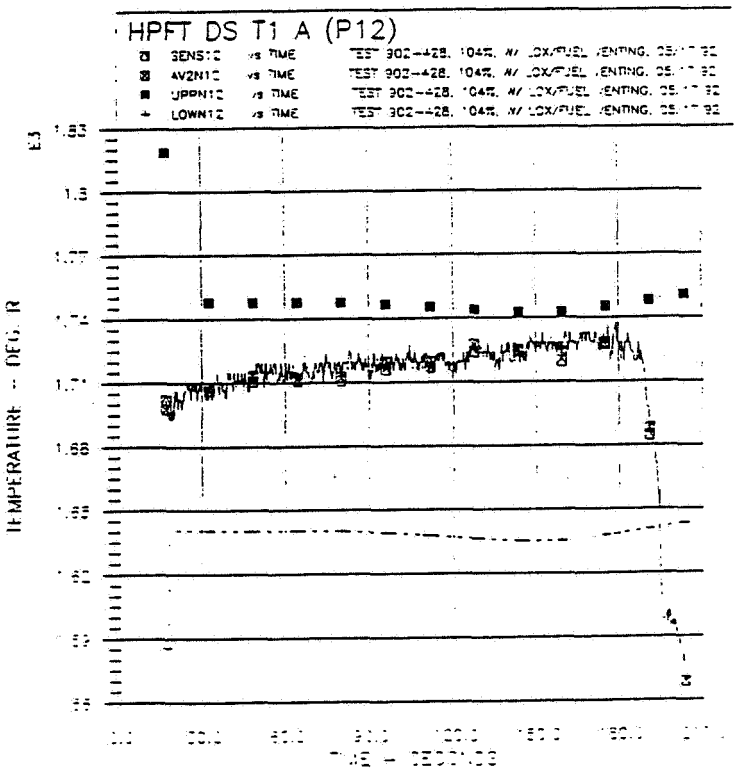

Figure 73.

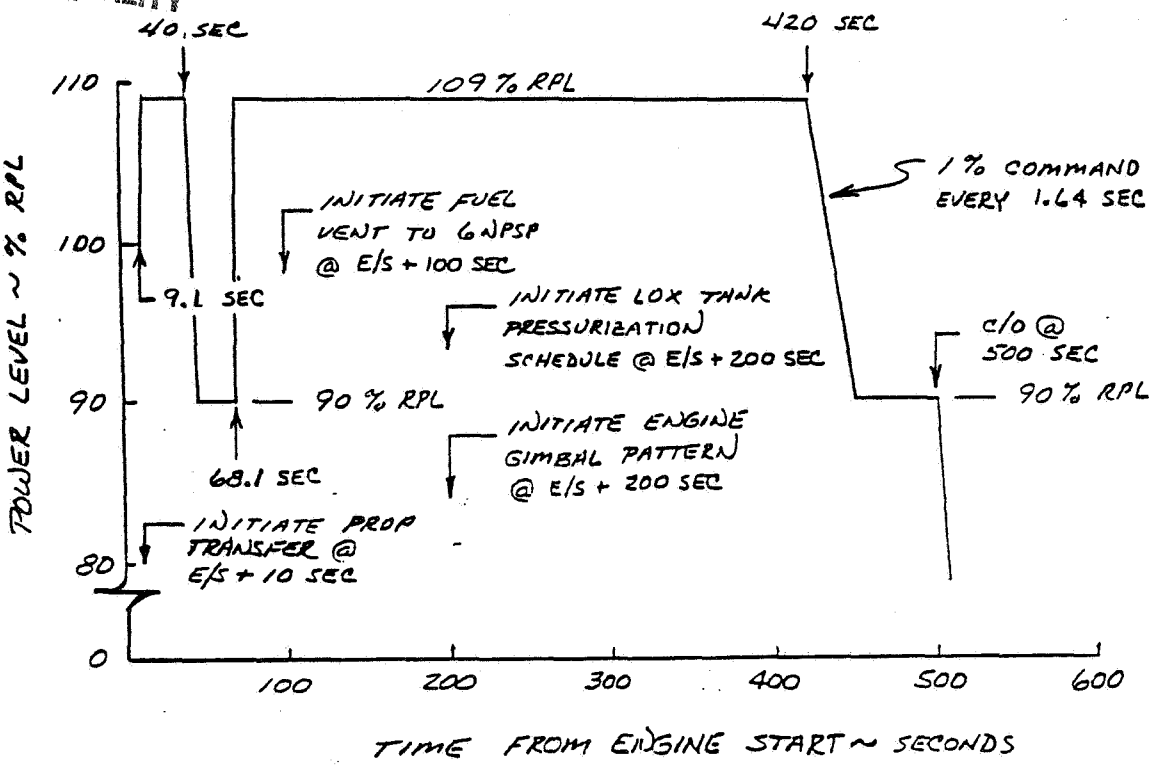

Figure 74. Thrust Profile, Test 901-364

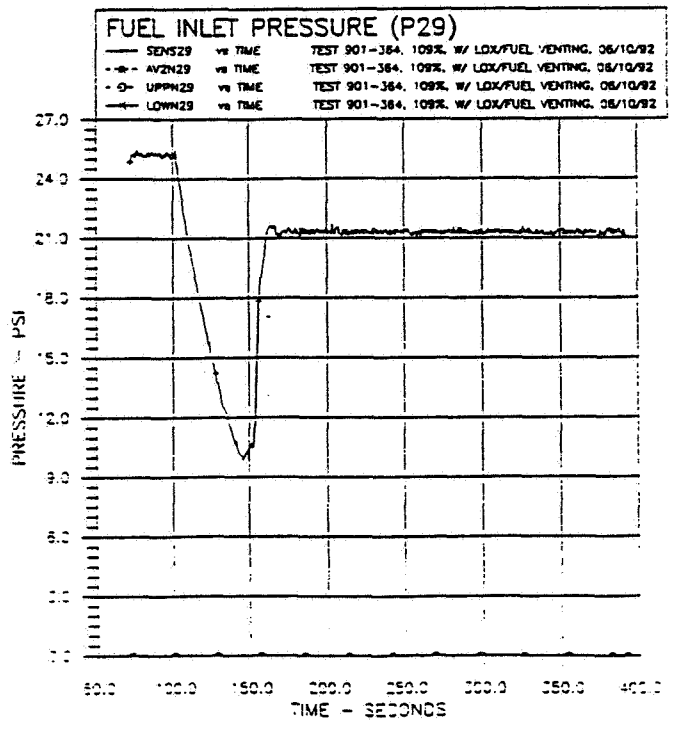

Figure 75.

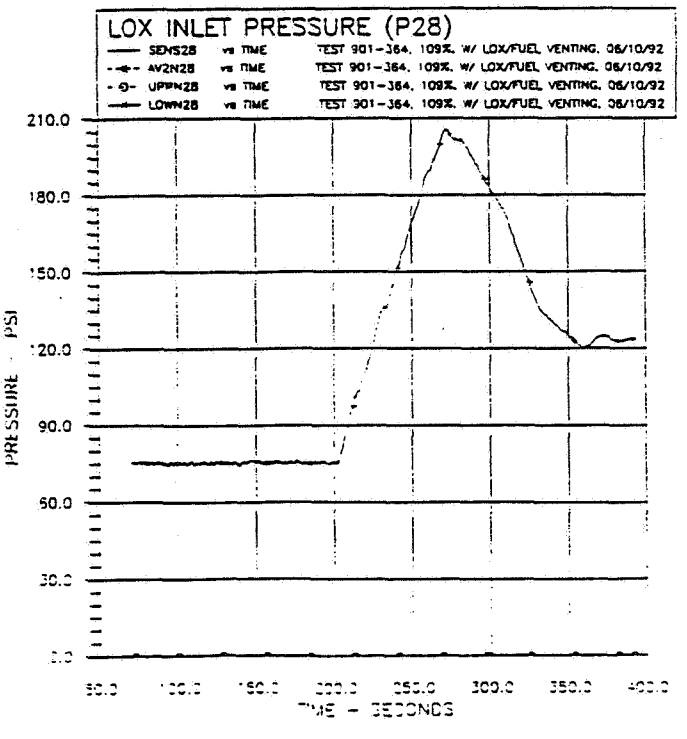

Figure 76.

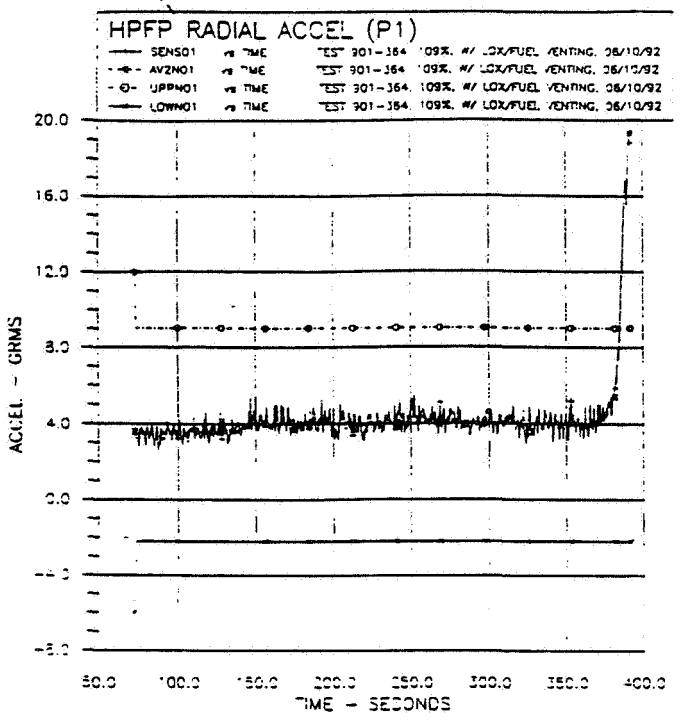

Figure 77.

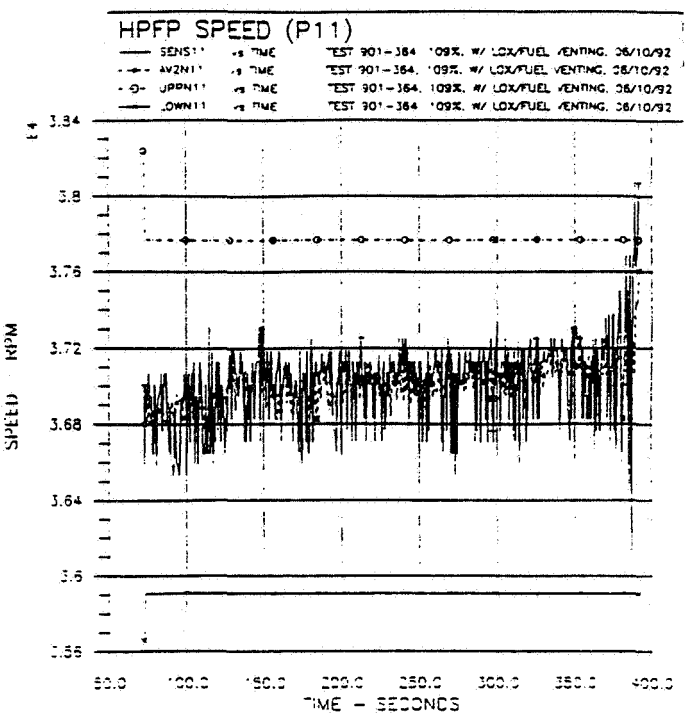

Figure 78.

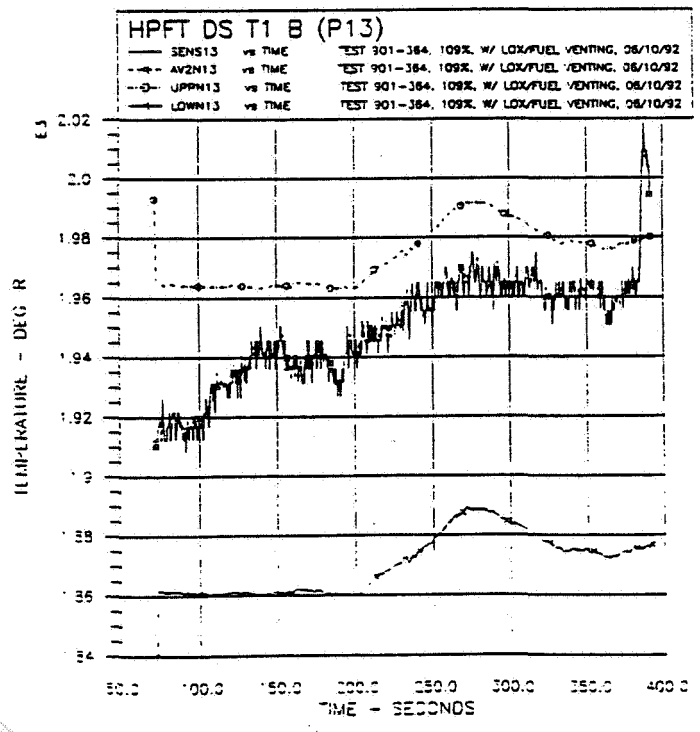

Figure 79.

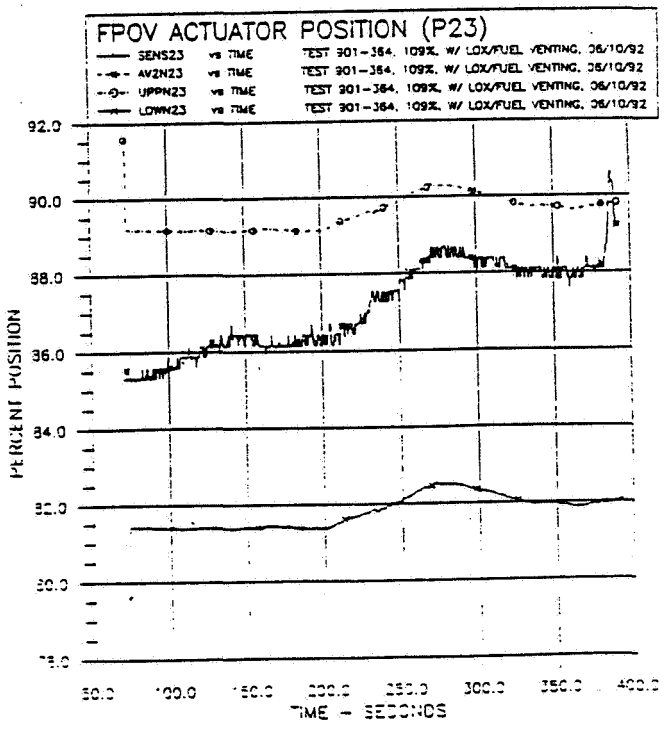

Figure 80.

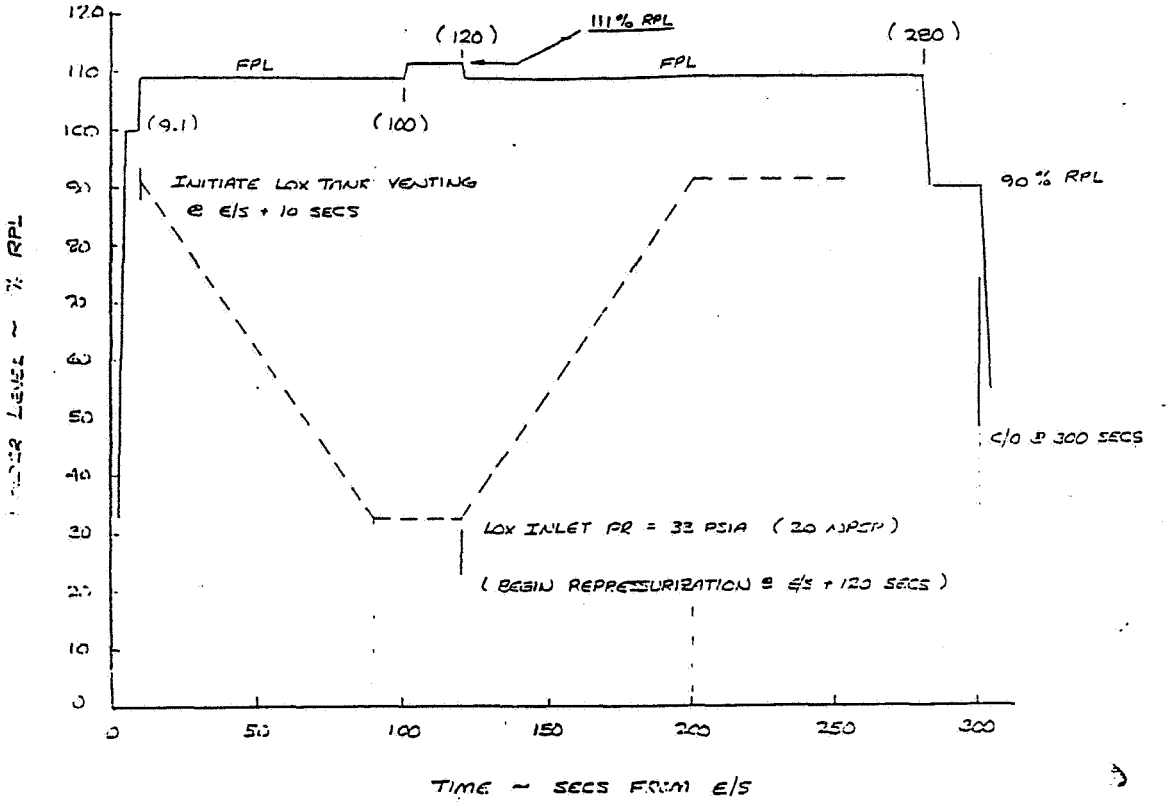

Figure 81. Thrust Profile, Test 750-175

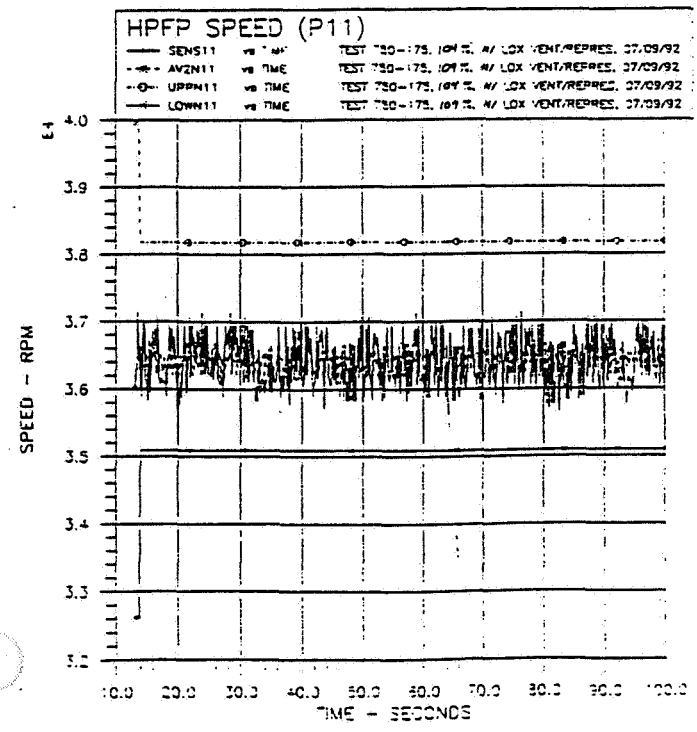

Figure 82.

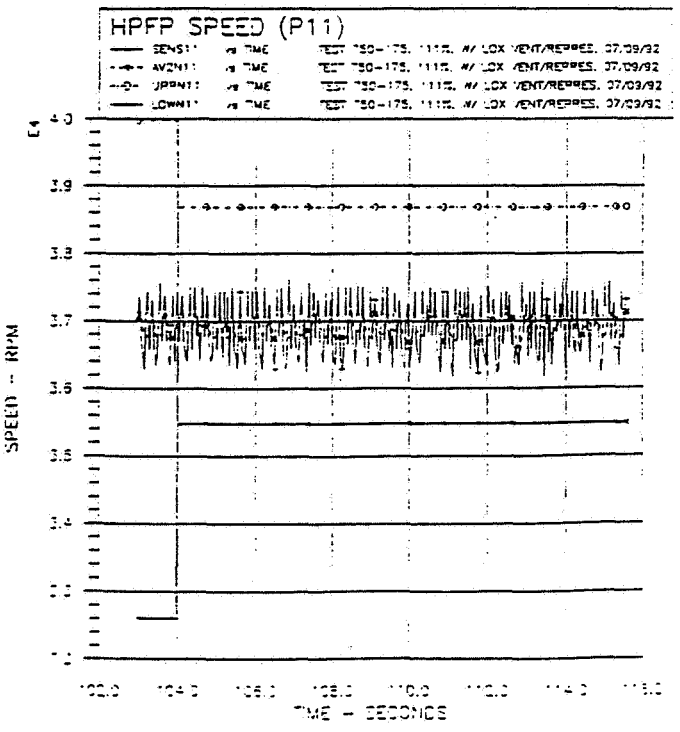

Figure 83.

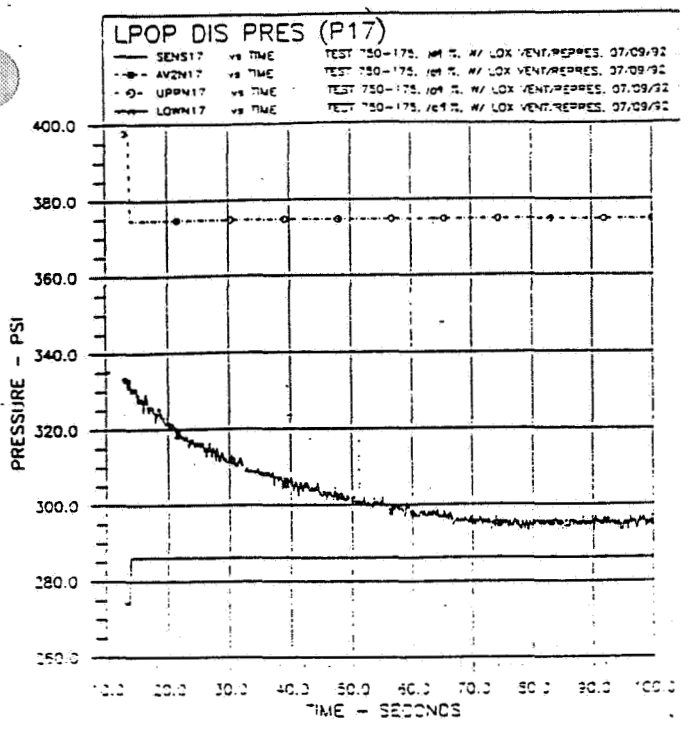

Figure 84.

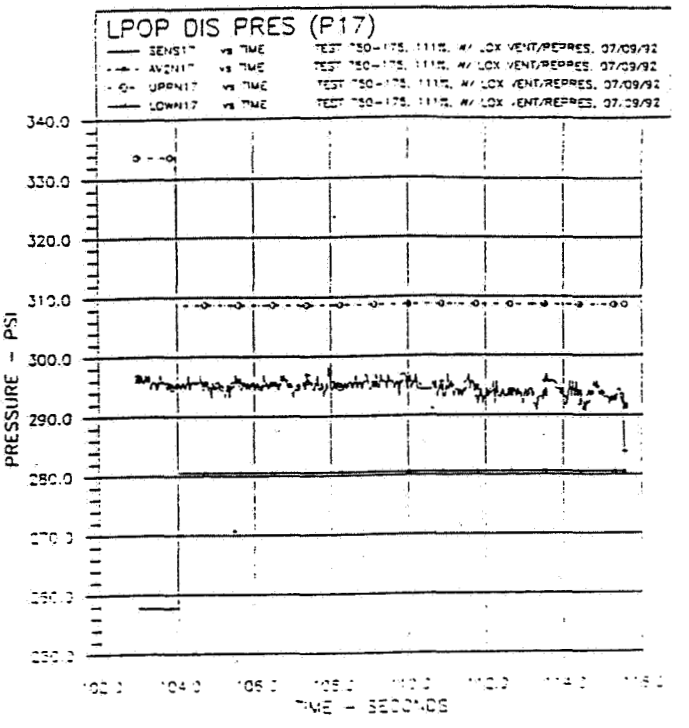

Figure 85.

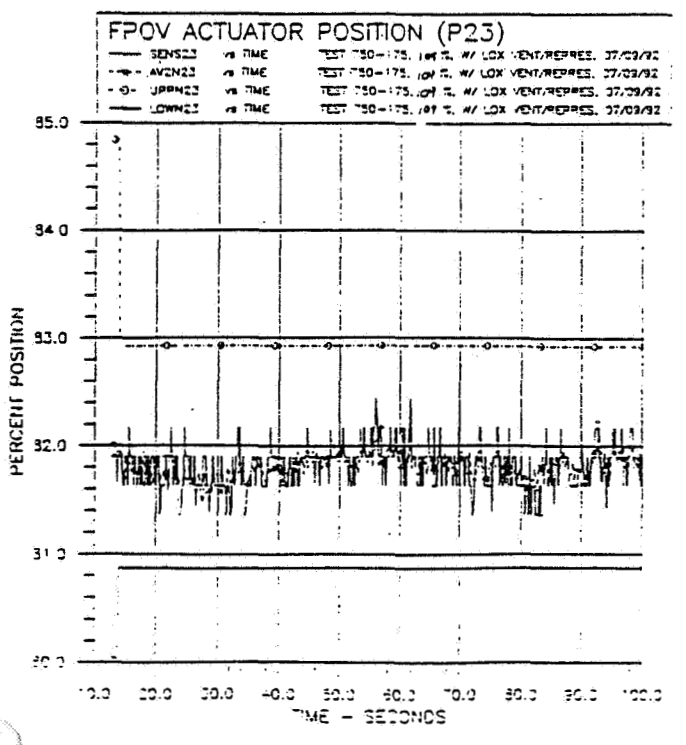

Figure 86.

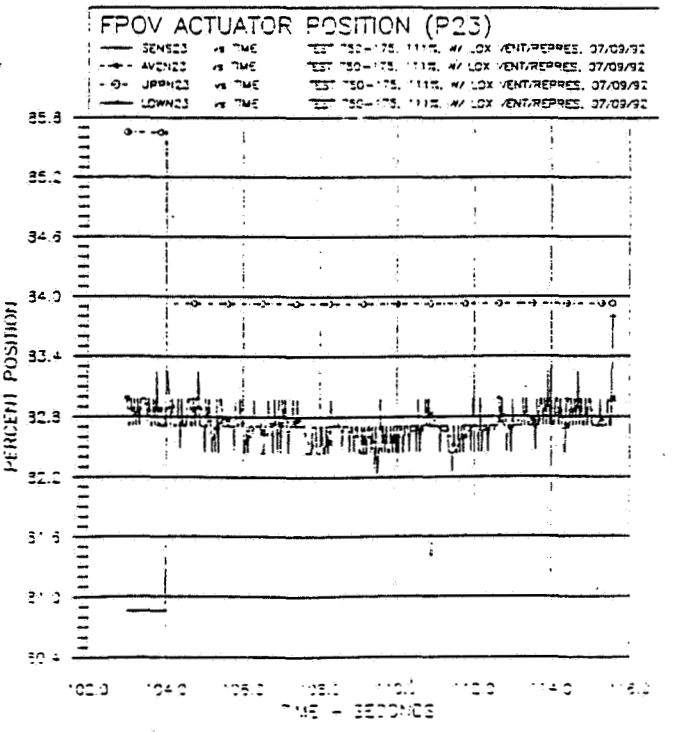

Figure 87.

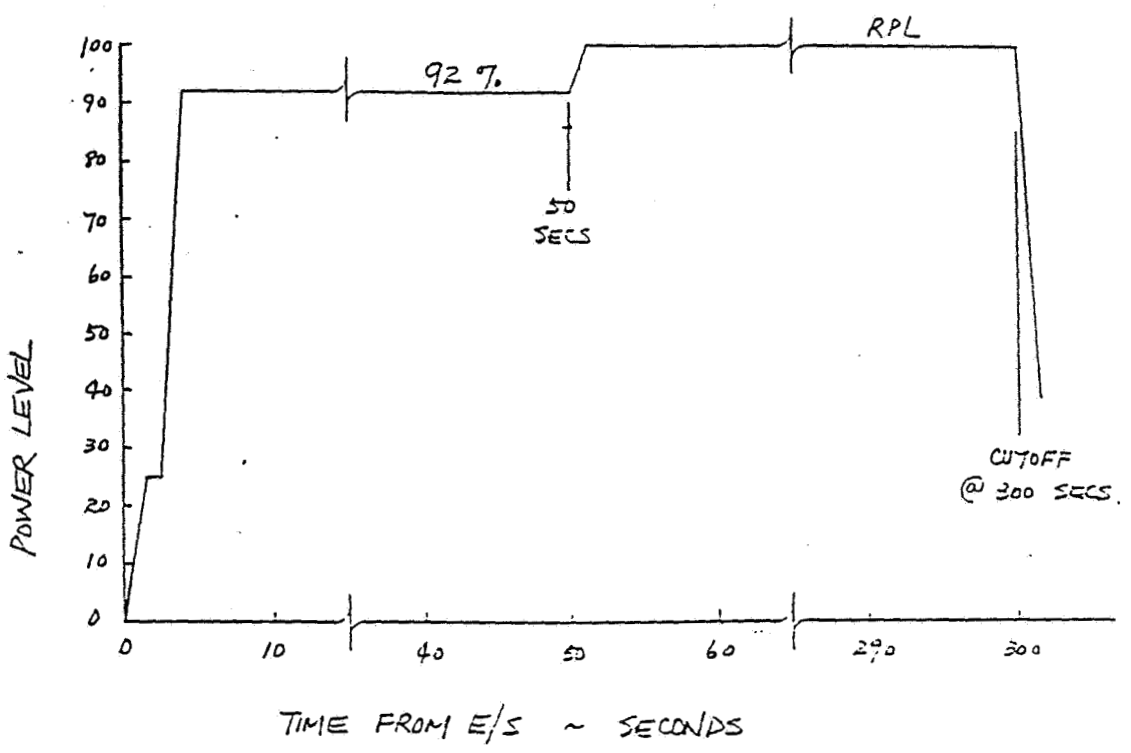

Figure 88. Thrust Profile, Test 901-183

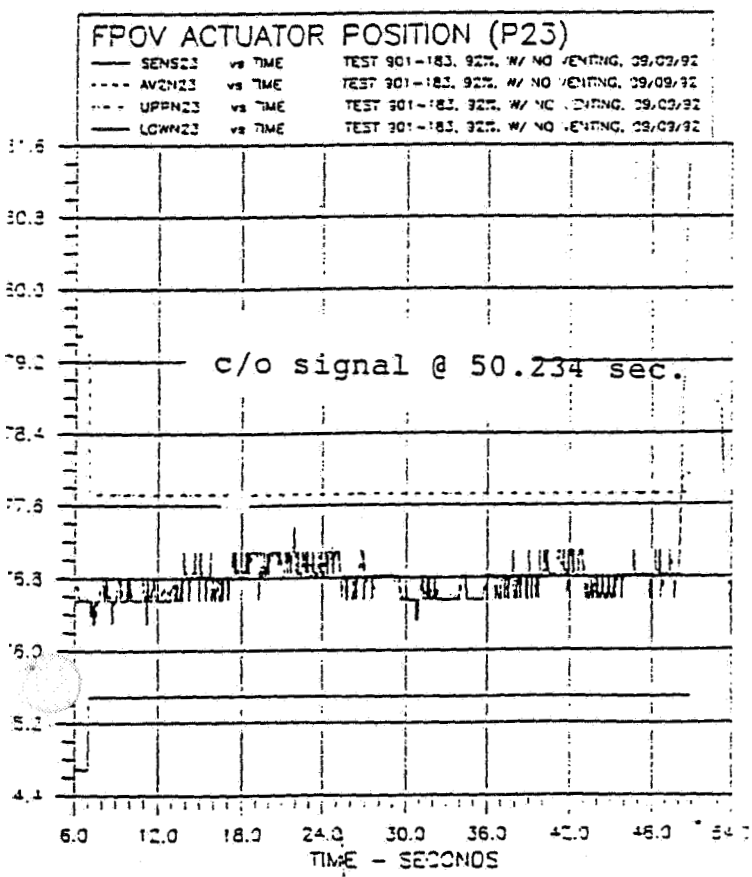

Figure 89.

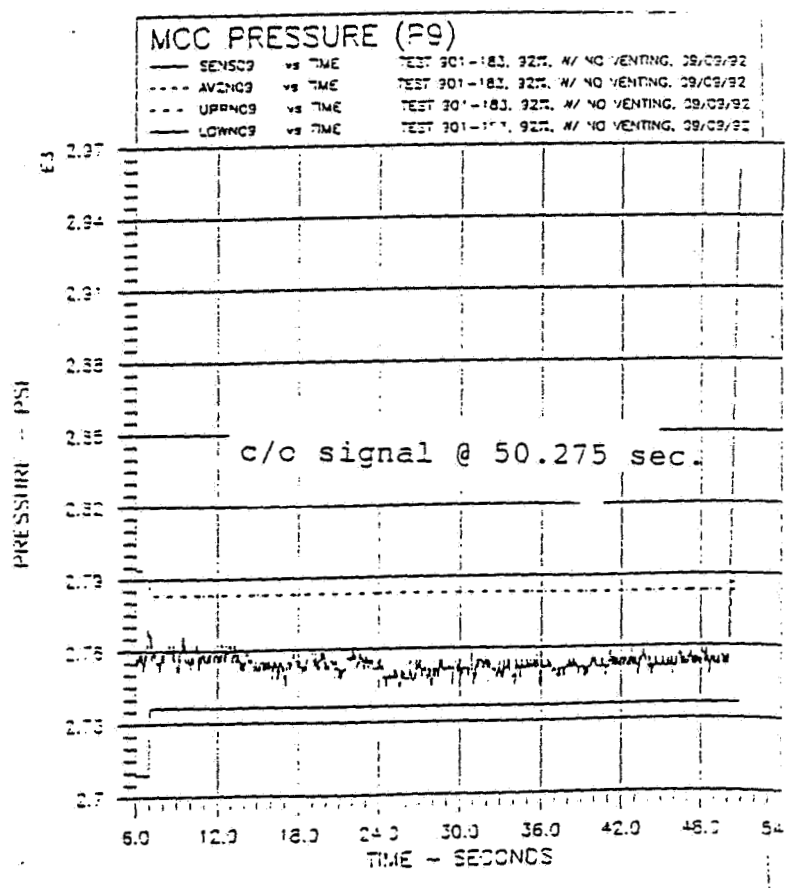

Figure 90.

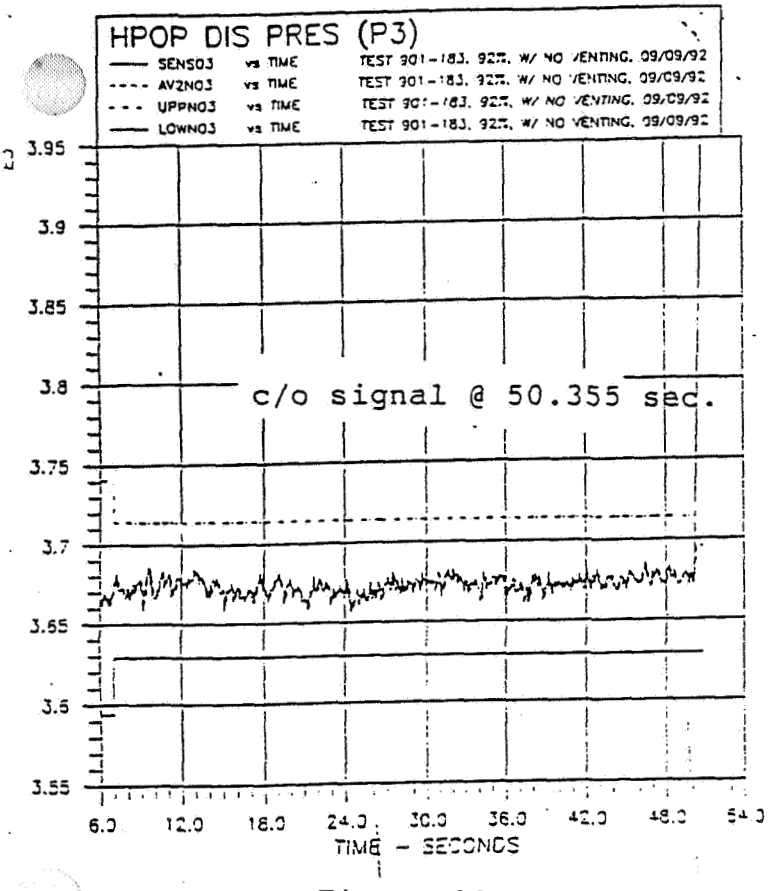

Figure 91.

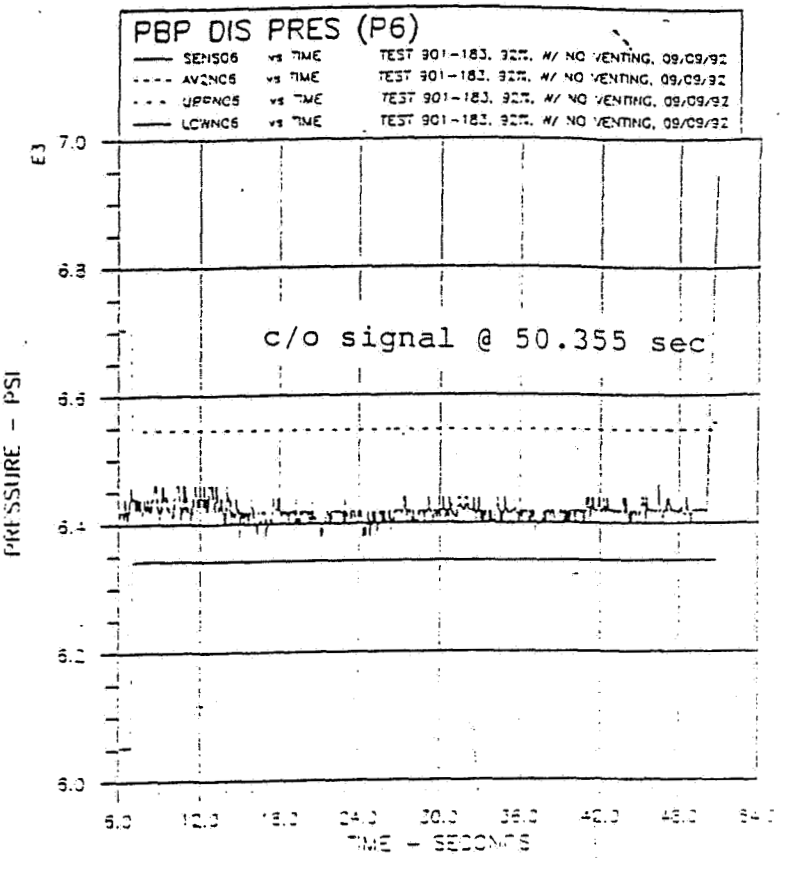

Figure 92.

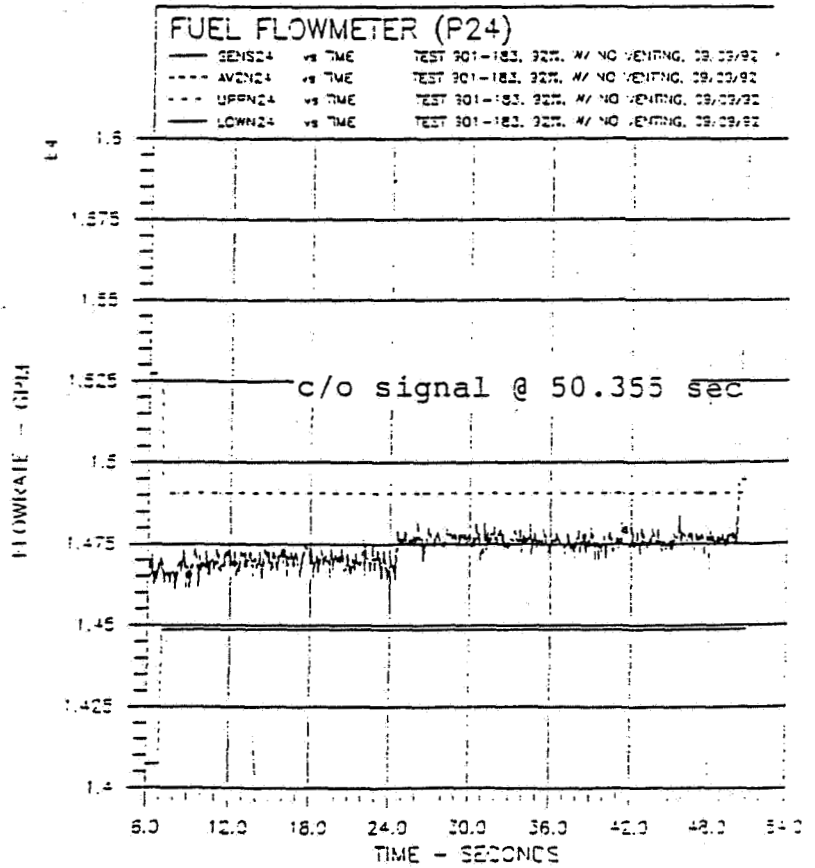

Figure 93.

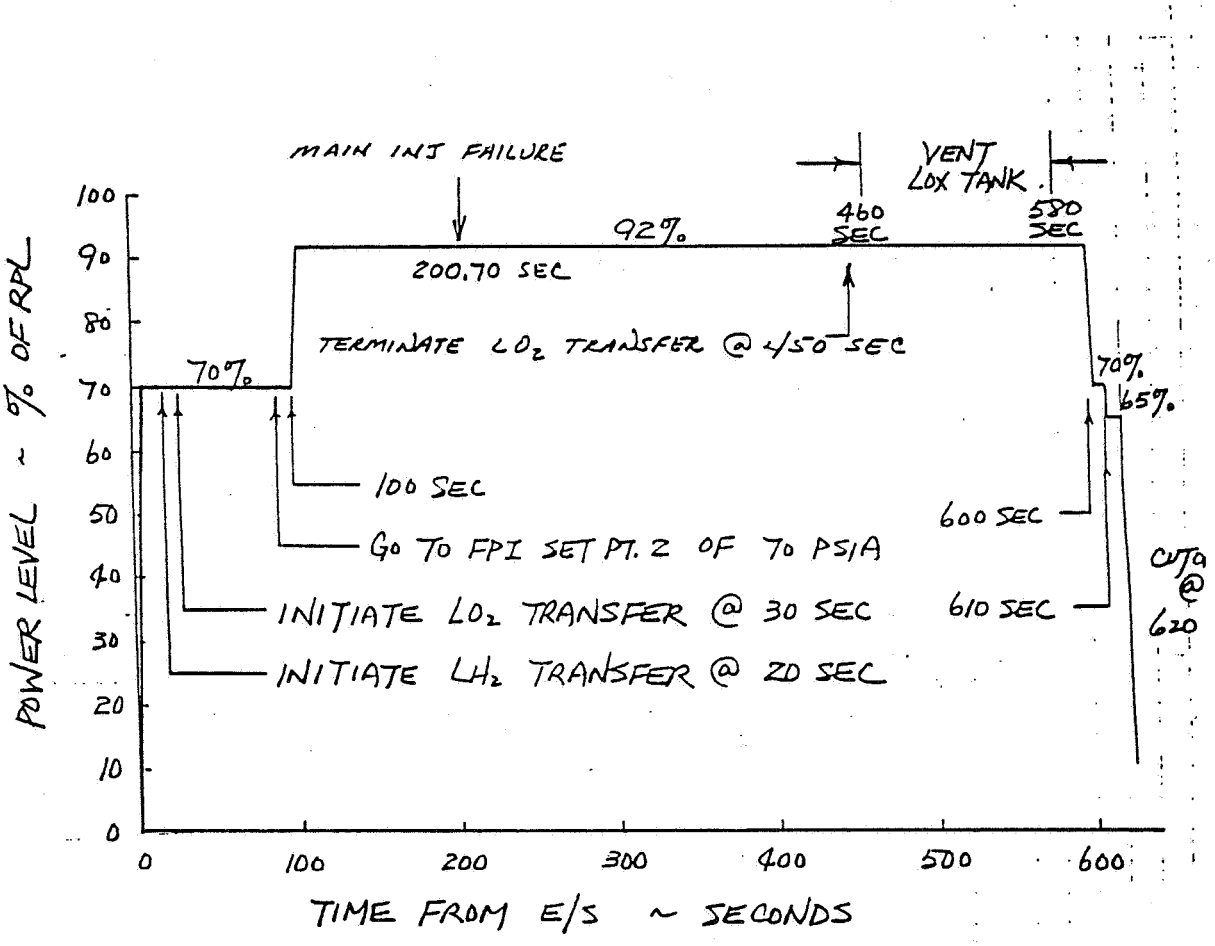

Figure 1

Figure 94. Thrust Profile, Test 901-173

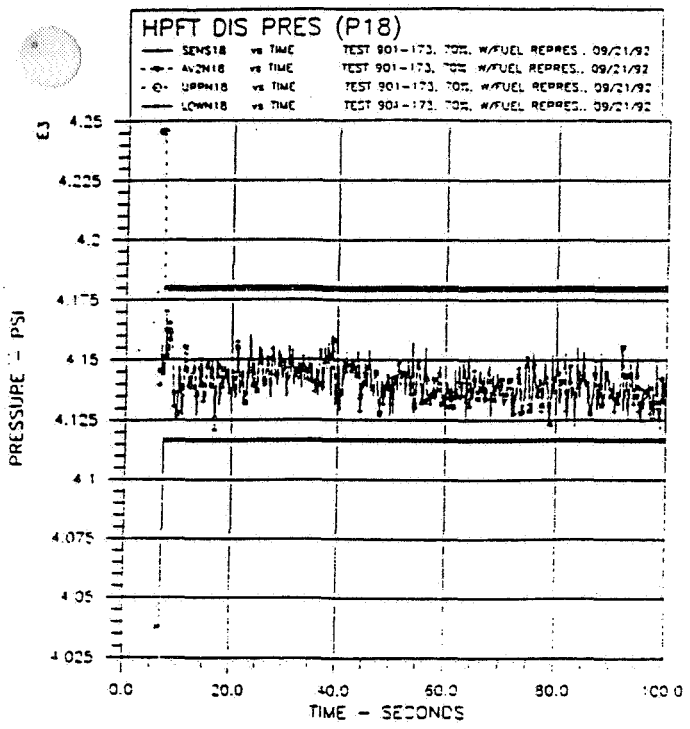

Figure 95.

HPFT DIS PRES, 70% RPL

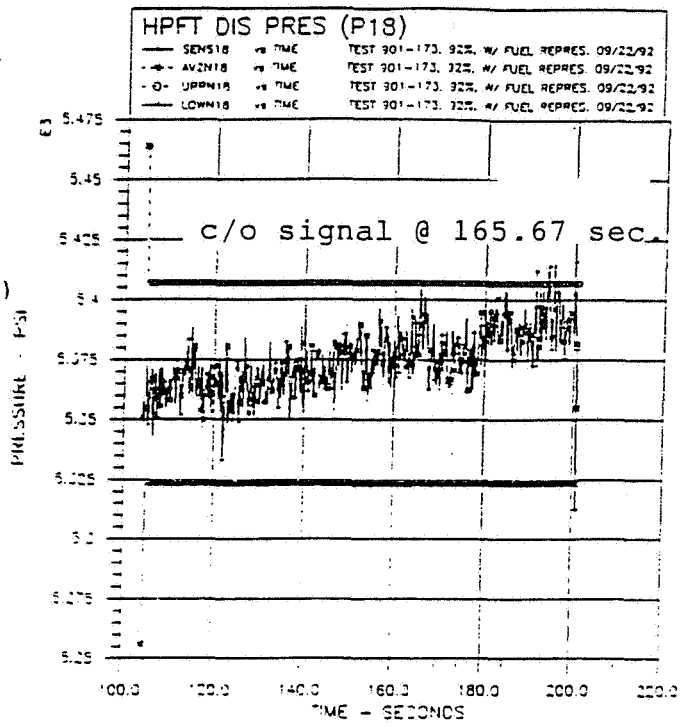

Figure 96.

HPFT DIS PRES, 92% RPL

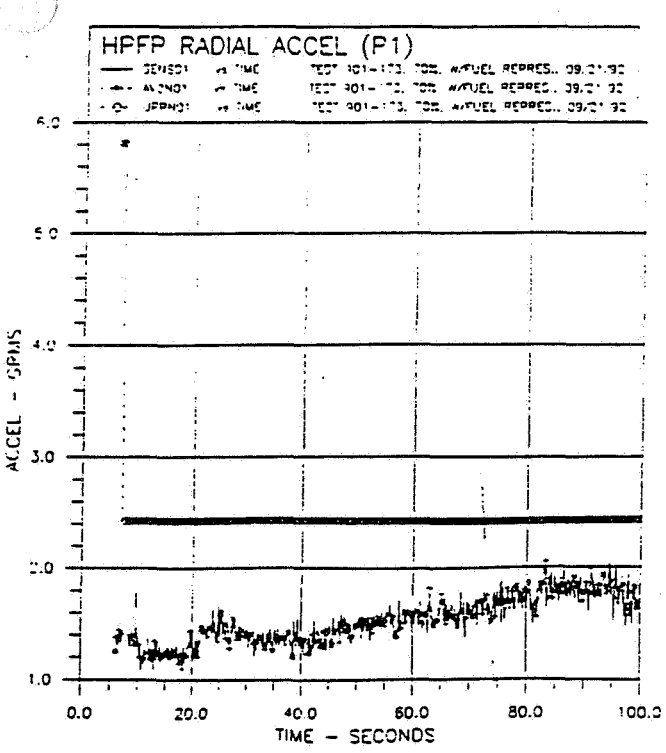

Figure 97.

HPFP RAD ACCEL, 70% RPL

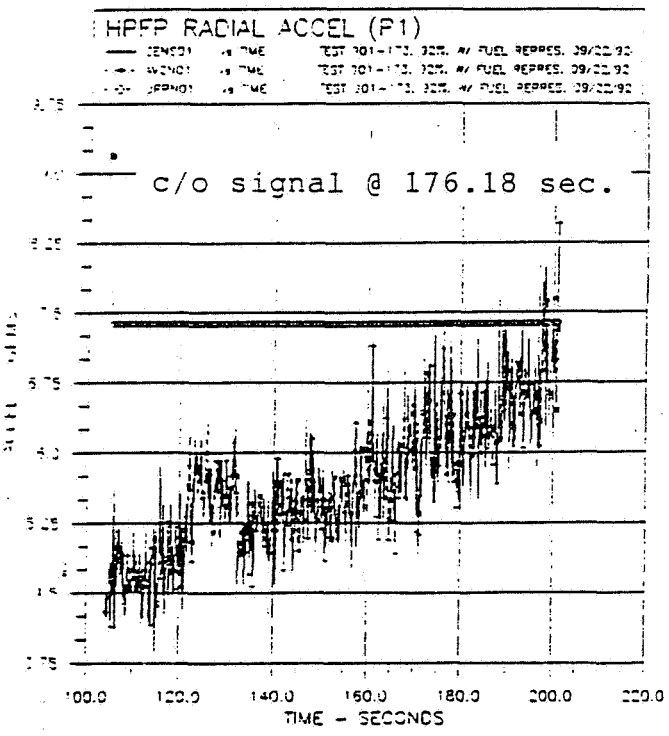

Figure 98.

HPFP RAD ACCEL, 92% RPL

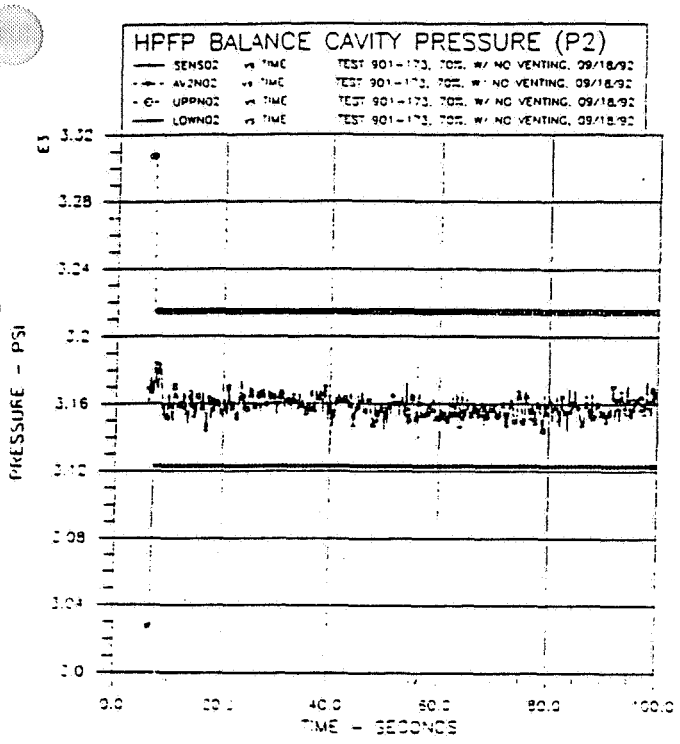

Figure 99.
HPFP BAL CAV PRES, 70% RPL

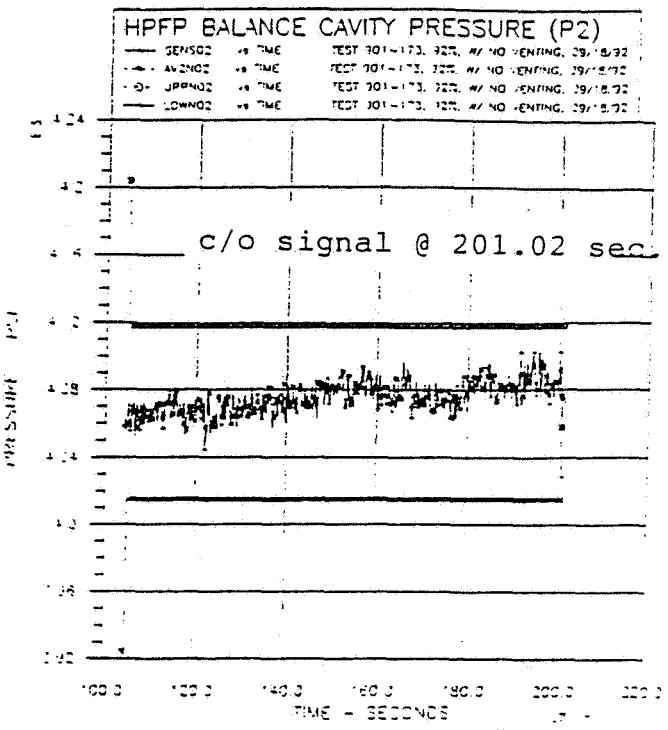

Figure 100.
HPFP BAL CAV PRES, 92% RPL

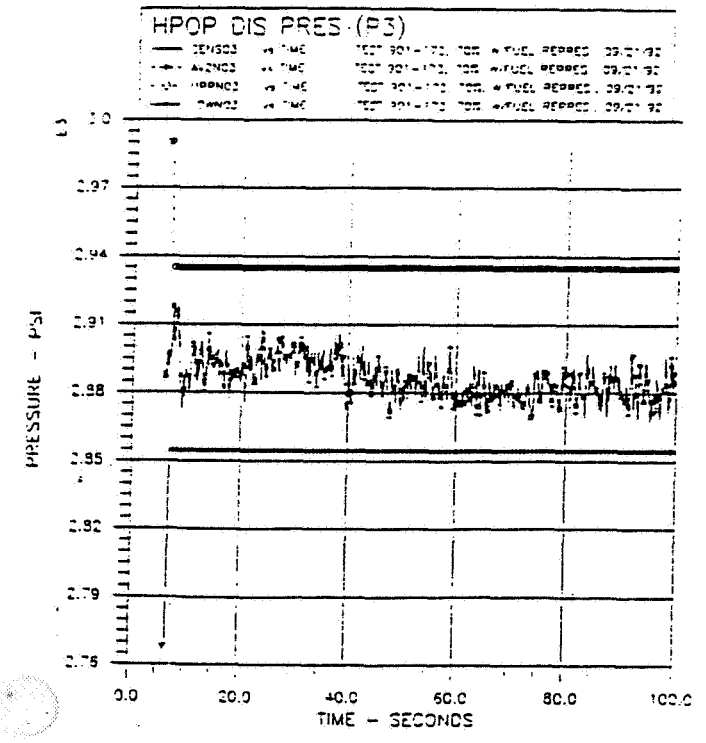

Figure 101.
HPOP DIS PRES, 70% RPL

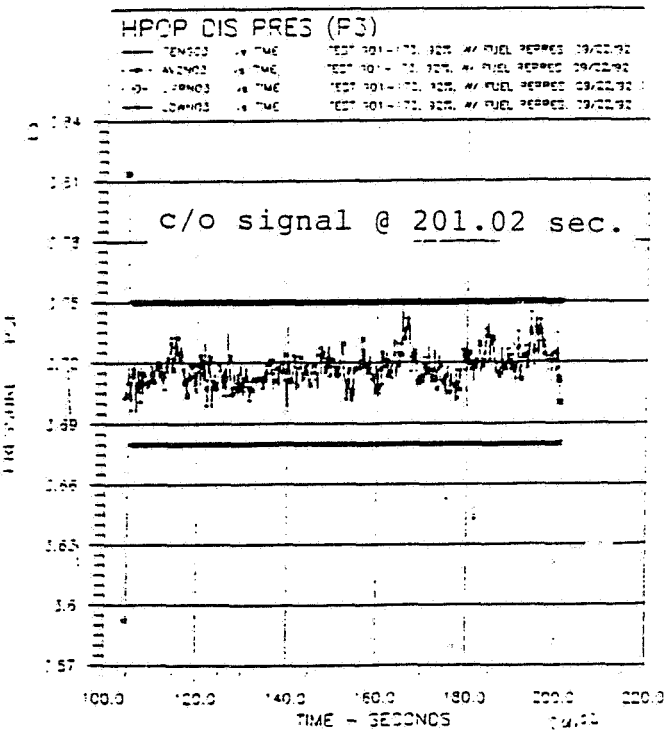

Figure 102.
HPOP DIS PRES, 92% RPL

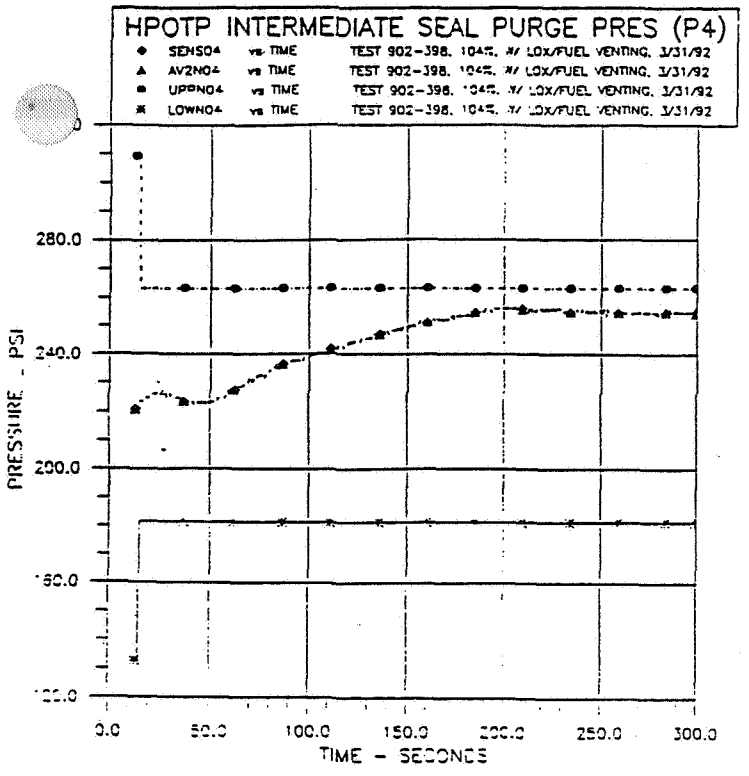

Figure 103.

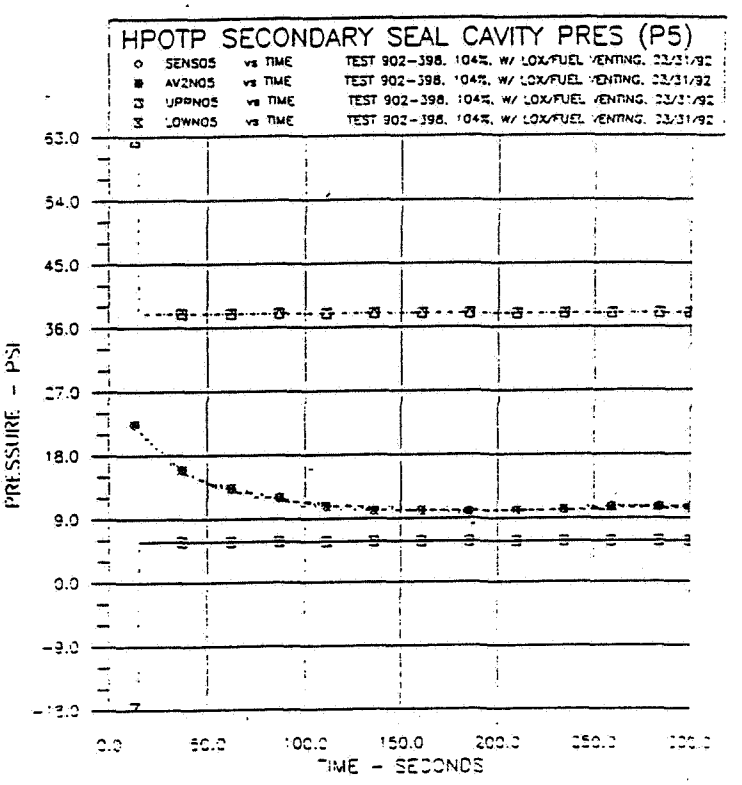

Figure 104.

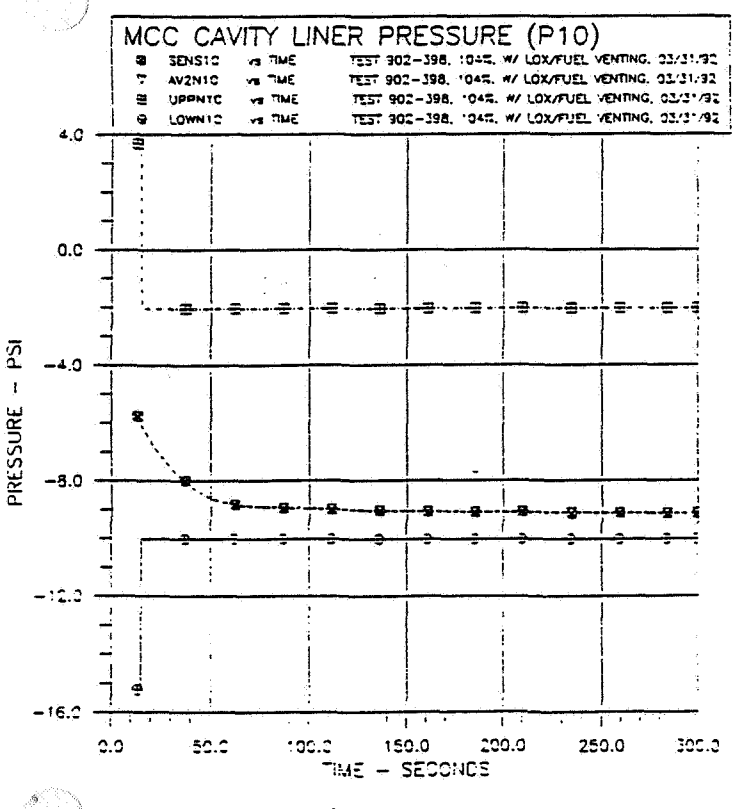

Figure 105.

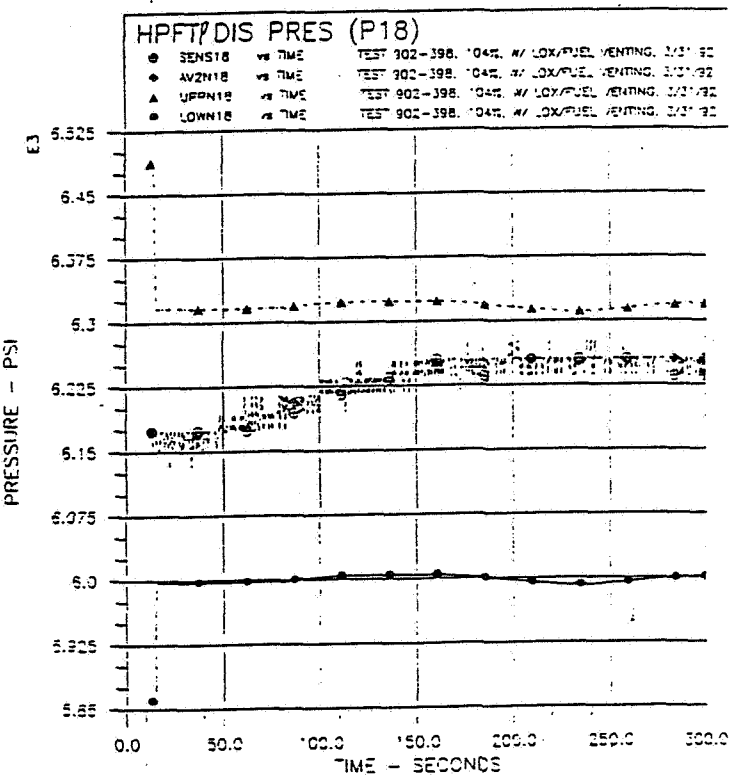

Figure 106.

Figure 103 - 106. Examples Of Parameters Exhibiting Non-Linear Behavior

SSME REAL-TIME FAILURE CONTROL SCHEDULE